P-138

AN INITIAL INVESTIGATION INTO METHODS OF COMPUTING TRANSONIC AERODYNAMIC SENSITIVITY COEFFICIENTS

AEROSPACE ENGINEERING DEPARTMENT

Semiannual Progress Report

January 1, 1988 - June 30, 1988

TEXAS A&M UNIVERSITY

TAMRF Report No. 5802-88-02

July 1988

NASA Grant No. NAG 1-793

Leland A. Carlson
Professor of Aerospace Engineering
Texas A&M University
College Station, Texas 77843-3141

(NASA-CR-183061) AN INITIAL INVESTIGATION INTO METHODS OF COMPUTING TRANSONIC AERODYNAMIC SENSITIVITY COEFFICIENTS Semiannual Progress Report, 1 Jan. - 30 Jun. 1988 (Texas A&M Univ.) 138 p CSCL 01A G3/02

N88-26332

Unclas
0149246

TEXAS ENGINEERING EXPERIMENT STATION

AN INITIAL INVESTIGATION INTO METHODS OF COMPUTING TRANSONIC AERODYNAMIC SENSITIVITY COEFFICIENTS

Semiannual Progress Report

January 1, 1988 -- June 30, 1988

TAMRF Report No. 5802-88-02

July 1988

NASA Grant No. NAG 1 -793

Leland A. Carlson
Professor of Aerospace Engineering
Texas A&M University
College Station, TX 77843-3141

AN INITIAL INVESTIGATION INTO METHODS OF COMPUTING TRANSONIC AERODYNAMIC SENSITIVITY COEFFICIENTS

I. Introduction

This report covers the period from January 1, 1988 thru June 30, 1988. The primary tasks during this were were to complete and formally report on the methods developed for computing aerodynamic sensitivity coefficients using the quasi-analytical approach.

II. Personnel

The staff associated with this project during the present reporting period were Dr. Leland A. Carlson, Principal Investigator, and Hesham El Banna, Graduate Research Assistant.

III. Research Progress

As previously reported (Ref. 1), this initial effort has concentrated on developing the quasi-analytical approach for two-dimensional transonic flow. To keep the problem computationally efficient and straightforward, this initial study has only considered two-dimensional flow and has modeled the problem using the transonic small perturbation equation equation. During this reporting period, this initial development has been essentially completed and formally reported in the Master of Science thesis of Hesham El Banna. Mr. El Banna received his M.S. degree in May 1988, and is continuing his studies at Texas A&M towards a Ph.D.

Since Mr. El Banna's thesis is an excellent summary of much of the work to date, it is included as an appendix of this report. In addition, a shortened version of this thesis has been submitted for possible presentation at the 1989 AIAA Aerospace Sciences Meeting under applied aerodynamics.

IV. Future Efforts

As you are aware, the present project has been granted a no-cost extension until 31 December 1988. Currently studies are underway to compute aerodynamic sensitivity coefficients over a a series of transonic freestream Mach numbers in order to determine how rapidly the coefficients vary with Mach number and whether or not the present method detects or predicts these variations properly. In addition, new solution schemes for the quasi-analytical equation are in progress of being developed and tested. The objective, of course, is to decrease the computational time required to solve the quasi-analytical equation. Particular attention is currently being devoted to tri-diagonal iterative schemes which may carry over to three dimensions. These efforts will be reported in the next progress report.

Finally, it is anticipated that a proposal will be submjitted to continue this work and to extend it to three dimensional transonic flows about wings.

V. References

1. Carlson, L. A., "An Initial Investigation into Methods of Computing Transonic Aerodynamic Sensitivity Coefficients -- Semi-Annual Progress Report," Texas A&M Research Foundation Report NO. 5802-88-01, February 1988.

Appendix I

NUMERICAL COMPUTATION
OF AERODYNAMIC SENSITIVITY COEFFICIENTS
IN THE TRANSONIC AND SUPERSONIC REGIMES

A Thesis

by

HESHAM MAHMOUD ELBANNA

Submitted to the Graduate College of
Texas A&M University
in partial fulfillment of the requirements for the degree of

MASTER OF SCIENCE

May 1988

Major Subject: Aerospace Engineering

NUMERICAL COMPUTATION OF AERODYNAMIC SENSITIVITY COEFFICIENTS IN THE TRANSONIC AND SUPERSONIC REGIMES

A Thesis

by

HESHAM MAHMOUD ELBANNA

Approved as to style and content by:

Leland A. Carlson (Chair of Committee)	Cyrus Ostowari (Member)
Steven D. Taliaferro (Member)	W. E. Haisler (Head of Department)

May 1988

ABSTRACT

Numerical Computation of Aerodynamic Sensitivity Coefficients in the Transonic and Supersonic Regimes. (May 1988)

Hesham M. Elbanna, B.S., Cairo University, Egypt

Chair of Advisory Committee: Dr. Leland Carlson

The quasi-analytical approach is developed to compute the aerodynamic sensitivity coefficients in the transonic and supersonic flight regimes. Initial investigation verifies the feasibility of this approach as applied to the transonic small perturbation residual expression. Results are compared to those obtained by the direct (finite difference) approach and both methods are evaluated to determine their computational efficiencies. A Gauss-Seidel procedure is used to solve the large set of equations associated with the quasi-analytical approach. On a medium grid, the quasi-analytical method is more efficient than the finite difference approach. However, on a fine grid, time comparisons are not as competitive.

ACKNOWLEDGMENTS

The author wishes to extend his sincere appreciation to Professor Leland A. Carlson for his patience and understanding as well as his technical guidance, and to the members of the Advisory Committe for their assistance. Of great benefit were comments and suggestions of Professor Michael S. Pilant who has been a source of inspiration and encouragement.

Principal funding for this research effort was provided by the National Aeronautics and Space Administration, Langley Research Center, under NASA Grant No. NAG 1-793 with E. Carson Yates, Jr. as technical monitor.

TABLE OF CONTENTS

	Page
INTRODUCTION	1
BACKGROUND	4
PROBLEM STATEMENT	6
DESIGN VARIABLES AND AIRFOIL DEFINITION	8
MATHEMATICAL TREATMENT AND SOLUTION PROCEDURE	12
Problem Discretization	12
Solution about a Fixed Design Point	14
Differentiation of the Residual	15
Assembling $(\partial R/\partial \varphi)$ and $(\partial R/\partial XD_i)$	21
Solution by Gauss-Seidel	22
TEST CASES	24
RESULTS AND DISCUSSION	27
Accuracy of the Quasi-Analytical Method	27
Subsonic Cases (M_∞ = 0.2)	27
Transonic Cases (M_∞ = 0.8)	44
Supersonic Cases (M_∞ = 1.2)	59
Time Comparisons	72
CONCLUSIONS AND RECOMMENDATIONS	77
REFERENCES	79
APPENDIX A GENERAL EQUATION FOR SENSITIVITY	81
APPENDIX B RESIDUAL EXPRESSIONS AND DERIVATIVES	85
VITA	118

LIST OF FIGURES

Figure		Page
1	Computational and Physical Domains	13
2	Various Types of Grid Boundary Points	17
3	Pressure Distribution, P1406 Airfoil, $M_\infty = 0.2$, $\alpha = 1°$	29
4	Sensitivity of Pressure to Maximum Thickness, P1406 Airfoil, $M_\infty = 0.2$, $\alpha = 1°$	30
5	Sensitivity of Pressure to Mach Number, P1406 Airfoil, $M_\infty = 0.2$, $\alpha = 1°$	32
6	Sensitivity of Pressure to Angle of Attack, P1406 Airfoil, $M_\infty = 0.2$, $\alpha = 1°$	33
7	Sensitivity of Pressure to Maximum Camber, P1406 Airfoil, $M_\infty = 0.2$, $\alpha = 1°$	35
8	Sensitivity of Pressure to Location of Maximum Camber, P1406 Airfoil, $M_\infty = 0.2$, $\alpha = 1°$	36
9	Pressure Distribution, NACA 1406 Airfoil, $M_\infty = 0.2$, $\alpha = 1°$	38
10	Sensitivity of Pressure to Maximum Thickness, NACA 1406 Airfoil, $M_\infty = 0.2$, $\alpha = 1°$	39
11	Sensitivity of Pressure to Mach Number, NACA 1406 Airfoil, $M_\infty = 0.2$, $\alpha = 1°$	40
12	Sensitivity of Pressure to Angle of Attack, NACA 1406 Airfoil, $M_\infty = 0.2$, $\alpha = 1°$	41

Figure		Page
13	Sensitivity of Pressure to Maximum Camber, NACA 1406 Airfoil, $M_\infty = 0.2$, $\alpha = 1°$	42
14	Sensitivity of Pressure to Location of Maximum Camber, NACA 1406 Airfoil, $M_\infty = 0.2$, $\alpha = 1°$	43
15	Pressure Distribution, P1406 Airfoil $M_\infty = 0.8$, $\alpha = 1°$	45
16	Sensitivity of Pressure to Maximum Thickness, P1406 Airfoil, $M_\infty = 0.8$, $\alpha = 1°$	46
17	Sensitivity of Pressure to Mach Number, P1406 Airfoil, $M_\infty = 0.8$, $\alpha = 1°$	48
18	Sensitivity of Pressure to Angle of Attack, P1406 Airfoil, $M_\infty = 0.8$, $\alpha = 1°$	49
19	Sensitivity of Pressure to Maximum Camber, P1406 Airfoil, $M_\infty = 0.8$, $\alpha = 1°$	50
20	Sensitivity of Pressure to Location of Maximum Camber, P1406 Airfoil, $M_\infty = 0.8$, $\alpha = 1°$	51
21	Pressure Distribution, NACA 1406 Airfoil, $M_\infty = 0.8$, $\alpha = 1°$	52
22	Sensitivity of Pressure to Maximum Thickness, NACA 1406 Airfoil, $M_\infty = 0.8$, $\alpha = 1°$	54
23	Sensitivity of Pressure to Mach Number, NACA 1406 Airfoil, $M_\infty = 0.8$, $\alpha = 1°$	55
24	Sensitivity of Pressure to Angle of Attack, NACA 1406 Airfoil, $M_\infty = 0.8$, $\alpha = 1°$	56

Figure		Page
25	Sensitivity of Pressure to Maximum Camber, NACA 1406 Airfoil, $M_\infty = 0.8$, $\alpha = 1°$	57
26	Sensitivity of Pressure to Location of Maximum Camber, NACA 1406 Airfoil, $M_\infty = 0.8$, $\alpha = 1°$	58
27	Pressure Distribution, P1406 Airfoil, $M_\infty = 1.2$, $\alpha = 1°$	60
28	Sensitivity of Pressure to Maximum Thickness, P1406 Airfoil, $M_\infty = 1.2$, $\alpha = 1°$	61
29	Sensitivity of Pressure to Mach Number, P1406 Airfoil, $M_\infty = 1.2$, $\alpha = 1°$	62
30	Sensitivity of Fressure to Angle of Attack, P1406 Airfoil, $M_\infty = 1.2$, $\alpha = 1°$	63
31	Sensitivity of Pressure to Maximum Camber, P1406 Airfoil, $M_\infty = 1.2$, $\alpha = 1°$	64
32	Sensitivity of Pressure to Location of Maximum Camber, P1406 Airfoil, $M_\infty = 1.2$, $\alpha = 1°$	65
33	Pressure Distribution, NACA 1406 Airfoil, $M_\infty = 1.2$, $\alpha = 1°$	66
34	Sensitivity of Pressure to Maximum Thickness, NACA 1406 Airfoil, $M_\infty = 1.2$, $\alpha = 1°$	67
35	Sensitivity of Pressure to Mach Number, NACA 1406 Airfoil, $M_\infty = 1.2$, $\alpha = 1°$	68
36	Sensitivity of Pressure to Angle of Attack, NACA 1406 Airfoil, $M_\infty = 1.2$, $\alpha = 1°$	69

Figure Page

37 Sensitivity of Pressure to Maximum Camber, NACA 1406 Airfoil, $M_\infty = 1.2$, $\alpha = 1°$ 70

38 Sensitivity of Pressure to Location of Maximum Camber, NACA 1406 Airfoil, $M_\infty = 1.2$, $\alpha = 1°$ 71

LIST OF TABLES

Table		Page
1	Lift Coefficients	25
2	Accuracy of Quasi-Analytical Method for Computing Lift Coefficient Sensitivity Coefficients	28
3	Time Comparisons for Obtaining Sensitivity Coefficients for Five Design Variables, Grid 41*20	73
4	Time Comparisons for Obtaining Sensitivity Coefficients for Five Design Variables, Grid 81*20	74

NOMENCLATURE

A1, A2	Coordinate stretching constants
C	Maximum camber
Cp	Pressure coefficient
IM, JM	Grid dimensions
L	Chordwise location of maximum camber
M	Mach number
N	Size of Jacobian matrix
R	Residual expression
T	Maximum thickness
f,g	Cartesian coordinate stretching functions
n	Quadrant number in two-dimensions
x,y	Cartesian coordinates
α	Angle of attack
γ	Ratio of specific heats
Γ	Circulation
φ	Perturbation potential function
Subscripts	
∞	Free stream condition
p	Pressure
b	Body
u,l	Upper, lower
i,j	Grid point
ii,jj	Counters

INTRODUCTION

Over the past few years, computational fluid dynamics has evolved rapidly as a result of the immense advancements in the computational field and the impact of the use of computers on obtaining numerical solutions to complex problems. Accordingly, researchers are now capable of calculating aerodynamic forces on wing-body-nacelle-empennage configurations subject to subsonic or transonic flows. A next logical step would be to compute the sensitivity of these forces to configuration geometry.

In the transonic regime, one of the main difficulties facing the aircraft designer is the prediction of the aerodynamic loads. The difficulty is caused by the fact that in this regime even the most primitive representation of the aerodynamics must be described by a nonlinear equation or a set of equations. In addition, aerodynamic prediction in the transonic regime is extremely important since it is in this speed range that most civil aircraft maneuver. Consequently, the transonic regime is probably the most critical flow regime for present day aircraft.

Format in accordance with AIAA Journal.

In order to improve the design of transonic vehicles, design codes are being developed which use optimization techniques; and, in order to be successful, these codes require aerodynamic sensitivity coefficients, which are defined as the derivatives of the aerodynamic functions with respect to the design variables. Obviously, it is desirable that such sensitivity coefficients be easily obtained.

Consequently, the primary objective of this effort is to investigate the feasibility of using the quasi-analytical method[1-5] for calculating the aerodynamic sensitivity derivatives in the transonic and supersonic flight regimes. As part of this work, the resulting sensitivity coefficients are compared to those obtained from the finite difference approach. Finally, both methods are evaluated to determine their computational efficiencies.

As mentioned earlier, knowledge of the sensitivity coefficients is essential information in any design optimization process. Obviously these calculations cannot be performed without the availability of solutions for the problem under consideration.

In the transonic regime, a variety of methods for computing solutions to the flow field do exist. These

range from full Navier-Stokes solvers to transonic small perturbation equation solvers. The complexity of the equations that need to be solved depends upon the flow phenomena in question and the objective of the analysis. Since it is not the objective of this work to develop flowfield algorithms, the present research uses the transonic small perturbation equation to determine and, as mentioned earlier, verify the existence of efficient methods for calculating the aerodynamic sensitivity derivatives.

This research is original in that it aims to include sensitivity analysis procedures as part of aerodynamic analyses. Thus, it will provide a reference point for aeronautical engineers[1] who need sensitivity information when conducting aerodynamic optimization as part of the aircraft design process.

BACKGROUND

Most recently, sensitivity methodology has been successfully used in structural design[2] and optimization programs[3] primarily to assess the effects of the variation of various fundamental properties relative to the important physical design variables. Moreover, researchers have developed and applied sensitivity analysis for analytical model improvement and assessment of design trends. In most cases, a predominant contributor to the cost and time in the optimization procedures is the calculation of derivatives. For this reason it is desirable in aerodynamic optimization to have efficient methods of determining the aerodynamic sensitivity coefficients and, wherever possible, to develop appropriate numerical methods for such computations.

Currently, most methods for calculating transonic aerodynamic sensitivity coefficients are based upon the finite difference approximation to the derivatives. In this approach, a design variable is perturbed from its previous value, a new complete solution is obtained, and the differences between the new and the old solutions are used to obtain the sensitivity coefficients.

This direct, or brute force, technique has the disadvantage of being potentially very computer intensive,

especially if the governing equations are expensive to solve. Accordingly, the need to eliminate these costly and repetitive analyses is the primary motivation for the development of alternative efficient computational methods to determine the aerodynamic sensitivity coefficients.

In steady-state transonic flow problems, implicit approximate-factorization (AF) algorithms[6] have been used successfully and efficiently to solve the nonlinear two-dimensional transonic small-disturbance equation. This governing equation permits capturing of important physical phenomena while being easy to handle from a coding standpoint. For this reason it would seem desirable to initiate the study of the quasi-analytical method in the transonic regime using the transonic small perturbation equation as a practical object of this investigation.

PROBLEM STATEMENT

Based on the foregoing discussion, the current problem is formulated starting from the generic quasi-analytical approach and manipulated according to the rules given in Appendix A of Ref.1 which is reproduced in this thesis because of its direct significance to the derivation of the general sensitivity equation.

In this study, the general sensitivity equation is applied to the residual expression (R) of the transonic small perturbation equation. As mentioned earlier, this expression is chosen because of its simplicity as well as its adequate description of the nonlinear phenomena occurring in the transonic regime. Although this expression is nonlinear in the perturbation potential (φ), the general sensitivity equation, Eq.(1), is linear with respect to the unknown sensitivity ($\partial\varphi/\partial XD_i$), (see Appendix A).

It is to be noticed that the practical implementation of the above step is not achieved until the residual expression is approximated on a finite domain and the mathematical form of the problem rendered to that of one in linear algebra. This discretization process will be explained in a later section.

Following the previous formulation, the sensitivity equation as applied to the residual expression of the transonic small perturbation equation is given by,

$$\left[\frac{\partial R}{\partial \varphi}\right]\left\{\frac{\partial \varphi}{\partial XD_i}\right\} = -\left\{\frac{\partial R}{\partial XD_i}\right\} \tag{1}$$

where

$$R = (B_1+B_2\varphi_x)\,\varphi_{xx} + \varphi_{yy} = 0 \tag{2}$$

$$B_1 = 1 - M_\infty^2$$

$$B_2 = -(\gamma+1)\,M_\infty^2$$

for air γ = const. = 1.4

$$\varphi = \varphi\,(x,y,XD) \tag{3}$$

XD = set of design variables

XD_i = i^{th} design variable

subject to,

Airfoil Boundary Condition

$$\varphi_y(x_b,0) = \left[\frac{dy}{dx}\right]_b = F(x,XD) \tag{4}$$

Infinity Boundary Condition

subsonic : $\varphi_\infty = \Gamma\theta/(2\pi)$, $\theta = n\pi/2$, n=0,1,2,3,4

supersonic : $\varphi_\infty = 0$, $\theta = n\pi/2$, n=1,2,3

$\varphi_x = 0$, $\theta = n\pi/2$, n=0,4 (5)

Kutta Condition

$\Delta P = 0$ ($\Gamma = \Delta\varphi$ = const.), $x_{TE} < x \leq \infty$ (6)

DESIGN VARIABLES AND AIRFOIL DEFINITION

Equation (1) is discretized into a system of linear equations to be solved for the unknown sensitivity vector. The solution of this system is obtained, as explained in the following section, by using a Gauss-Seidel iterative procedure which utilizes the sparsity pattern characterizing the coefficient matrix ($\partial R/\partial \varphi$). An advantage of using this scheme is that several unknown vectors can be obtained simultaneously, each vector representing the sensitivity of the potential (φ) with respect to some design variable XD_i.

At this stage, it is convenient to define the vector of design variables

$$XD = (XD_1, XD_2, \ldots, XD_n) \qquad (7)$$

and to exactly determine which variables influence the solution of Eq.(2). In doing so, the relation between the sensitivity coefficients corresponding to these variables and the form of the optimization algorithm that utilizes this information needs to be considered.

For the transonic flow problem, an appropriate choice of the first design variable is the free stream Mach Number (M_∞). This variable appears in the governing Eq.(2) and has an important influence on the character of the equation via its influence on local Mach number (for $M<1$,

the equation is elliptic, for M>1, the equation is hyperbolic) and thus on the nature of the solution. For this reason, it is desirable to have M_∞ as one of the design variables.

Next, it is appropriate to examine the boundary condition given by Eq.(5). In the transonic small perturbation formulation, the angle of attack (α) enters the problem through the boundary condition and thus,

$$F_{u_1} = \left[\frac{dy}{dx}\right]_b - y_{u_1}' - \alpha \qquad (8)$$

For simplicity, the function (F) should be easily differentiable with respect to the design variables defining the airfoil geometry. This desirable feature is explained later on and has to do with the computation of the right hand side term of the sensitivity equation. Therefore, it would seem plausible to have a simple analytical expression for modeling the upper and lower surfaces of the airfoil.

For the present studies, it was decided to limit consideration to two basic airfoil sections, namely parabolic-arc sections, and the NACA four-digit sections. These families of wing sections are obtained by combining a mean line and a thickness distribution[7]. The resultant expressions possess the necessary features that suit the

problem, mainly the concise description of the airfoil surfaces in terms of several geometric design variables. The expressions are as follows :

For parabolic-arc sections

$$y_{u_l} = \begin{cases} C(2Lx-x^2)/L^2 & \pm 2Tx(1-x), \quad x \le L \\ C[(1-2L)+2Lx-x^2]/(1-L)^2 & \pm 2Tx(1-x), \quad x > L \end{cases} \tag{9}$$

For NACA four-digit sections

$$y_{u_l} = \begin{cases} C(2Lx-x^2)/L^2 \\ \pm 5T(0.2969\sqrt{x}-0.126x-0.3516x^2+0.2843x^3-0.1015x^4) \\ \qquad\qquad x \le L \\ C[(1-2L)+2Lx-x^2]/(1-L)^2 \\ \pm 5T(0.2969\sqrt{x}-0.126x-0.3516x^2+0.2843x^3-0.1015x^4) \\ \qquad\qquad x > L \end{cases} \tag{10}$$

where

C = Maximum ordinate of mean line (camber)

L = Chordwise location of maximum ordinate of camber

T = Maximum thickness

Each of the quantaties C, L, and T is expressed as a fraction of the chord (e.g. if T is 6% chord then T = 0.06). Differentiating Eqs.(9) and (10) with respect to x and substituting the results into Eq.(8) yields :

For parabolic-arc sections

$$F_{u,1} = 2C(L-x)/LL - \alpha \pm 2T(1-2x) \qquad (11)$$

For NACA four-digit sections

$$F_{u,1} = 2C(L-x)/LL - \alpha \pm 5T(0.14845/\sqrt{x}-0.126-0.7032x+0.8529x^2-0.406x^3) \qquad (12)$$

where

$$LL = \begin{cases} L^2 & \text{forward of maximum ordinate of camber, } x \le L \\ (1-L)^2 & \text{aft of maximum ordinate of camber, } x > L \end{cases} \qquad (13)$$

Eqs.(11) and (12) are simple analytical expressions in terms of the four variables T, L, C, and α. Thus,

$$XD = (T, M_\infty, \alpha, L, C) \qquad (14)$$

represents the complete set of design variables that define the present two-dimensional airfoil sensitivity problem. Notice that these variables are completely uncoupled and, thus the sensitivity equation can be solved independently with respect to each variable[8].

MATHEMATICAL TREATMENT AND SOLUTION PROCEDURE

Problem Discretization

Equation (1) resembles the general sensitivity equation (see Appendix A) applied to the residual R instead of the function F, φ instead of y, and XD_i instead of x. Now, in order to solve the problem numerically, Eq.(2) is formulated computationally on a finite domain. This transformation is achieved by using a stretched Cartesian grid that maps the infinite physical domain onto a finite computational grid, Fig.(1). In this study, the grid used is based upon a hyperbolic tangent transformation that places the outer boundaries at infinity. Accordingly, the computational variables used are given by,

$$\xi = \tanh A_2 x \tag{15}$$

$$\eta = \tanh A_1 y \tag{16}$$

or,

$$x = \{ \ln[(1+\xi)/(1-\xi)] \} / (2A_2) \tag{17}$$

$$y = \{ \ln[(1+\eta)/(1-\eta)] \} / (2A_1) \tag{18}$$

In terms of the grid nodes (i,j), we have,

$$\xi = -1 + (i-1)\Delta\xi \tag{19}$$

$$\eta = -1 + (j-1)\Delta\eta \tag{20}$$

Equations (15)-(20) are the equations that govern the hyperbolic tangent transformation.

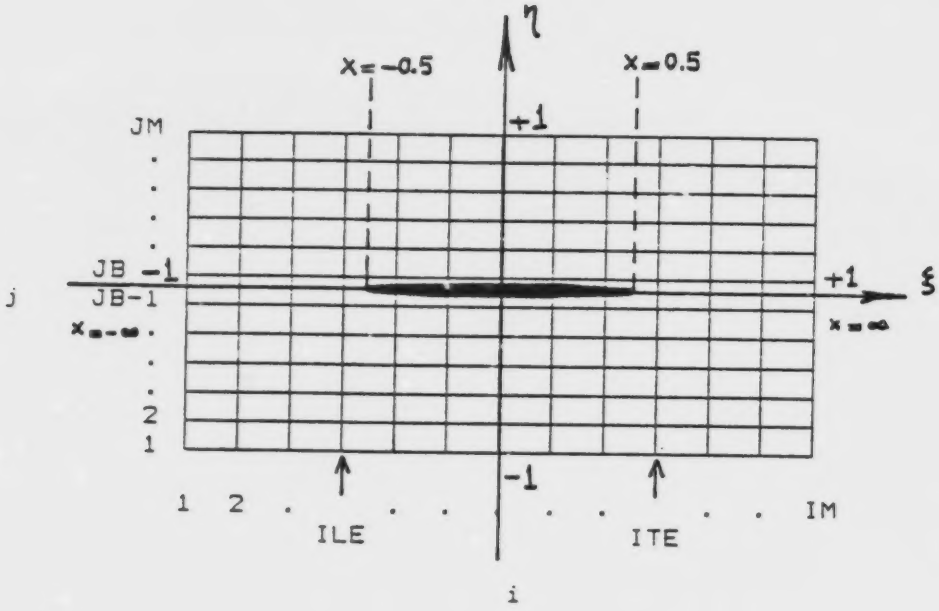

Fig.1 Computational and Physical Domains

In addition, the stretching functions are defined as,

$$f = (d\xi/dx) = A_2(1-\xi^2) \tag{21}$$

$$g = (d\eta/dy) = A_1(1-\eta^2) \tag{22}$$

so that,

$$\varphi_x = f\varphi_\xi \tag{23}$$

$$\varphi_y = g\varphi_\eta \tag{24}$$

$$\varphi_{xx} = f\,(f\varphi_\xi)_\xi \tag{25}$$

$$\varphi_{yy} = g\,(g\varphi_\eta)_\eta \tag{26}$$

Solution about a Fixed Design Point

Substituting from Eqs.(23)-(26) into Eq.(2), yields the transformed residual expression,

$$R = [B_1+B_2f\varphi_\xi]\, f(f\varphi_\xi)_\xi + g(g\varphi_\eta)_\eta = 0 \tag{27}$$

This equation is solved numerically by an approximate factorization scheme[6] in which the objective is to force the residual to zero at each point of the computational domain. In finite difference form, Eq.(27) can be written as,

$$\begin{aligned} R_{i,j} = {} & [B_1 + B_2(\varphi_{i+1,j}-\varphi_{i-1,j})/(2\Delta\xi)]\, f_i/\Delta\xi^2 \\ & [\nu_{i,j}f_{i+\frac{1}{2}}(\varphi_{i+1,j}-\varphi_{i,j}) - (2\nu_{i,j-1})f_{i-\frac{1}{2}} \\ & (\varphi_{i,j}-\varphi_{i-1,j}) - (1-\nu_{i,j})f_{i-3/2}(\varphi_{i-1,j}-\varphi_{i-2,j})] \\ & + [g_{j+\frac{1}{2}}(\varphi_{i,j+1}-\varphi_{i,j}) - g_{j-\frac{1}{2}}(\varphi_{i,j}-\varphi_{i,j-1})]\, g_j/\Delta\eta^2 \end{aligned} \tag{28}$$

where

$\nu_{i,j} = 1$ if point (i,j) is subsonic

$\nu_{i,j} = 0$ if point (i,j) is supersonic

Eq.(28) is the discretized form of the residual at a general point (i,j) in terms of φ values at surrounding points. Consequently, R at i,j can be viewed as a function of the φ values at neighboring points; and, therefore, the differentiation of the residual expression is straight forward.

Differentiation of the Residual

Rearranging Eq.(28) yields

$$R_{i,j} = c_1\varphi_{i,j} + c_2\varphi_{i+1,j}\varphi_{i-1,j} + c_3\varphi_{i+1,j}\varphi_{i,j} + c_4\varphi_{i-1,j}\varphi_{i,j} + c_5\varphi_{i+1,j}\varphi_{i-2,j} + c_6\varphi_{i-1,j}\varphi_{i-2,j} + c_7\varphi_{i-1,j}^2 + c_8\varphi_{i+1,j}^2 + c_9\varphi_{i+1,j} + c_{10}\varphi_{i-1,j} + c_{11}\varphi_{i,j+1} + c_{12}\varphi_{i,j-1} + c_{13}\varphi_{i-2,j} \qquad (29)$$

where the coefficients $c_1, c_2, \ldots, c_{13}$ are given by :

$$c_1 = \{ -g_j(g_{j+\frac{1}{2}}+g_{j-\frac{1}{2}})/\Delta\eta^2 - f_iB_1[\nu_{i,j}f_{i+\frac{1}{2}}+(2\nu_{i,j}-1)f_{i-\frac{1}{2}}]/\Delta\xi^2 \}$$

$$c_2 = \{ -n_{i,j}B_2f_i^2f_{i+\frac{1}{2}}/(2\Delta\xi^3) + f_i^2B_2[(2\nu_{i,j}-1)f_{i-\frac{1}{2}}-(1-\nu_{i,j})f_{i-3/2}]/(2\Delta\xi^3) \}$$

$$c_3 = \{ -f_i^2B_2[\nu_{i,j}f_{i+\frac{1}{2}}+(2\nu_{i,j}-1)f_{i-\frac{1}{2}}]/(2\Delta\xi^3) \}$$

$$c_4 = \{ +f_i^2B_2[\nu_{i,j}f_{i+\frac{1}{2}}+(2\nu_{i,j}-1)f_{i-\frac{1}{2}}]/(2\Delta\xi^3) \}$$

$$c_5 = \{ +(1-\nu_{i,j})B_2f_i^2f_{i-3/2}/(2\Delta\xi^3) \}$$

$$c_6 = \{ - (1-\nu_{i,j})B_2 f_i^2 f_{i-3/2}/(2\Delta\xi^3) \}$$

$$c_7 = \{ - f_i^2 B_2[(2\nu_{i,j}-1)f_{i-\frac{1}{2}}-(1-\nu_{i,j})f_{i-3/2}]/(2\Delta\xi^3) \}$$

$$c_8 = \{ + \nu_{i,j}B_2 f_i^2 f_{i+\frac{1}{2}}/(2\Delta\xi^3) \}$$

$$c_9 = \{ + \nu_{i,j}B_1 f_i f_{i+\frac{1}{2}}/\Delta\xi^2 \}$$

$$c_{10} = \{ + f_i B_1[(2\nu_{i,j}-1)f_{i-\frac{1}{2}}-(1-\nu_{i,j})f_{i-3/2}]/\Delta\xi^2 \}$$

$$c_{11} = \{ + g_j g_{j+\frac{1}{2}}/\Delta\eta^2 \}$$

$$c_{12} = \{ + g_j g_{j-\frac{1}{2}}/\Delta\eta^2 \}$$

$$c_{13} = \{ + (1-\nu_{i,j})B_1 f_i f_{i-3/2}/\Delta\xi^2 \}$$

(30)

For a fixed computational grid, the coefficients given by Eq.(30) are functions only of B_1 and B_2 which in turn are functions of M_∞. This fact is used later when differentiating Eq.(29) with respect to M_∞ in order to obtain the right hand side $(\partial R/\partial M_\infty)$.

At this stage, it is necessary to consider the treatment of various types of grid points and examine the effect on the general residual expression. As can been seen from the distribution of points on the computational domain, Fig.2, several groups of points need special treatment as a result of applying various types of boundary conditions. Accordingly, it is necessary to revise the residual expression at these boundary points to include the boundary conditions.

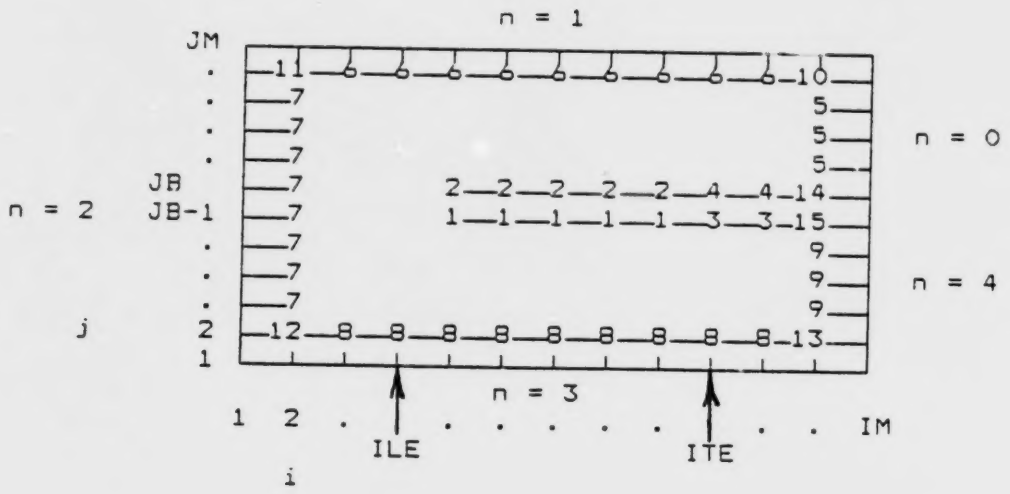

Fig.2 Various Types of Grid Boundary Points

In the following, each group of boundary points (see Fig.2) is denoted by a number and their corresponding revision is specified. It is to be noticed that applying the infinity boundary condition, Eq.(5), gives rise to two sets of updates for groups [5] thru [15]. The first corresponds to a subsonic free stream (i.e. if $M_\infty<1$), whereas the second set corresponds to a supersonic free stream (i.e. if $M_\infty>1$).

Points	Replace	By
[1] ILE<i<ITE, j=JB-1	$\varphi_{i,j+1}$	$\varphi_{i,j} + \Delta\eta(y'_1-\alpha)/g_{j+\frac{1}{2}}$
[2] ILE<i<ITE, j=JB	$\varphi_{i,j-1}$	$\varphi_{i,j} - \Delta\eta(y'_u-\alpha)/g_{j-\frac{1}{2}}$
[3] ITE≤i≤IM-2, j=JB-1	$\varphi_{i,j+1}$	$\varphi_{i,j+1} - \Gamma$
[4] ITE≤i≤IM-2, j=JB	$\varphi_{i,j-1}$	$\varphi_{i,j-1} + \Gamma$
For a subsonic free-stream,		
[5] i=IM-1, JB<j≤JM-2	$\varphi_{i+1,j}$	0
[6] 3≤i≤IM-2, j=JM-1	$\varphi_{i,j+1}$	$-\Gamma/4$
[7] i=2, 3≤j≤JM-2	$\varphi_{i-1,j}$	$-\Gamma/2$
[8] 3≤i≤IM-2, j=2	$\varphi_{i,j-1}$	$-3\Gamma/4$
[9] i=IM-1, 3≤j≤JB-1	$\varphi_{i+1,j}$	$-\Gamma$
[10] i=IM-1, j=JM-1	$\varphi_{i+1,j}$	0
	$\varphi_{i,j+1}$	$-\Gamma/4$

[11] i-2, j-JM-1	$\varphi_{i,j+1}$	$-\Gamma/4$
	$\varphi_{i-1,j}$	$-\Gamma/2$
[12] i-2, j-2	$\varphi_{i-1,j}$	$-\Gamma/2$
	$\varphi_{i,j-1}$	$-3\Gamma/4$
[13] i-IM-1, j-2	$\varphi_{i,j-1}$	$-3\Gamma/4$
	$\varphi_{i+1,j}$	$-\Gamma$
[14] i-IM-1, j-JB	$\varphi_{i+1,j}$	0
	$\varphi_{i,j-1}$	$\varphi_{i,j-1} + \Gamma$
[15] i-IM-1, j-JB-1	$\varphi_{i+1,j}$	$-\Gamma$
	$\varphi_{i,j+1}$	$\varphi_{i,j+1} - \Gamma$

For a supersonic free-stream,

[5] i-IM-1, JB<j≤JM-2	$\varphi_{i+1,j}$	$\varphi_{i,j}$
[6] 3≤i≤IM-2, j-JM-1	$\varphi_{i,j+1}$	0
[7] i-2, 3≤j≤JM-2	$\varphi_{i-1,j}$	0
[8] 3≤i≤IM-2, j-2	$\varphi_{i,j-1}$	0
[9] i-IM-1, 3≤j≤JB-1	$\varphi_{i+1,j}$	$\varphi_{i,j}$
[10] i-IM-1, j-JM-1	$\varphi_{i+1,j}$	$\varphi_{i,j}$
	$\varphi_{i,j+1}$	0
[11] i-2, j-JM-1	$\varphi_{i,j+1}$	0
	$\varphi_{i-1,j}$	0
[12] i-2, j-2	$\varphi_{i-1,j}$	0
	$\varphi_{i,j-1}$	0

[13] i-IM-1, j-2	$\varphi_{i,j-1}$	0
	$\varphi_{i+1,j}$	$\varphi_{i,j}$
[14] i-IM-1, j-JB	$\varphi_{i+1,j}$	$\varphi_{i,j}$
	$\varphi_{i,j-1}$	$\varphi_{i,j-1} + \Gamma$
[15] i-IM-1, j-JB-1	$\varphi_{i+1,j}$	$\varphi_{i,j}$
	$\varphi_{i,j+1}$	$\varphi_{i,j+1} - \Gamma$

The above updates are used to modify the residual equation, Eq.(29), and yield a set of expressions, each being valid for a group of boundary points. The details of these operations are shown in Appendix B.

In setting up the complete quasi-analytical problem the circulation and its dependence upon trailing edge potentials must be carefully included. Since the circulation is determined by the difference in potentials at the trailing edge,

$$\Gamma = \varphi_{uTE} - \varphi_{lTE} \tag{31}$$

or, by interpolating the trailing edge values

$$\begin{aligned}\Gamma = T_1 \, [\, & 1.5 \, (\varphi_{ITE-1,JB} - \varphi_{ITE-1,JB-1}) \\ & - 0.5 \, (\varphi_{ITE-1,JB+1} - \varphi_{ITE-1,JB-2}) \,] \\ + T_2 \, [\, & 1.5 \, (\varphi_{ITE,JB} - \varphi_{ITE,JB-1}) \\ & - 0.5 \, (\varphi_{ITE,JB+1} - \varphi_{ITE,JB-2}) \,]\end{aligned} \tag{32}$$

where

$$T_2 = [\, \xi(x-0.5) - \xi(ITE-1) \,] \, / \, \Delta\xi \tag{33}$$

$$T_1 = [\, 1 - T_2 \,] \tag{34}$$

and since a branch cut extends from the trailing edge to downstream infinity, the trailing edge potentials appear in the residual expressions at points adjacent to the outer boundaries. Consequently, the resultant matrix $(\partial R/\partial \varphi)$, while banded, also contains many nonzero elements far from the central band. Notice that the presence of these elements greatly complicates the rapid and efficient solution of the sensitivity equation, Eq.(1), which will be explained later.

Assembling $(\partial R/\partial \varphi)$ and $(\partial R/\partial XD_i)$

The residual expressions obtained from the previous step are differentiated analytically with respect to the potential (φ). To be more specific, each equation is differentiated with respect to the potential at neighboring points and trailing edge points (the later enters as a result of the implicit nature of the circulation effects). These points are denoted by the counters (ii,jj) and are given by,

(i,j-1), (i,j), (i,j+1), (i-2,j), (i-1,j), (i+1,j),
(ITE-1,JB-2), (ITE-1,JB-1), (ITE-1,JB), (ITE-1,JB+1),
(ITE,JB-2), (ITE,JB-1), (ITE,JB), (ITE,JB+1).

The end result is that the coefficient matrix $(\partial R_{i,j}/\partial \varphi_{ii,jj})$ is of size (IM-2)*(JM-2)x(IM-2)*(JM-2).

Again, the details and results of this step are shown in Appendix B. Once these relations are obtained, the actual coefficients are assembled by evaluating the appropriate analytical expresssions using a flowfield solution obtained from Eq.(2) for a given set of conditions (i.e. about a fixed design point).

Similarly, the right hand side is evaluated by differentiating the analytical expressions for the residual (see Appendix B) with respect to each design variable.

Solution by Gauss-Seidel

For a general (IM*JM) grid, the system given by Eq.(1) is of size (IM-2)*(JM-2)x(IM-2)*(JM-2). This system is large, of block structure, and sparse; and, as mentioned earlier while banded, also contains many nonzero elements far from the central band. As a result of this size and structure, and since the primary objective of this study is to establish the feasibility of the quasi-analytical method, it was obvious that a reasonably efficient scheme for solving Eq.(1) was needed and that an elimination technique, while straightforward, would be too time consuming. Consequently, the results presented in this thesis have been obtained using a Gauss-Seidel iterative

scheme[9]. This scheme has not been optimized for speed (through the choice of optimum acceleration parameters) but uses sparse matrix technology in processing only the nonzero elements; and, therefore, it is considerably faster and more efficient (with regard to storage requirements) than elimination methods.

In handling the sparsity pattern, the symbolic assembly of the coefficient matrix is performed only once for a given grid size and given free-stream (subsonic versus supersonic). The resultant structure is then stored on a diskfile. Before the numerical part is executed, the symbolic information is read into the code and used directly to assemble the new matrix. This procedure is followed in order to reduce the time consumed in assembling the coefficient matrix.

Once the sensitivities of the potentials, and thus the Cp distribution, to the design variables are known, the sensitivity of the lift coefficients to the design variables can be easily computed. To minimize errors, these coefficients are computed using

$$C_L = 2\Gamma = 2\,(\varphi_{uTE}-\varphi_{lTE}) \tag{35}$$

and hence,

$$\partial C_L/\partial XD = 2\,(\partial\varphi_{uTE}/\partial XD_i-\partial\varphi_{lTE}/\partial XD_i) \tag{36}$$

TEST CASES

In this study, the quasi-analytical method has been used to determine the aerodynamic sensitivity coefficients at three freestream Mach numbers (.2, .8, and 1.2) for two arbitrarily selected airfoils, each at one degree angle of attack. The first is a cambered parabolic arc section having 1% camber at 40% chord, a maximum thickness of 6% at 50% chord, and which is designated P1406; and the second is a NACA 1406 airfoil. Lift coefficients computed for these cases are shown in Table 1.

In the following, two types of results will be presented. The first will be plots of Cp versus chord for the three chosen Mach numbers and two airfoil sections. The second will be the corresponding plots of $(\partial Cp/\partial T)$, $(\partial Cp/\partial M_\infty)$, $(\partial Cp/\partial \alpha)$, $(\partial Cp/\partial C)$, and $(\partial Cp/\partial L)$ obtained by the quasi-analytical method. In addition, all of the figures will also contain results obtained using the direct (finite difference) approach in which each design variable was individually perturbed by a small amount, typically 0.001, and a new flowfield solution obtained. Then the sensitivities were computed using $\Delta Cp/\Delta XD$.

Finally, tables containing lift coefficients, lift coefficient sensitivity coefficients, and time comparisons are presented for all cases.

Table 1

Lift Coefficients

M_∞	P1406	NACA 1406
0.2	0.2066	0.2065
0.8	0.3827	0.3736
1.2	0.1024	0.0920

In all subsonic cases (M_∞ = 0.2, 0.8), an 81*20 stretched Cartesian grid was utilized. For the supersonic case (M_∞ = 1.2), a 41*20 grid was used. In addition, for these studies, the flowfield was normally computed using double precision arithmetic and the maximum residual reduced eight orders of magnitude. It was felt that this level of convergence was necessary in order to accurately evaluate sensitivity coefficients using a finite difference approach, although such convergence may not be required in the flowfield slover for the quasi-analytical method.

Notice also that in all cases the error tolerances used in the Gauss-Seidel solver for the coefficients involving maximum thickness, free stream Mach number, and location of maximum camber were 1.E-06 while those on angle of attack and maximum camber were 1.E-04.

RESULTS AND DISCUSSION

Accuracy of the Quasi-Analytical Method

In order to verify the accuracy of the quasi-analytical method, design sensitivity coefficients for Cp and C_L were obtained using the finite difference approach. In this procedure, a single design variable was perturbed by typically 0.001, while all others remained constant, and a new flowfield solution obtained using the approximate factorization solver. Then values of the various sensitivity coefficients were obtained by finite differences. The results obtained in this manner for the pressure distributions have been shown on all figures by dashed lines, and in many cases the dashed lines are coincident with the quasi-analytical results (solid lines). In addition, Table 2 compares results obtained by the two methods at Mach numbers 0.2, 0.8, and 1.2. In most cases the agreement is within significantly less than 1%.

Subsonic Cases (M_∞ = 0.2)

P1406 Airfoil: Initial studies concentrated on subsonic cases since such cases should run quickly and since at least approximate results would be known from thin airfoil theory. Figure 3 shows the pressure distribution for the P1406 airfoil while Figs.4a and 4b show the sensitivity of

Table 2

Accurary of Quasi-Analytical Method for Computing

Lift Coefficient Sensitivity Coefficients

P1406 Airfoil, Grid 81*20

XD_i	M_∞ = 0.2		M_∞ = 0.8		M_∞ = 1.2 *	
	QA	FD	QA	FD	QA	FD
T	0.0050	0.0053	1.1208	1.1177	-0.2505	-0.2476
M_∞	0.0472	0.0476	1.4556	1.4690	-0.1259	-0.1252
α	6.1075	6.1383	10.6667	10.7742	5.0899	5.0920
C	9.9140	9.9434	20.5295	20.4958	1.3152	1.3279
L	0.0692	0.0697	0.1647	0.1663	-0.1121	-0.1114

NACA 1406 Airfoil, Grid 81*20

XD_i	M_∞ = 0.2		M_∞ = 0.8		M_∞ = 1.2 *	
	QA	FD	QA	FD	QA	FD
T	0.0044	0.0044	0.5433	0.5231	-0.3322	-0.3305
M_∞	0.0466	0.0471	0.9891	0.9708	-0.0803	-0.0802
α	6.1077	6.1386	10.3861	10.5227	4.5982	4.5983
C	9.9086	9.9380	18.4786	19.5767	1.3495	1.3769
L	0.0690	0.0696	0.1482	0.1499	-0.0304	-0.0301

* Executed on Grid 41*20

QA Quasi-Analytical

FD Finite Differece

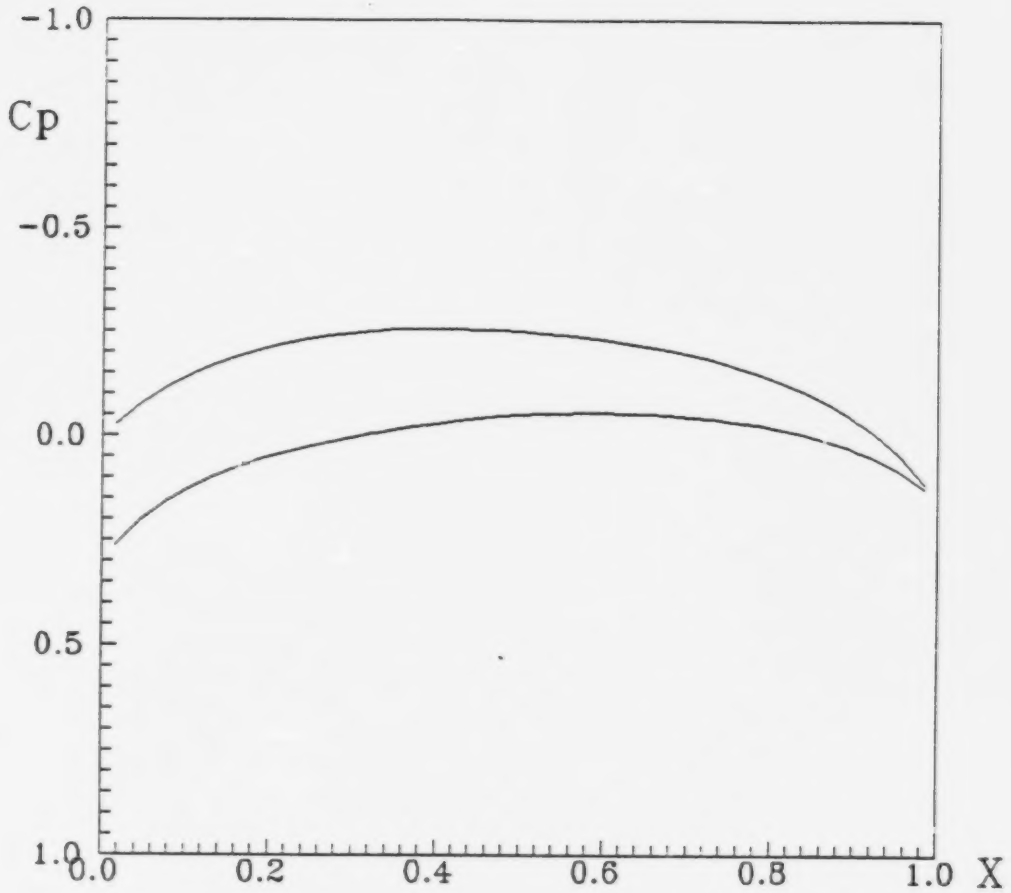

Fig.3 Pressure Distribution,

P1406 Airfoil, M_∞ = 0.2, α = 1 °

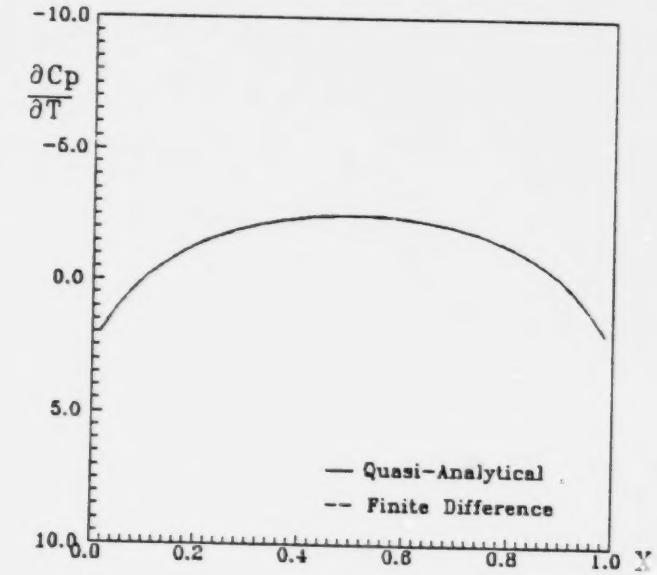

(a)

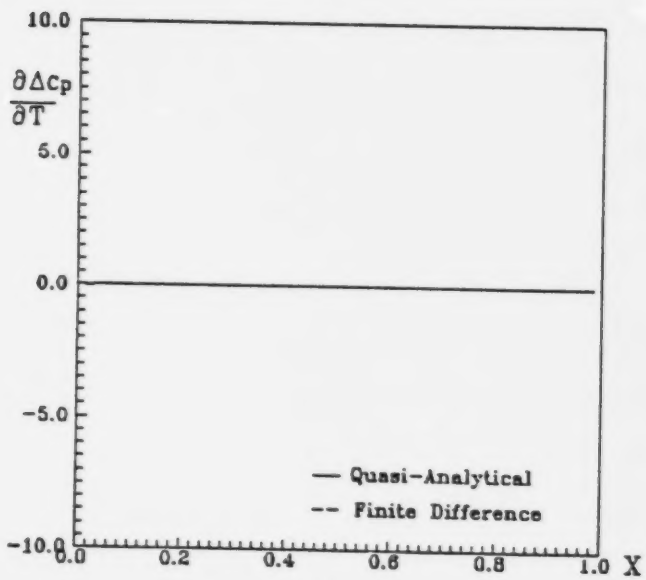

(b)

Fig.4 Sensitivity of Pressure to Maximum Thickness, P1406 Airfoil, $M_\infty = 0.2$, $\alpha = 1°$

the pressure to thickness for the same airfoil. As expected from thin airfoil theory, the upper and lower surface values are essentially identical and the difference is very small everywhere. Also shown on the same figure (and on subsequent figures) by the dashed line is the result obtained by using the finite difference approach; and as can be seen, the agreement betweeen the two approaches is excellent.

The sensitivity of pressure to freestream Mach number is plotted on Figs.5a and 5b. It is noticed that while the profiles for the upper and lower surfaces are similar, they are not equal in magnitude, indicating a nonlinear variation with Mach number as predicted by simple Prandtl-Glauret Theory. However, as indicated by the results on Fig.5b, the magnitudes for this subsonic Mach number are very low.

The sensitivity of the pressure coefficients to angle of attack are shown for this case on Figs.6a and 6b. As expected from linear thin airfoil theory, the upper and lower surface curves are essentially equal in magnitude but of opposite sign. Not surprisingly, the sensitivity of the delta Cp variation, Fig.6b, has the shape of the pressure difference curve for a flat plate at angle of

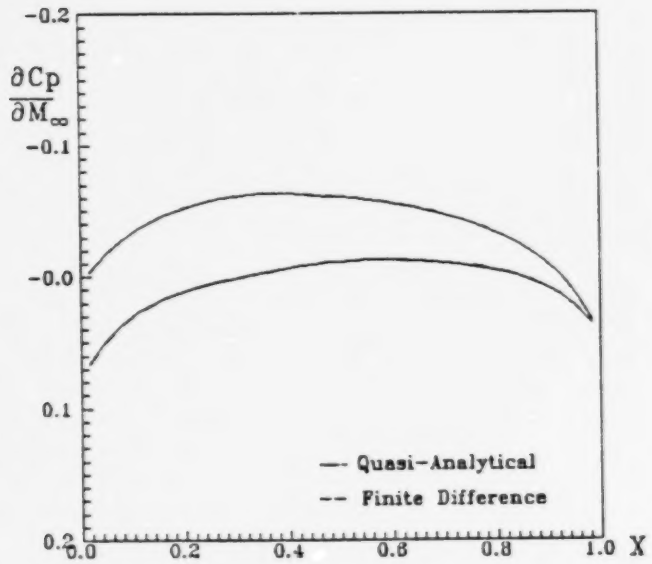

(a)

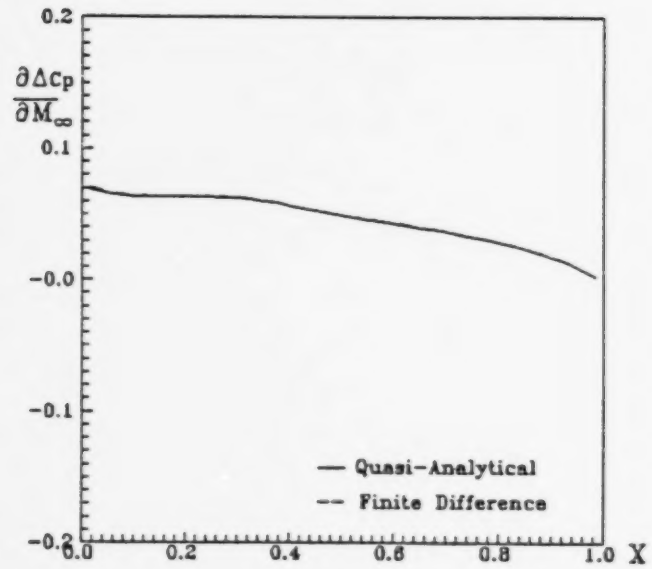

(b)

Fig.5 Sensitivity of Pressure to Mach Number, P1406 Airfoil, M_∞ = 0.2, α = 1 °

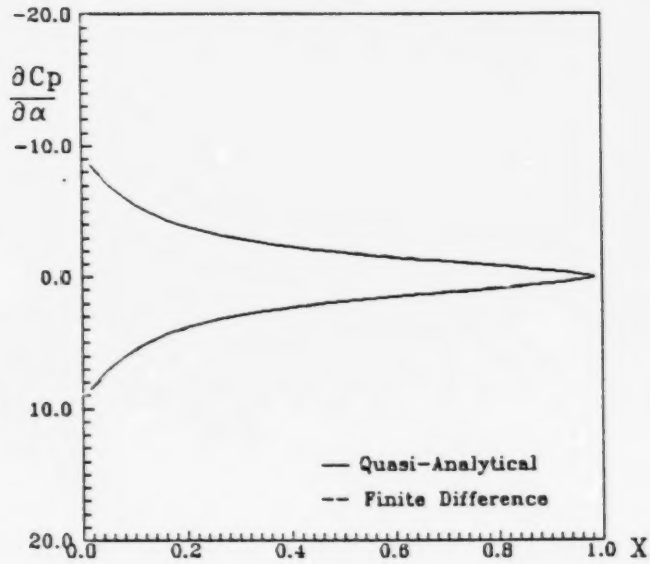

(a)

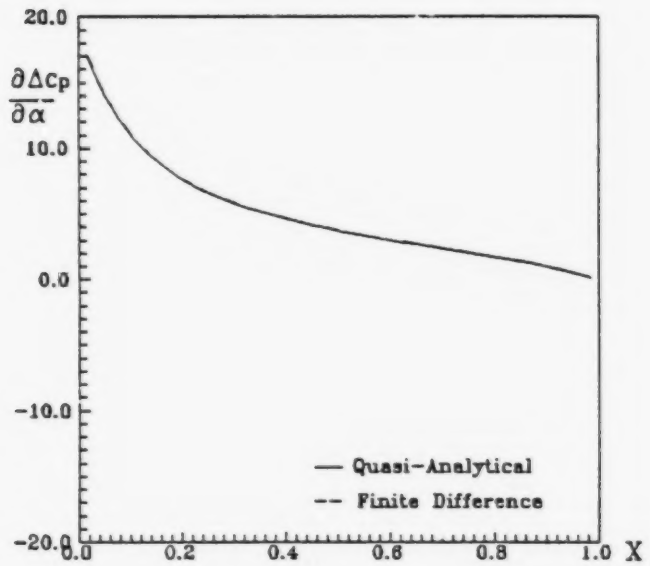

(b)

Fig.6 Sensitivity of Pressure to Angle of Attack, P1406 Airfoil, $M_\infty = 0.2$, $\alpha = 1°$

attack; and its magnitude, particularly near the leading edge is quite large.

On Figs.7a and 7b is plotted the sensitivity of the pressure coefficient to the amount of maximum camber. Since camber contributes to lift, it is expected from thin airfoil theory that these values should be "equal but opposite in sign" for the upper and lower surfaces. In addition, the pressure difference curve has the correct shape for that associated with a 14 mean line with the peak occuring at 30% chord[7] and has magnitude comparable to those for the $(\partial Cp/\partial \alpha)$ curves.

Finally, the sensitivity of pressure to the location of the maximum camber point is portrayed on Figs.8a and 8b, and to say the least the results are interesting. Since maximum camber location affects the camber profile and hence lift, the equal and opposite behavior of the upper and lower surface coefficients is expected. In addition, the pressure difference sensitivity is primarily negative forward of the point of maximum camber and positive aft of it. This result indicates that if the location of maximum camber were moved rearward slightly (i.e. a positive ΔL) that lift would be decreased on the forward portion of the airfoil and increased on the aft portion of the airfoil, which is in agreement with the results presented in Ref.7.

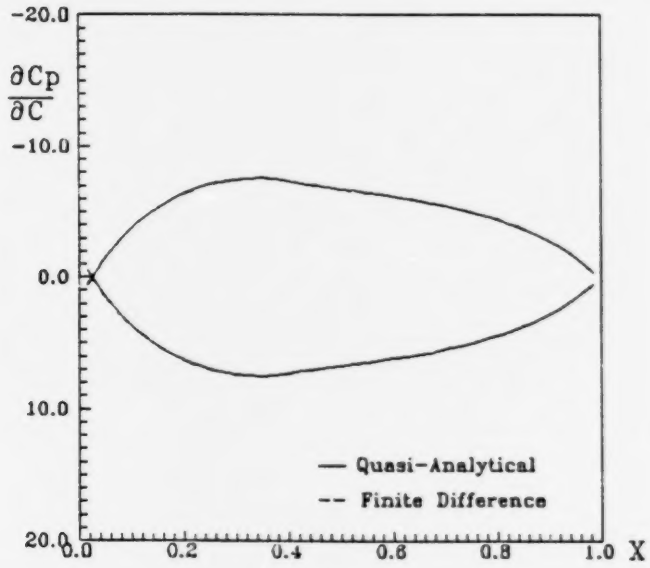

(a)

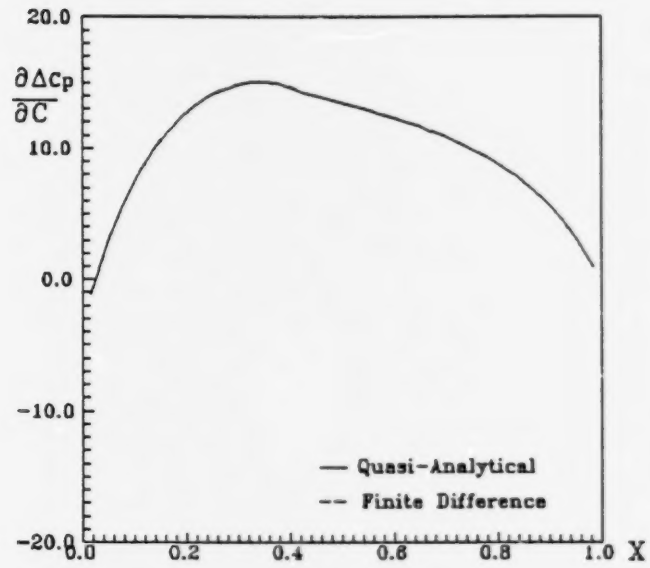

(b)

Fig.7 Sensitivity of Pressure to Maximum Camber, P1406 Airfoil, M_∞ = 0.2, α = 1 °

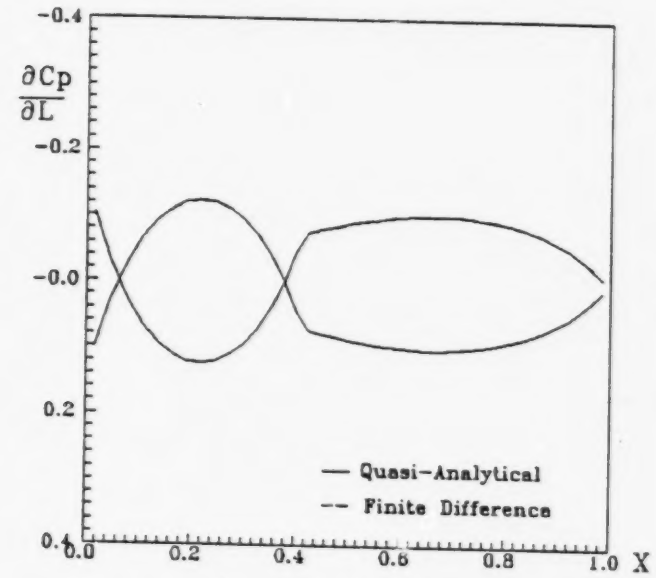

(a)

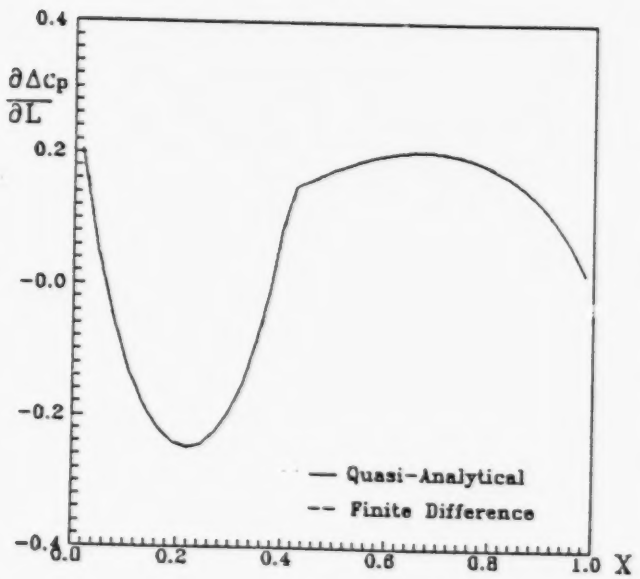

(b)

Fig.8 Sensitivity of Pressure to Location of Maximum Camber, P1406 Airfoil, $M_\infty = 0.2$, $\alpha = 1°$

NACA 1406 Airfoil: Figure 9 shows the pressure distribution for the NACA1406 airfoil at $M_\infty = 0.2$, and it should be noted that it is different than that obtained for the P1406 airfoil. This difference is basically due to the different thickness distributions describing each profile. Figs.10 to 14 show for the NACA 1406 airfoil the sensitivity of ΔCp with position for each of the five design variables. Since the NACA 1406 and the parabolic P1406 both have the same camber line and since for this low Mach number and thin airfoils the solutions should essentially be linear, the sensitivity to maximum camber and location of maximum camber should be essentially identical for the two airfoils. As can be seen by comparing Figs.7 with 13 and 8 with 14, the present quasi-analytiacl method does indeed yield this result. Likewise, the sensitivity to angle of attack, Figs.6 and 12, are also identical for the two airfoils.

However, the pressure sensitivity to thickness, Fig. 10, and freestream Mach number, Fig.11, while very small in magnitude compared to the other coefficients, have a different chordwise variation than that for the P1406 airfoil. The first, of course, is expected since the two airfoils have different thickness distributions; and the second is due to the fact that the two airfoils have

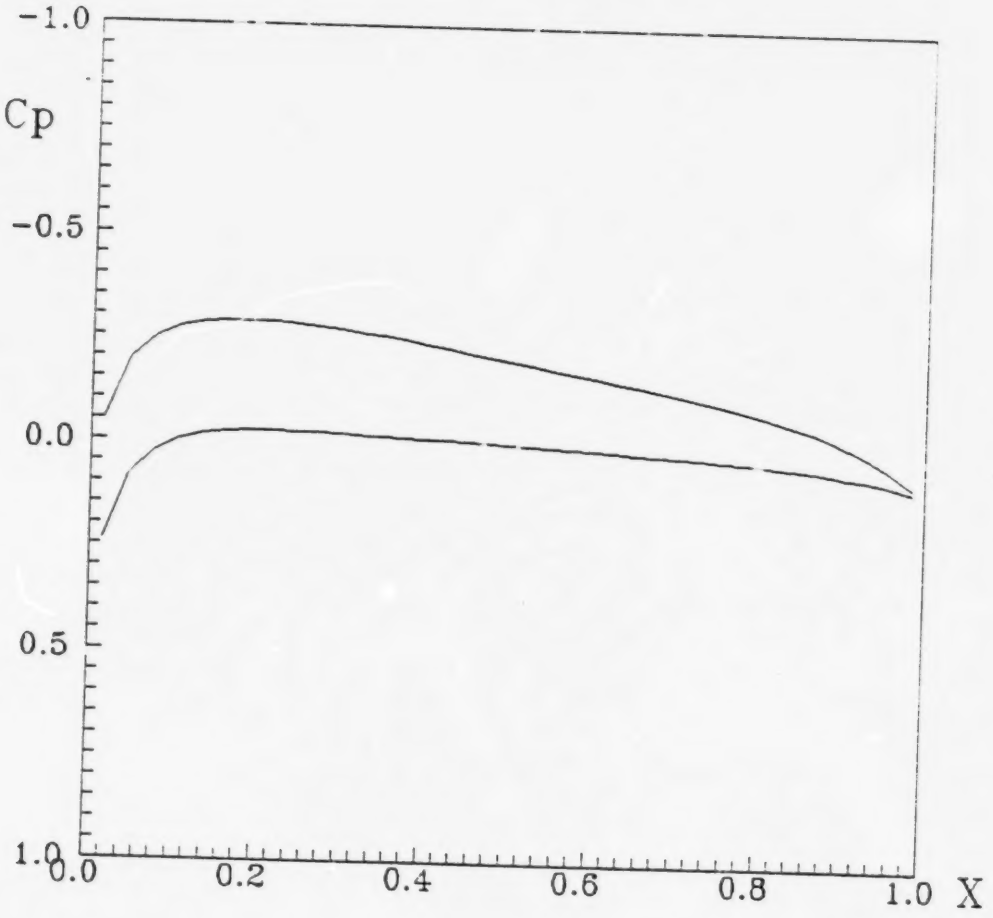

Fig.9 Pressure Distribution,

NACA 1406 Airfoil, $M_\infty = 0.2$, $\alpha = 1°$

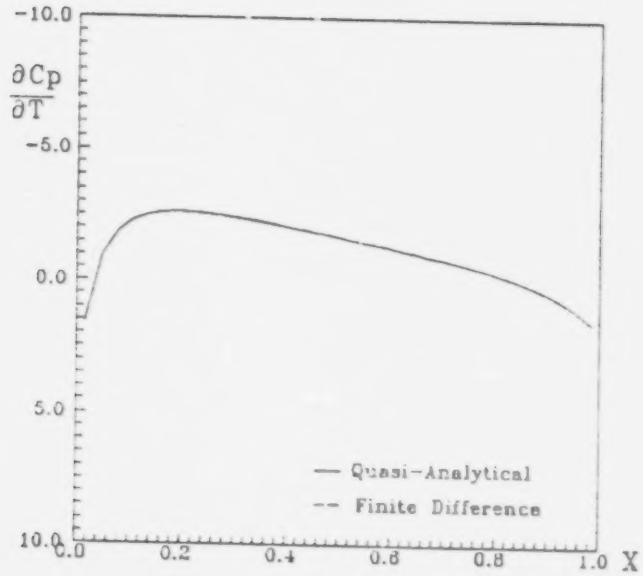

(a)

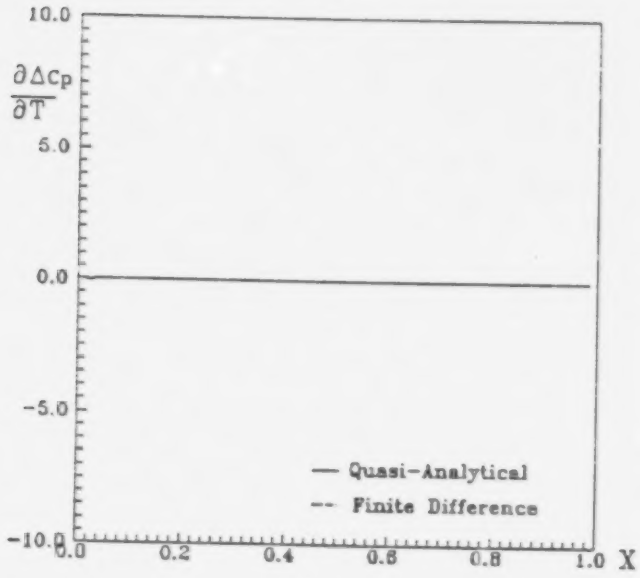

(b)

Fig.10 Sensitivity of Pressure to Maximum Thickness, NACA 1406 Airfoil, $M_\infty = 0.2$, $\alpha = 1°$

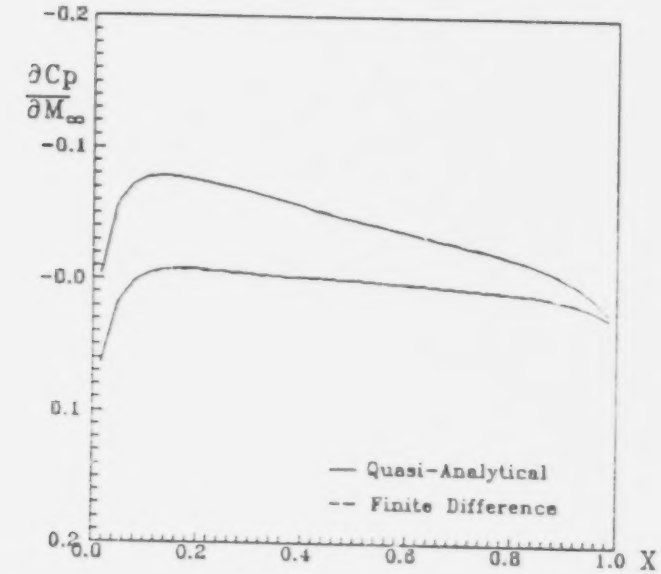

(a)

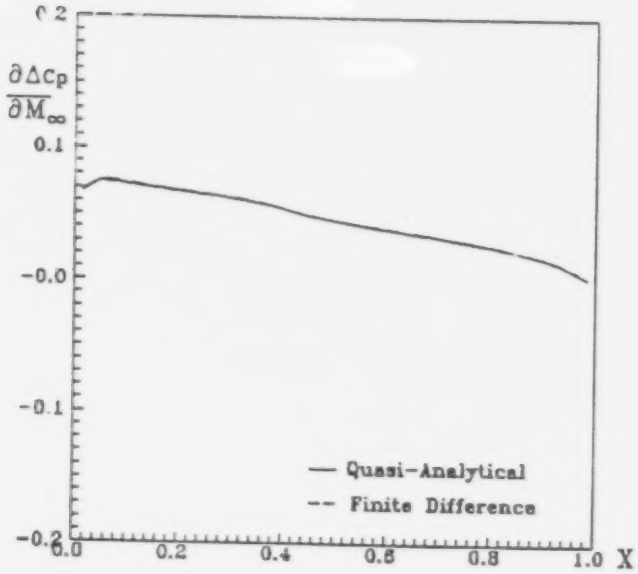

(b)

Fig.11 Sensitivity of Pressure to Mach Number, NACA 1406 Airfoil, $M_\infty = 0.2$, $\alpha = 1°$

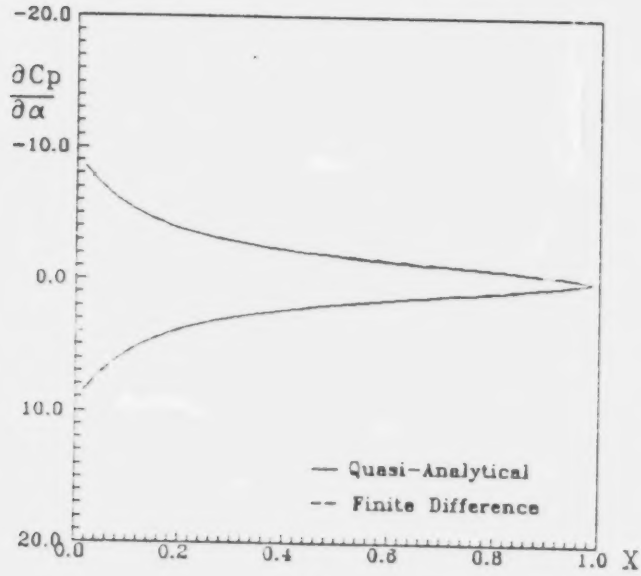

(a)

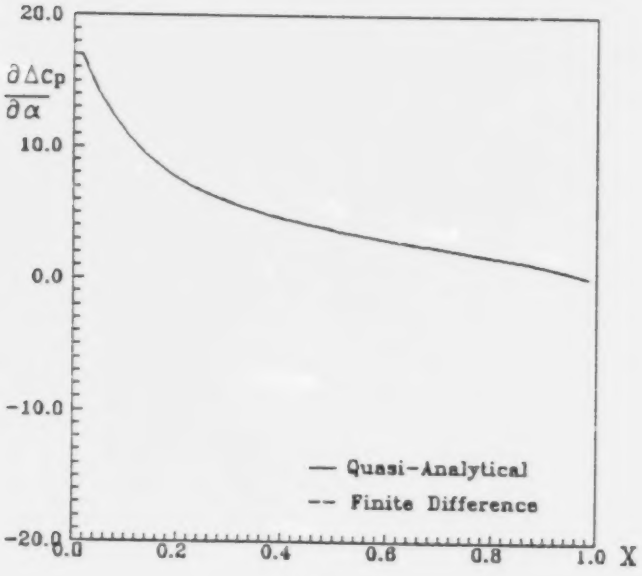

(b)

Fig.12 Sensitivity of Pressure to Angle of Attack, NACA 1406 Airfoil, $M_\infty = 0.2$, $\alpha = 1°$

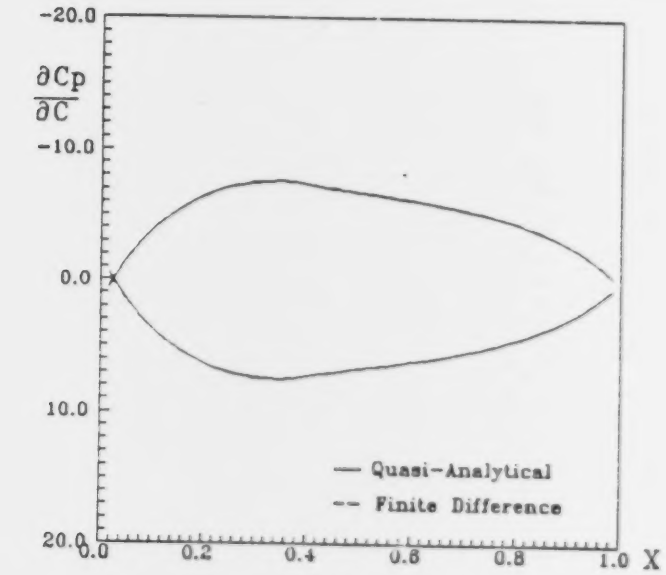

(a)

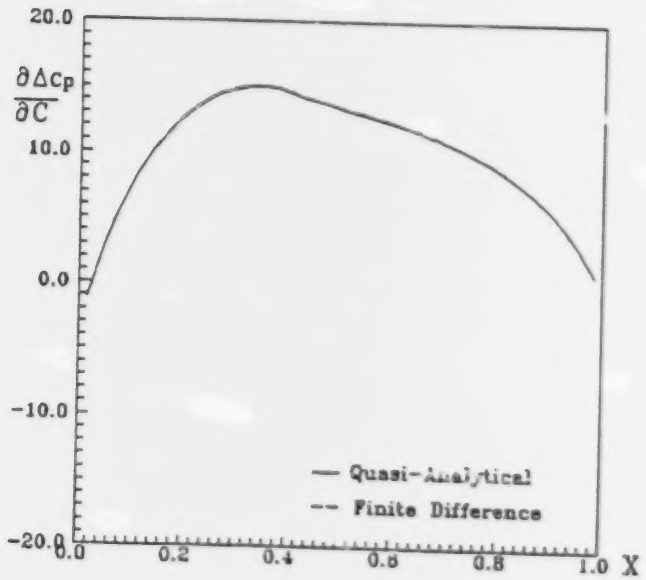

(b)

Fig.13 Sensitivity of Pressure to Maximum Camber, NACA 1406 Airfoil, $M_\infty = 0.2$, $\alpha = 1°$

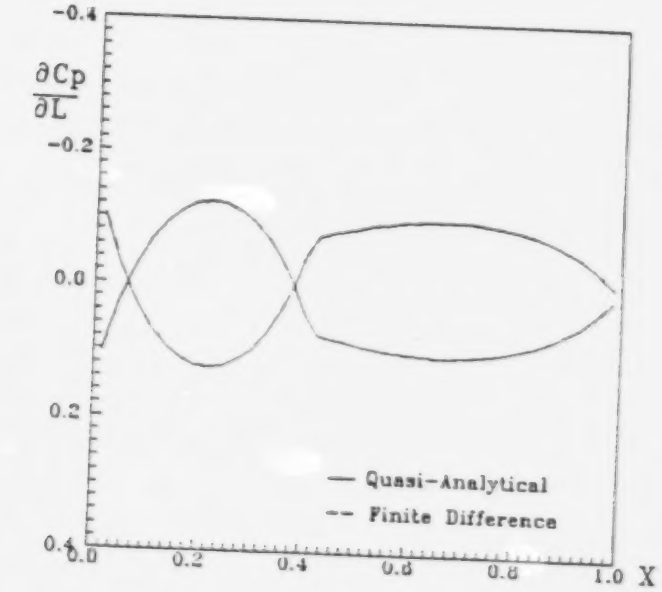

(a)

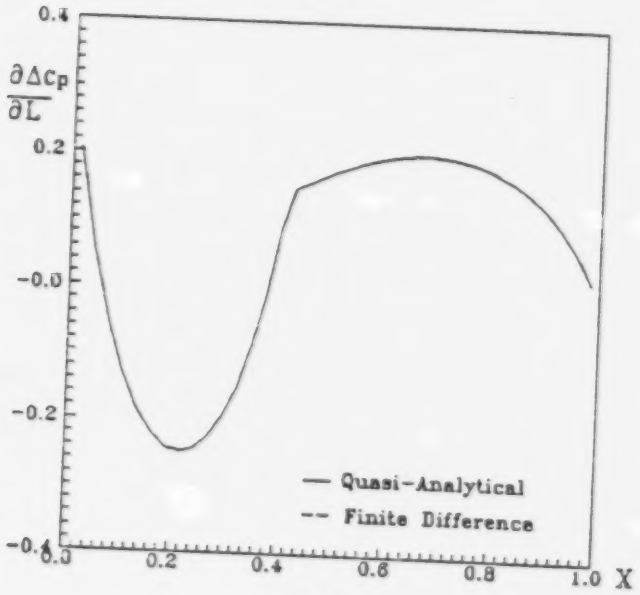

(b)

Fig.14 Sensitivity of Pressure to Location of Maximum Camber, NACA 1406 Airfoil, $M_\infty = 0.2$, $\alpha = 1°$

entirely different pressure distributions and, thus, sensitivity to Mach number.

The sensitivity of the lift coefficients to the design variables were shown in Table 2. It should be noticed that for the subsonic case that the lift sensitivities for the two airfoils are essentially identical. Since these airfoils are thin and since they have the same camber line, such agreement should exist.

Transonic Cases (M_∞ = 0.8)

P1406 Airfoil: For this case, the cambered parabolic airfoil is slightly supercritical with a weak shock on the upper surface at about 55% chord, Fig.15; and the lower surface is entirely subcritical with the minimum pressure point ocurring at 60% chord. As a consequence, the variation with chord of the sensitivity coefficients is considerably different than in the subsonic case.

Figs.16a and 16b show the sensitivity of pressure to the maximum thickness; and while the lower surface profile is similar to that obtained at subsonic conditions, the upper surface curve and the pressure difference coefficient plot show the effect of the upper surface shock wave. The large peak on the curves corresponds to the location of the shock wave and indicates that the

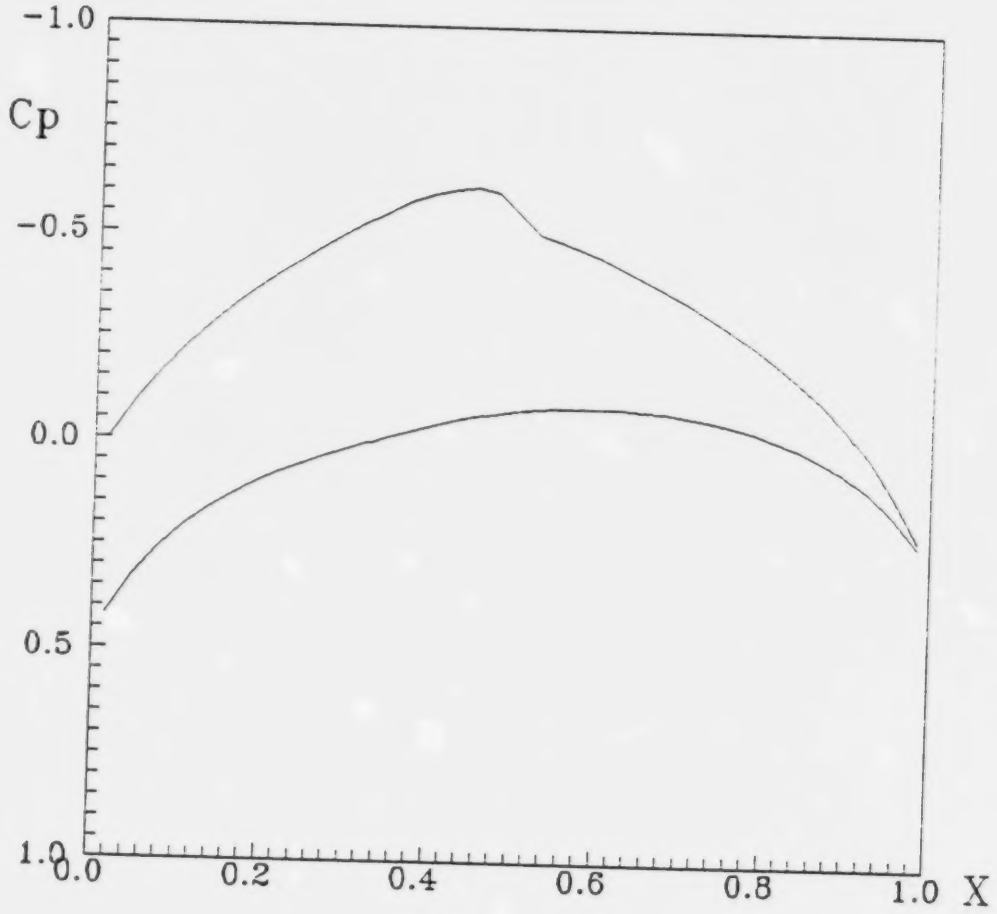

Fig.15 Pressure Distribution,

P1406 Airfoil, $M_\infty = 0.8$, $\alpha = 1°$

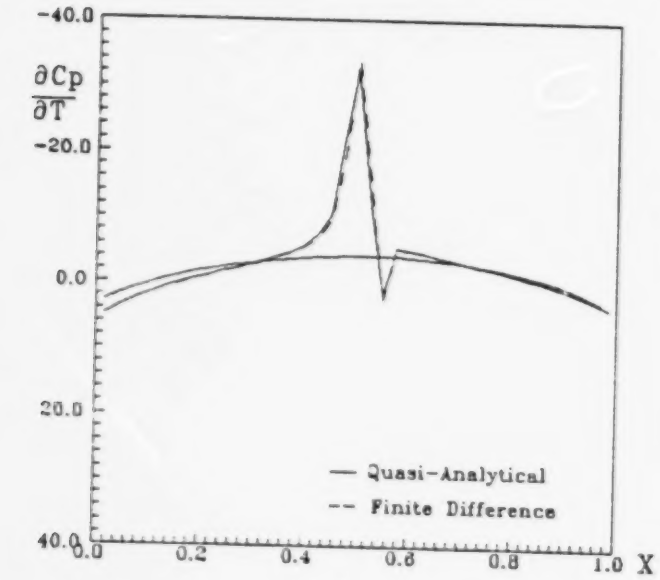

(a)

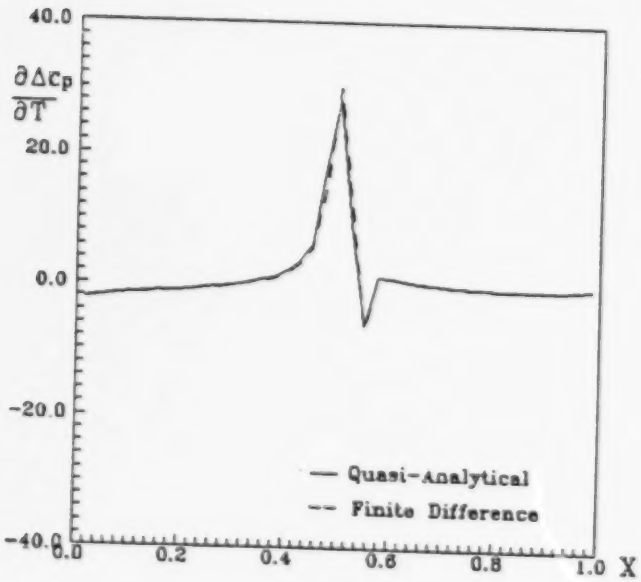

(b)

Fig.16 Sensitivity of Pressure to Maximum Thickness, P1406 Airfoil, $M_\infty = 0.8$, $\alpha = 1°$

shock wave location is very sensitive to maximum thickness. Notice on Figs.16a and 16b the excellent agreement of the quasi-analytical results indicated by the solid lines with those obtained using the finite-differece approach (dashed lines).

The results for $(\partial Cp/\partial M_\infty)$, which are shown on Figs.17a and 17b, are similar. The lower surface curve is typical of a subsonic flow, while the upper surface and the pressure difference coefficients reflect the presence of the upper surface shock wave. Similar comments can be made for the remaining design variable coeficients, which are plotted on Figs.18, 19, and 20.

Examination of the curves in the vicinity of the shock wave location indicates that the pressure sensitivity and indirectly the shock wave location is about equally influenced by the maximum thickness, freestream Mach number, and angle of attack.

However, in comparison it is relatively insensitive to location of maximum camber; but, perhaps surprisingly so, the pressure is twice as sensitive to the amount of maximum camber as it is to the other design variables.

NACA 1406: At $M_\infty = 0.8$, the flow about the NACA 1406 airfoil has a strong shock at 40% chord, Fig.21. As a

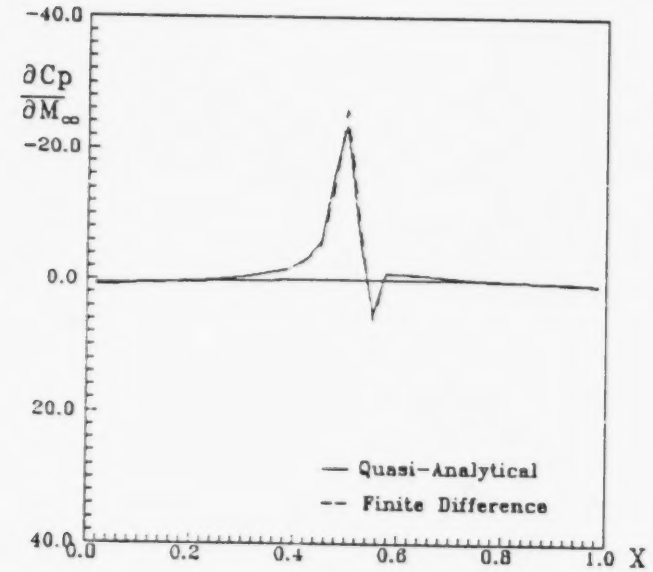

(a)

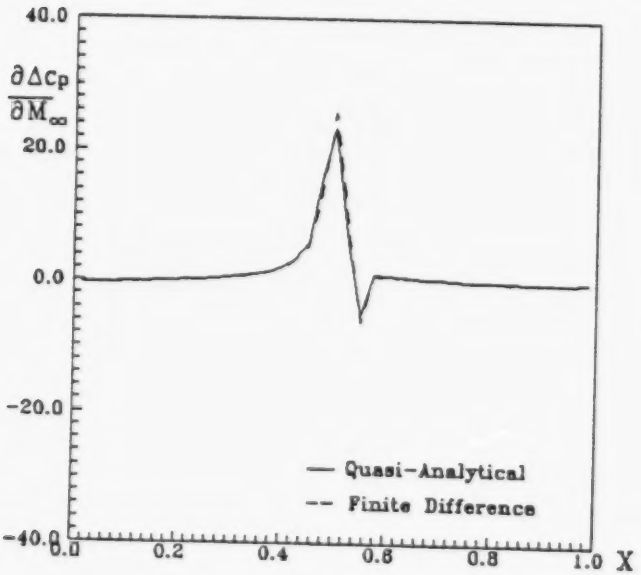

(b)

Fig.17 Sensitivity of Pressure to Mach Number, P1406 Airfoil, $M_\infty = 0.8$, $\alpha = 1°$

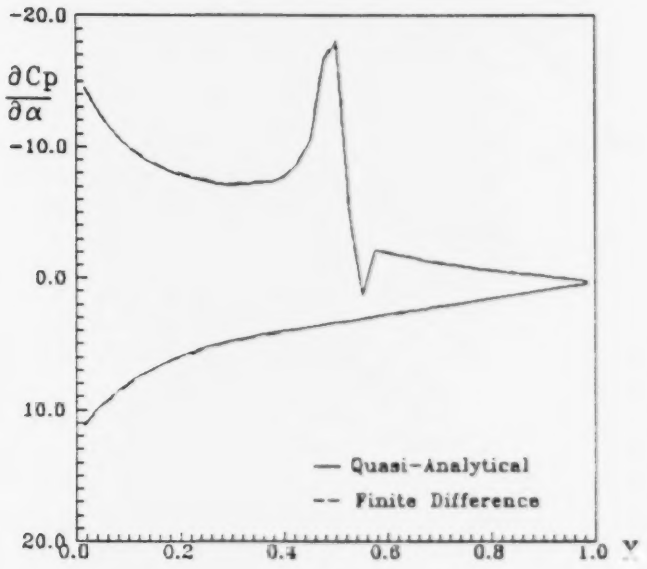

(a)

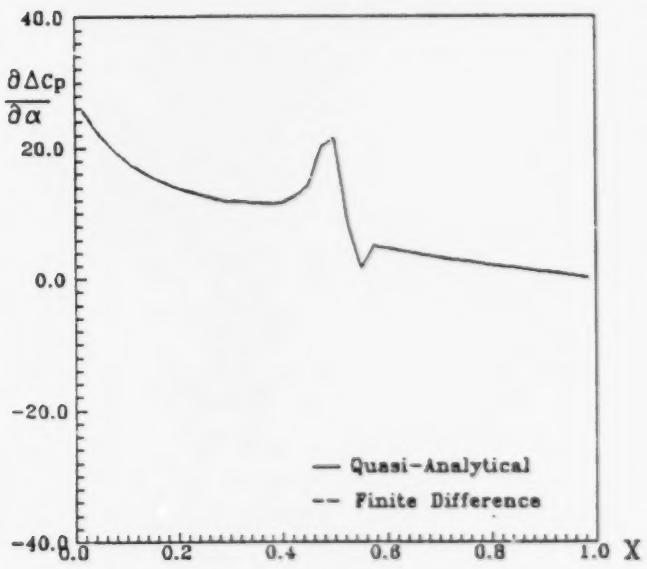

(b)

Fig.18 Sensitivity of Pressure to Angle of Attack, P1406 Airfoil, $M_\infty = 0.8$, $\alpha = 1°$

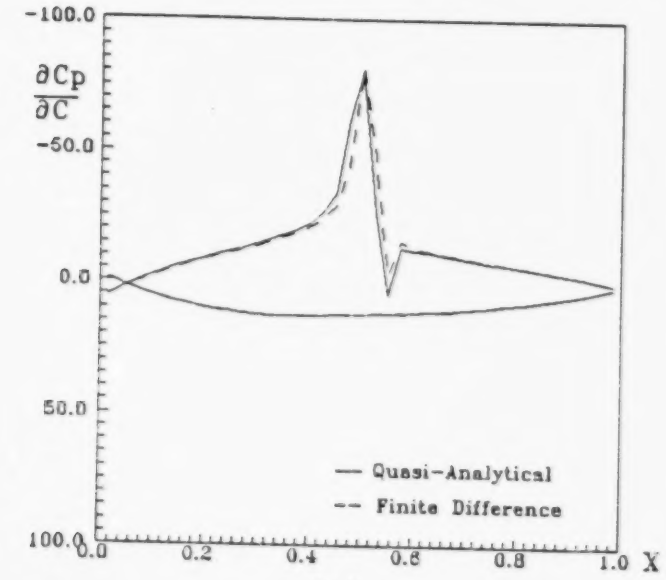

(a)

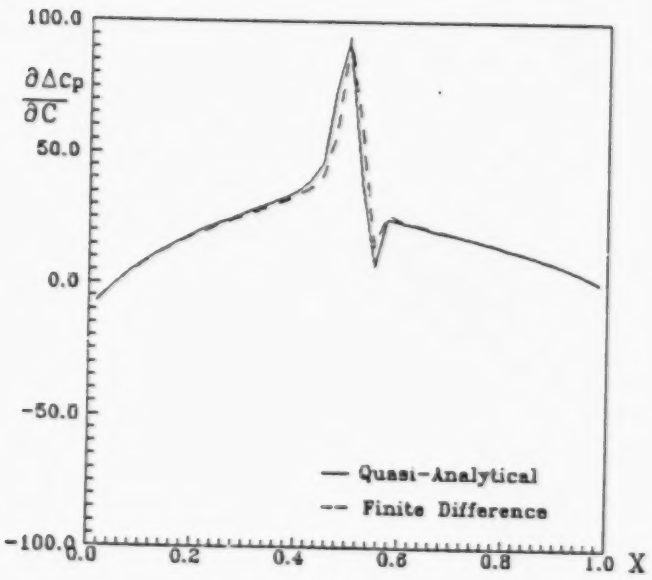

(b)

Fig.19 Sensitivity of Pressure to Maximum Camber, P1406 Airfoil, M_∞ = 0.8, α = 1 °

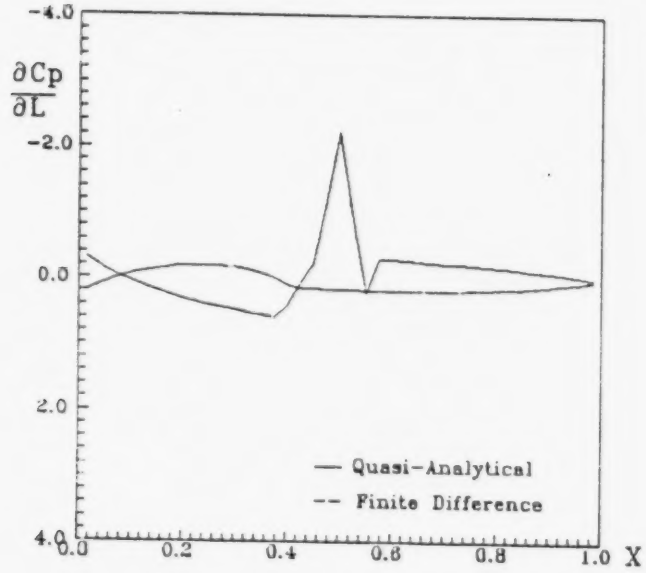

(a)

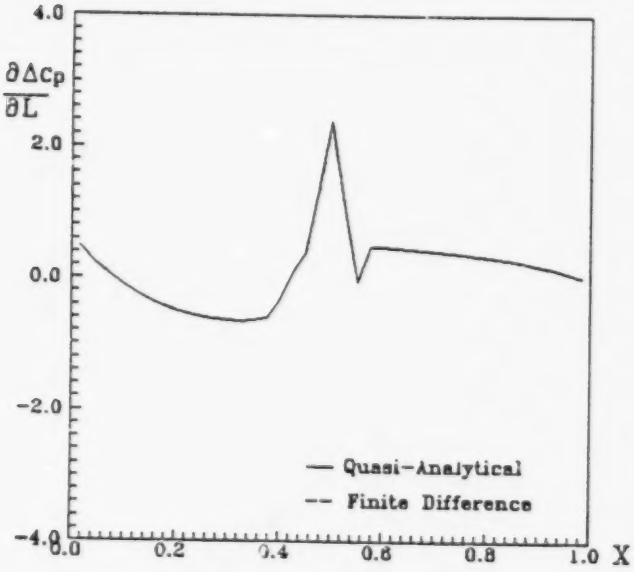

(b)

Fig.20 Sensitivity of Pressure to Location of Maximum Camber, P1406 Airfoil, $M_\infty = 0.8$, $\alpha = 1°$

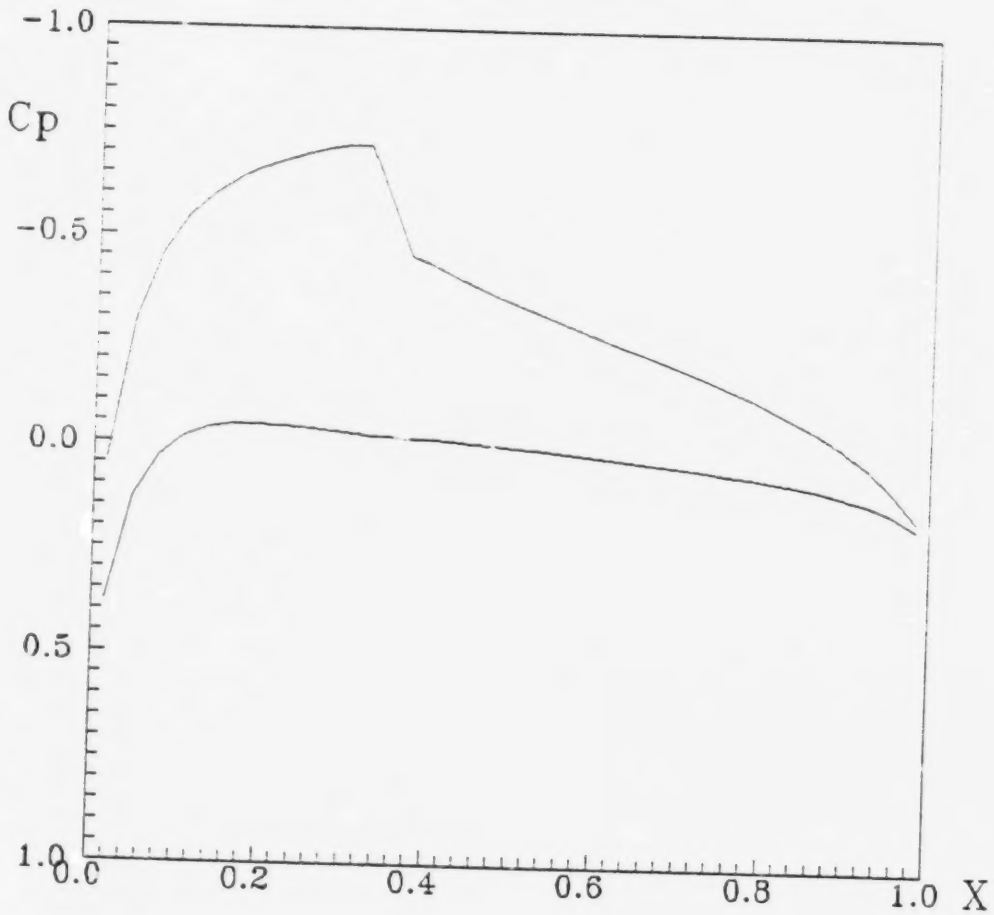

Fig.21 Pressure Distribution,

NACA 1406 Airfoil, M_∞ = 0.8, α = 1 °

result, the pressure design sensitivity coefficients, which are shown on Figs.22-26, have large peaks at the shock location. In addition, while the curves are similar to those obtained for the P1406 airfoil, they differ in details and some cases in magnitude. In particular, the peak value at the shock in the $\partial Cp/\partial\alpha$ curve for the NACA 1406 is significantly higher than that for the P1406 airfoil. Further, for the subsonic "linear" flow situation the sensitivity coefficients for angle of attack, maximum camber and location of maximum camber were identical for the two airfoils. However, at transonic conditions, the flow is highly nonlinear and the corresponding curves for the two airfoils are significantly different. Again the reasonable agreement between the quasi-analytical results (solid lines) and the finite difference results (dashed lines) is evident on the figures.

The sensitivity of lift to the design variables was also shown in Table 2 for both airfoils. While the values for the various design variables are similar in magnitude for the two airfoils, there are some significant differences. For example, the coefficients for maximum thickness differ by a factor of two between the two airfoils and those for Mach number differ by about fifty percent. Also, it should be noticed that for both airfoils

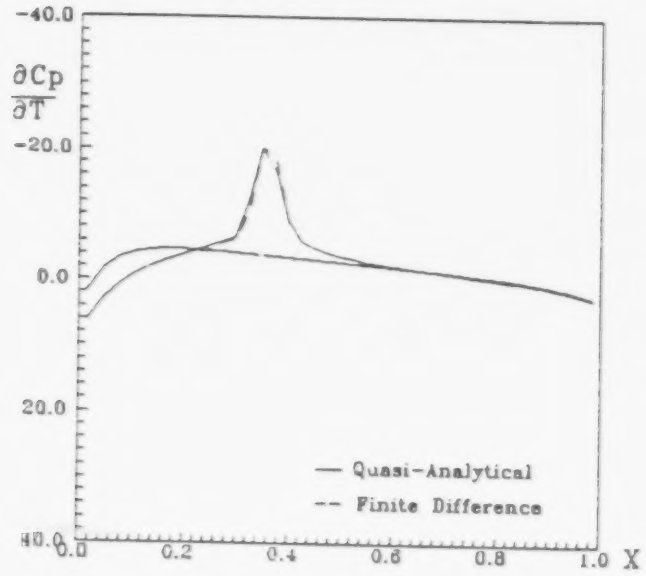

(a)

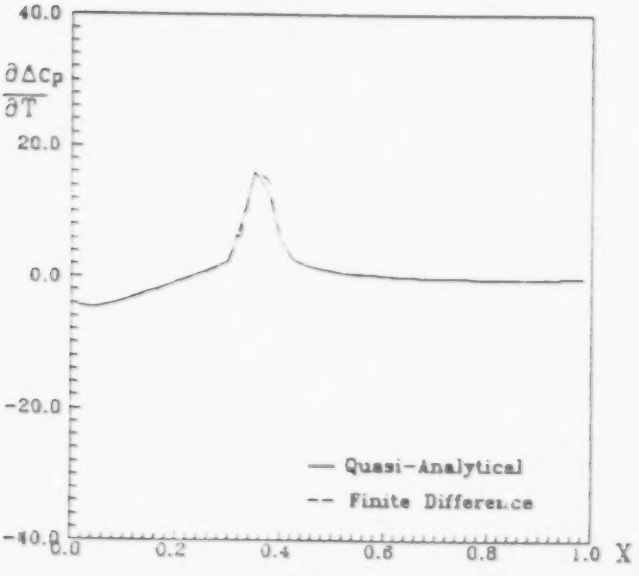

(b)

Fig.22 Sensitivity of Pressure to Maximum Thickness, NACA 1406 Airfoil, $M_\infty = 0.8$, $\alpha = 1°$

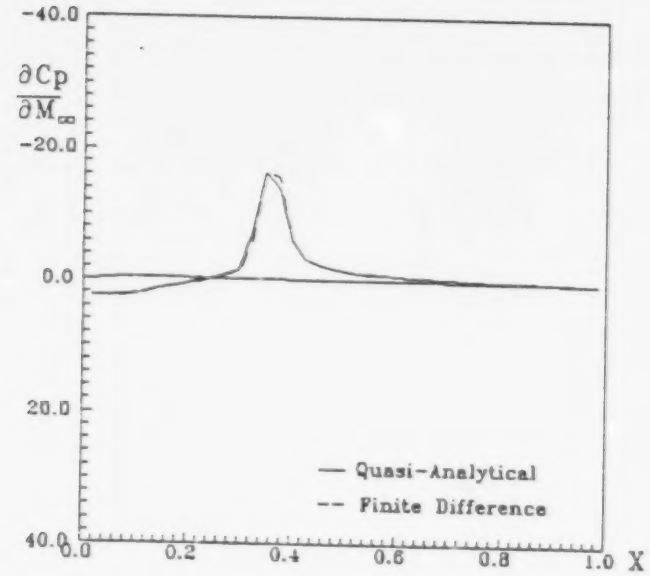

(a)

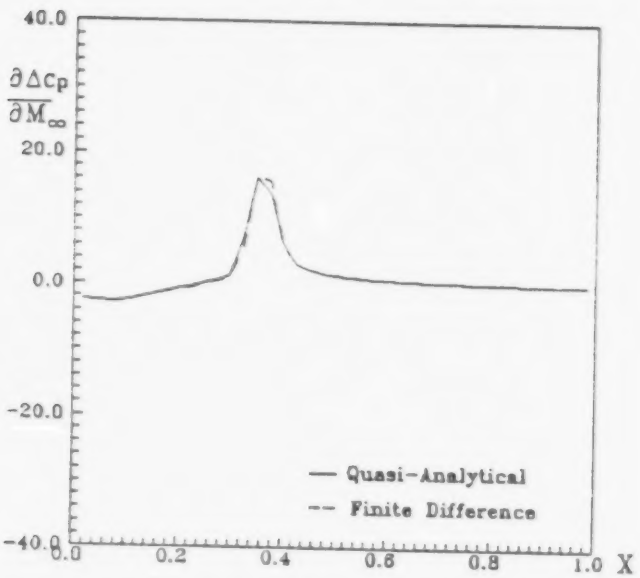

(b)

Fig.23 Sensitivity of Pressure to Mach Number

NACA 1406 Airfoil, $M_\infty = 0.8$, $\alpha = 1°$

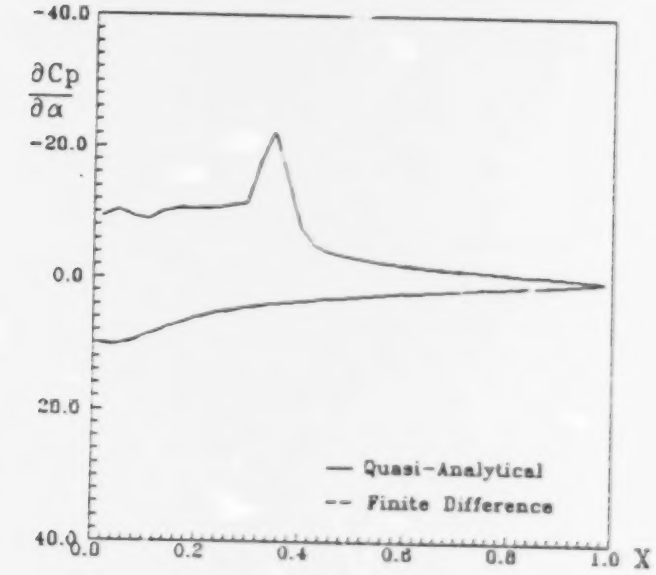

(a)

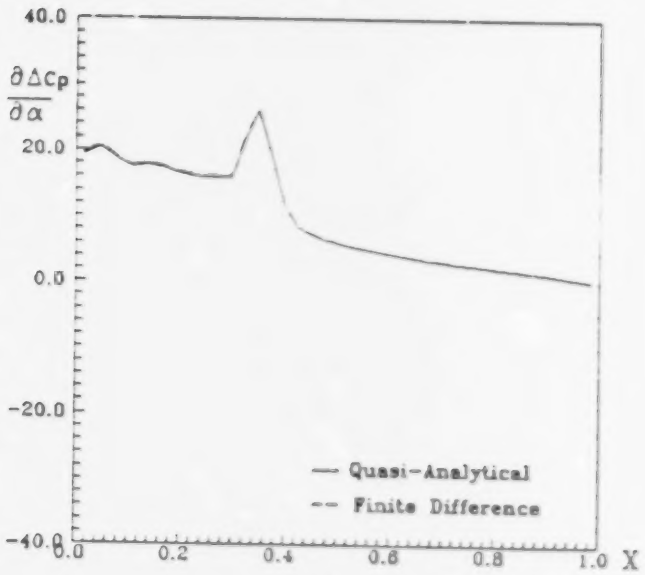

(b)

Fig.24 Sensitivity of Pressure to Angle of Attack, NACA 1406 Airfoil, $M_\infty = 0.8$, $\alpha = 1°$

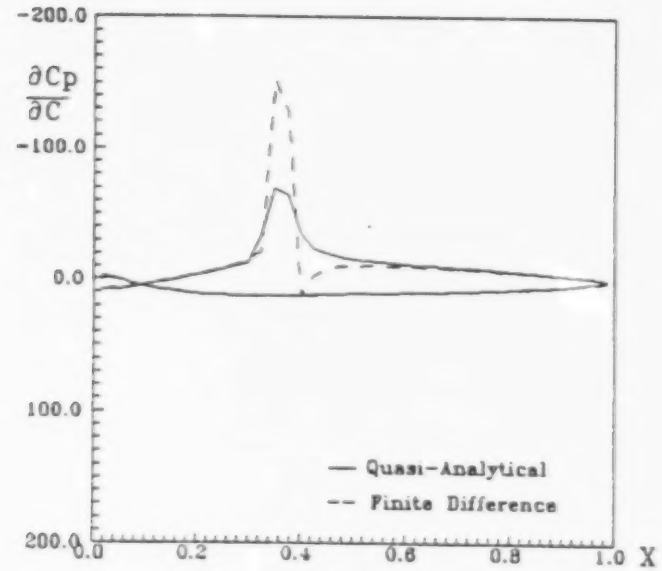

(a)

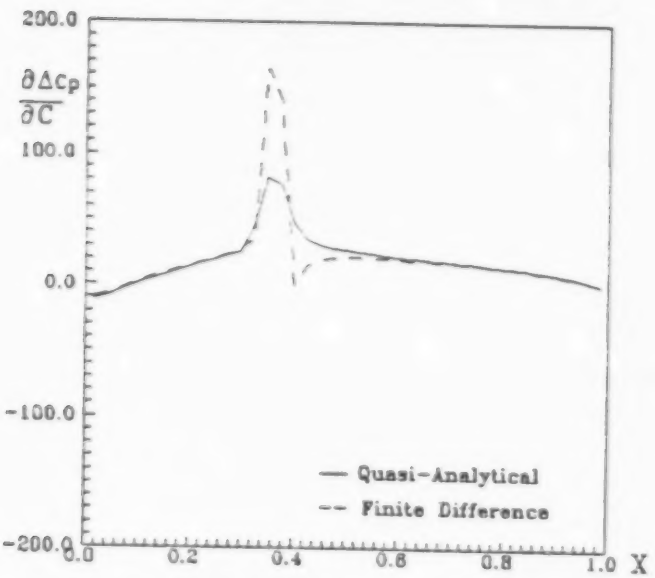

(b)

Fig.25 Sensitivity of Pressure to Maximum Camber, NACA 1406 Airfoil, $M_\infty = 0.8$, $\alpha = 1°$

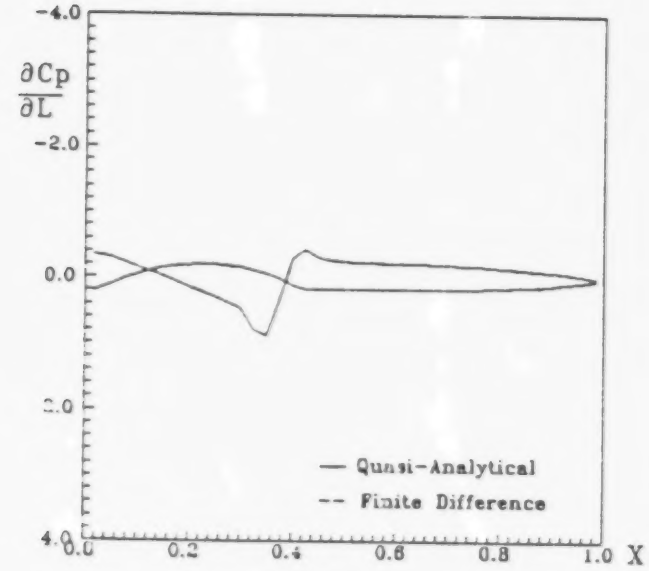

(a)

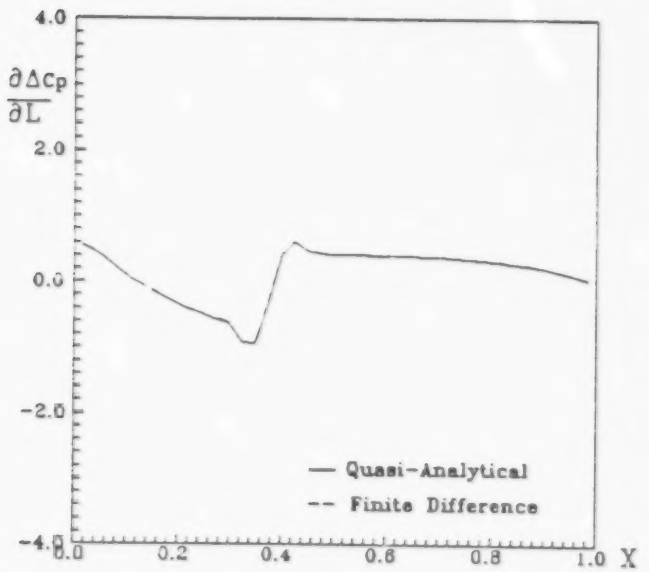

(b)

Fig.26 Sensitivity of Pressure to Location of Maximum Camber, NACA 1406 Airfoil, M_∞ = 0.8, α = 1 °

the lift is most sensitive to angle of attack and to maximum camber. In addition, Fig.25 shows a discrepancy between the results obtained by the direct approach and those obtained thru the quasi-analytical method. This discrepancy could be due to either the magnitude of the perturbation used to compute the sensitivities by the direct approach, or the tolerance values used in the stopping criteria of the Gauss-Seidel procedure.

C. Supersonic Cases (M_∞ = 1.2)

In order to investigate the applicability of the quasi-analytical method at supersonic freestream Mach numbers, solutions were obtained for the P1406 and the NACA 1406 airfoils at Mach 1.2. At this condition, the flow is transonic in that the bow shock is detached, and there is a region of subsonic flow extending to approximately the quarter chord, Figs.27 and 33. Figures 28-32 and 34-38 show the pressure sensitivities for these cases, and Table 2 listed the lift sensitivities. As mentioned earlier, notice that for these cases the solutions presented are for the 41*20 medium grid.

Examination of the plots shows that the pressure sensitivity coefficients have different trends and magnitudes from those computed for subsonic freestream

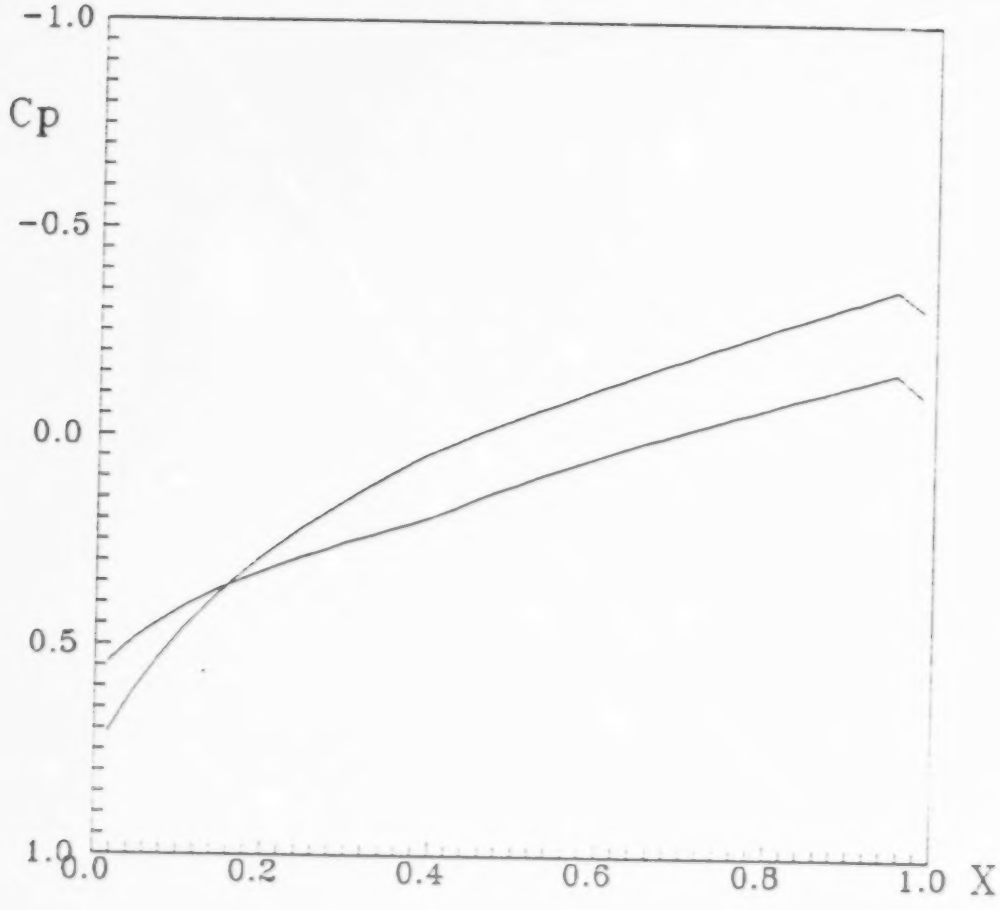

Fig.27 Pressure Distribution,

P1406 Airfoil, $M_\infty = 1.2$, $\alpha = 1°$

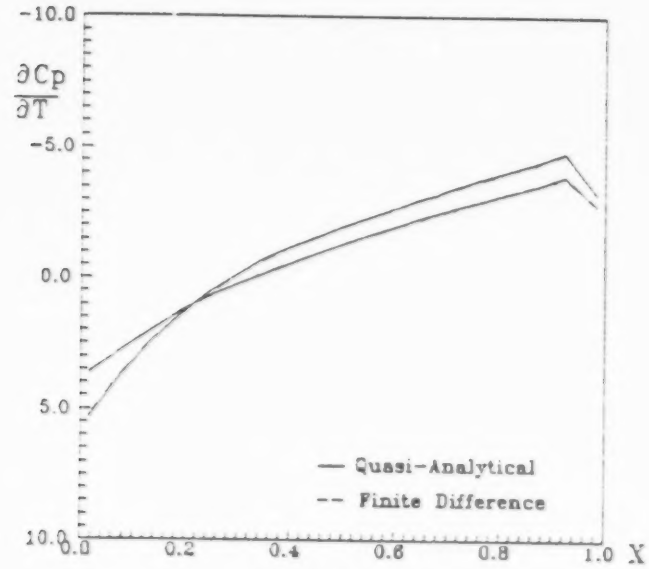

(a)

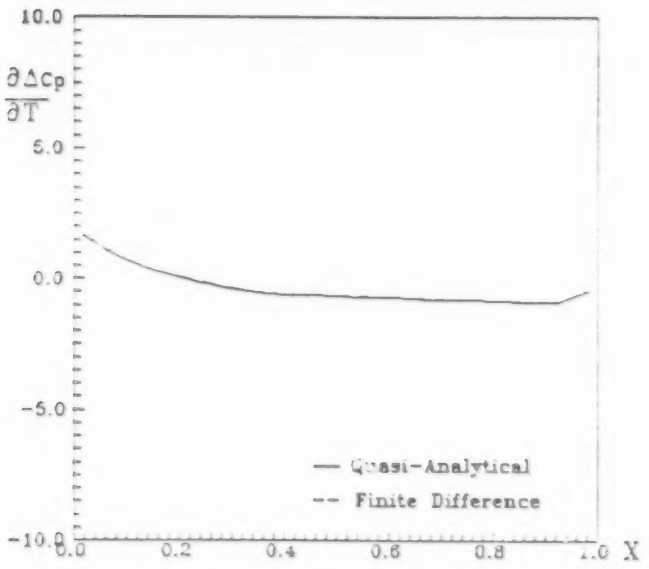

(b)

Fig.28 Sensitivity of Pressure to Maximum Thickness, P1406 Airfoil, $M_\infty = 1.2$, $\alpha = 1°$

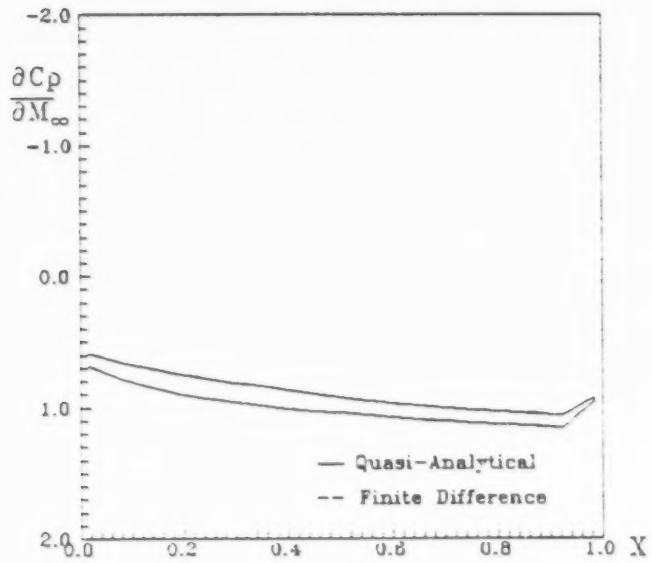

(a)

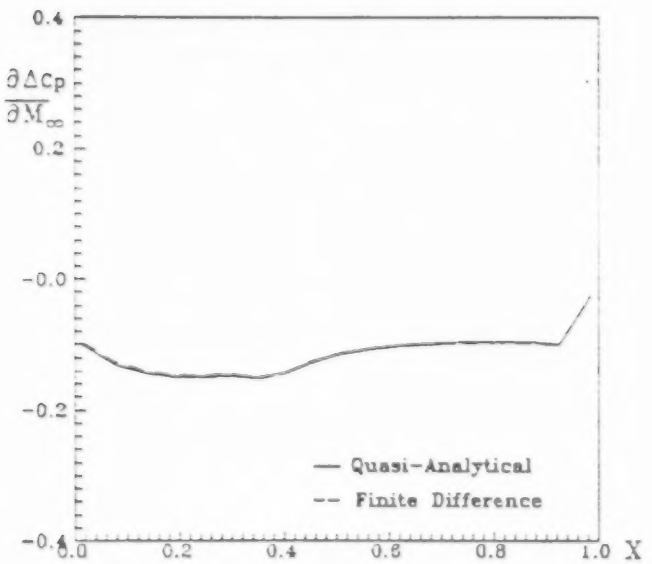

(b)

Fig.29 Sensitivity of Pressure to Mach Number, P1406 Airfoil, $M_\infty = 1.2$, $\alpha = 1°$

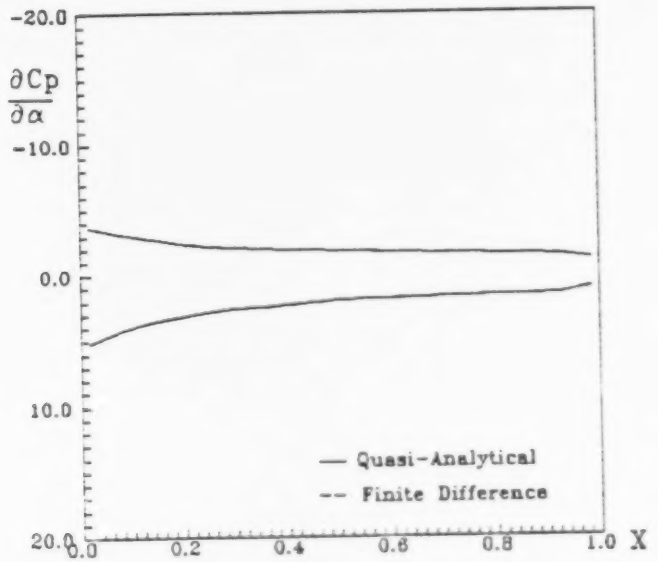

(a)

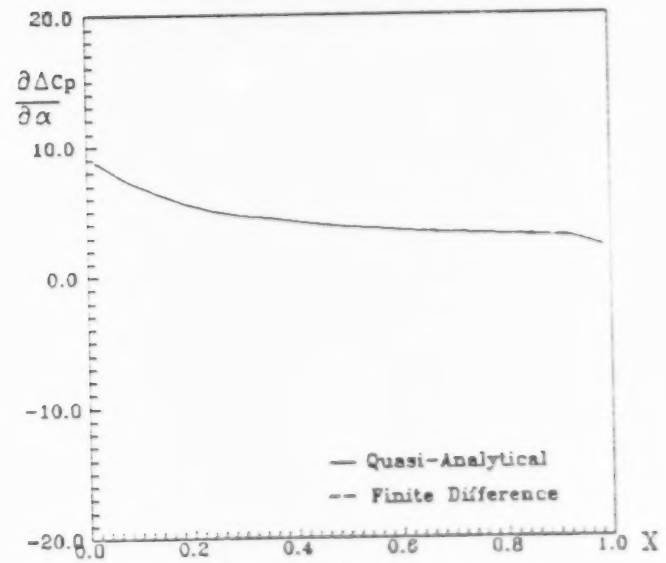

(b)

Fig 30 Sensitivity of Pressure to Angle of Attack, P1406 Airfoil, $M_\infty = 1.2$, $\alpha = 1°$

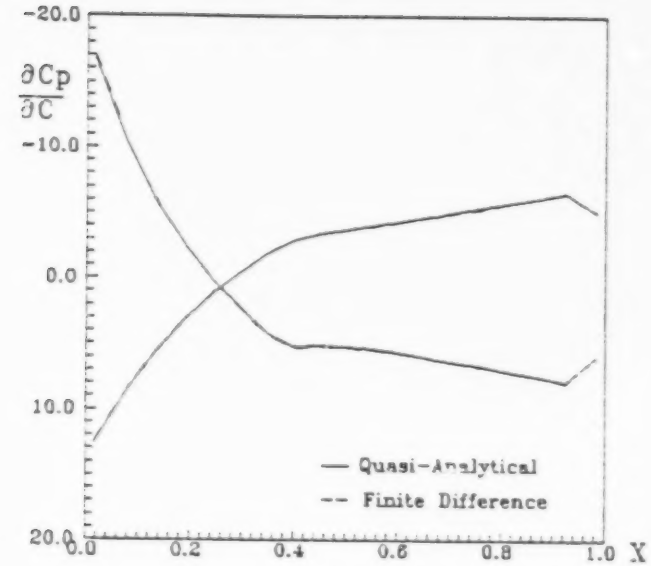

(a)

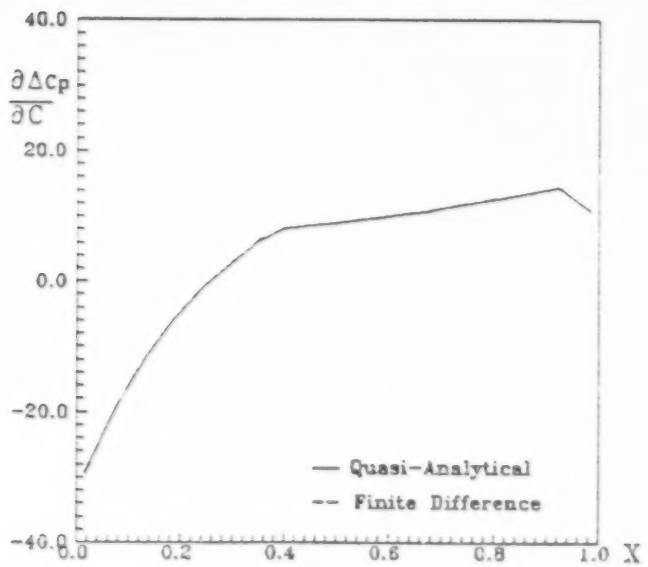

(b)

Fig.31 Sensitivity of Pressure to Maximum Camber, P1406 Airfoil, $M_\infty = 1.2$, $\alpha = 1°$

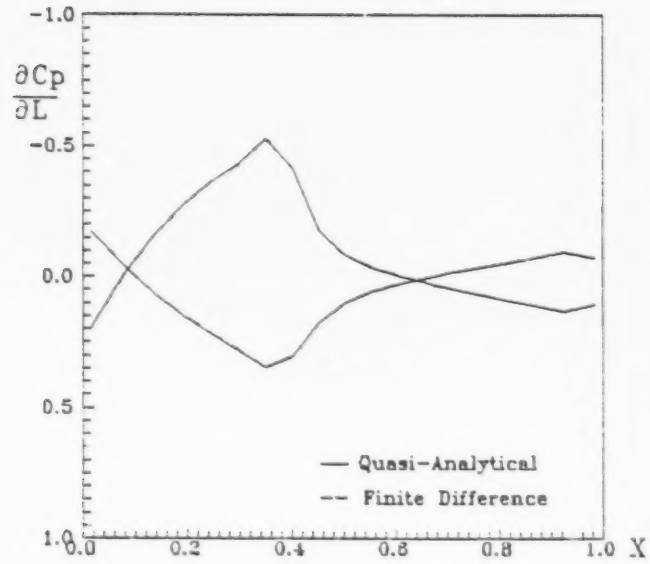

(a)

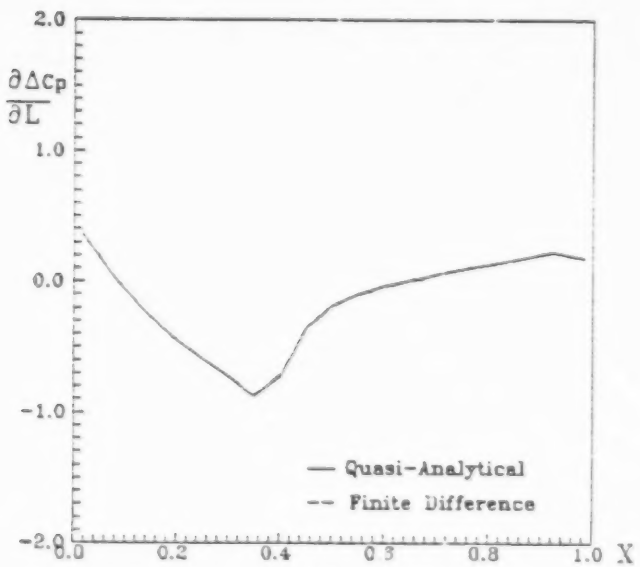

(b)

Fig.32 Sensitivity of Pressure to Location of Maximum Camber, P1406 Airfoil, M_∞ = 1.2 α = 1 °

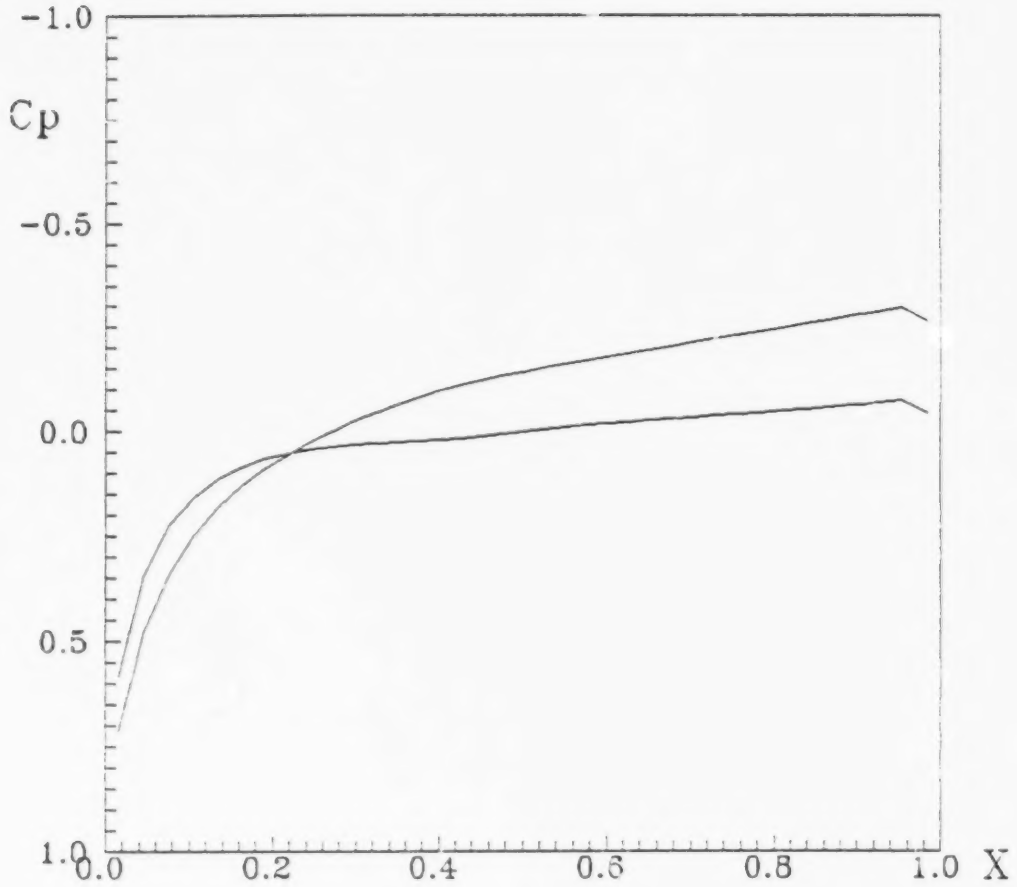

Fig.33 Pressure Distribution,

NACA 1406 Airfoil, $M_\infty = 1.2$, $\alpha = 1°$

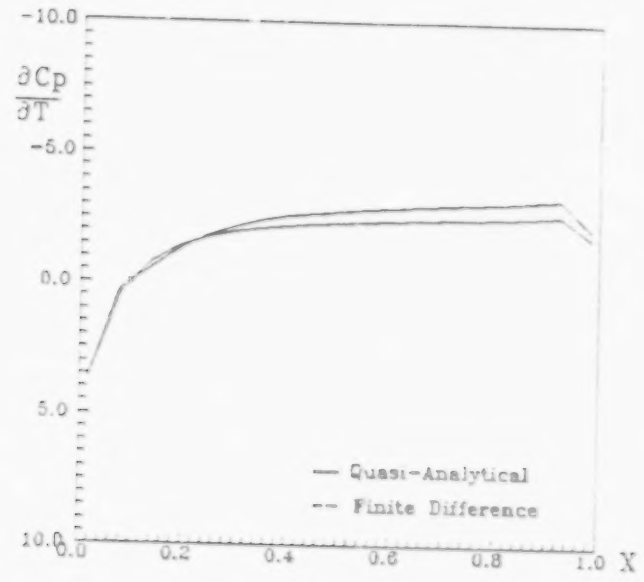

(a)

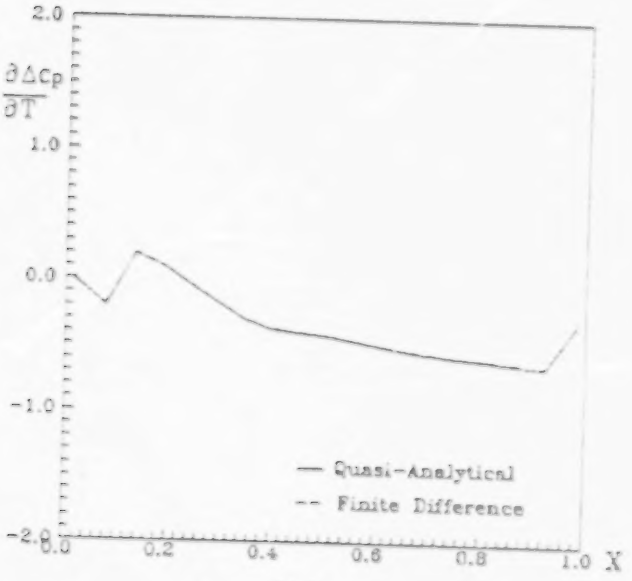

(b)

Fig.34 Sensitivity of Pressure to Maximum Thickness, NACA 1406 Airfoil, $M_\infty = 1.2$, $\alpha = 1°$

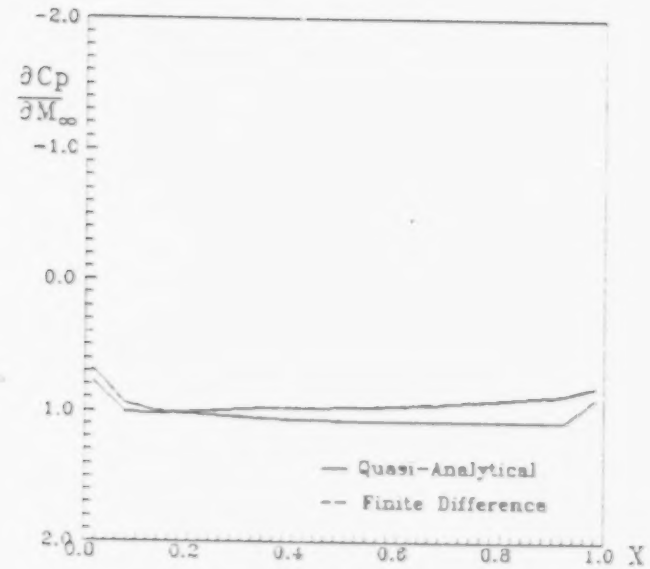

(a)

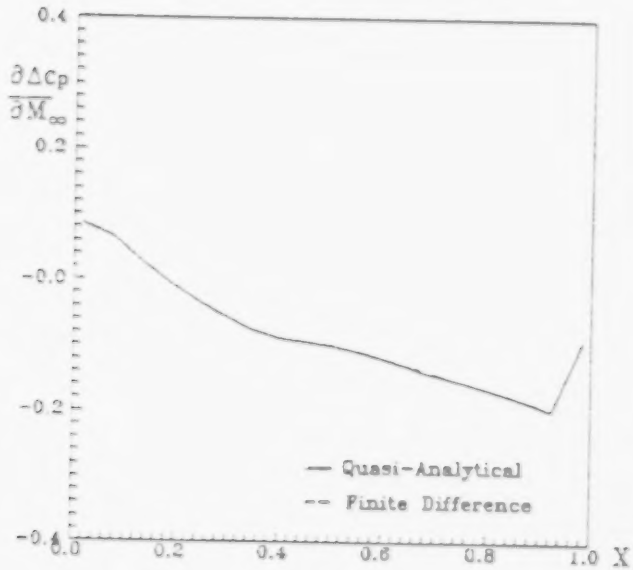

(b)

Fig.35 Sensitivity of Pressure to Mach Number, NACA 1406 Airfoil, $M_\infty = 1.2$, $\alpha = 1°$

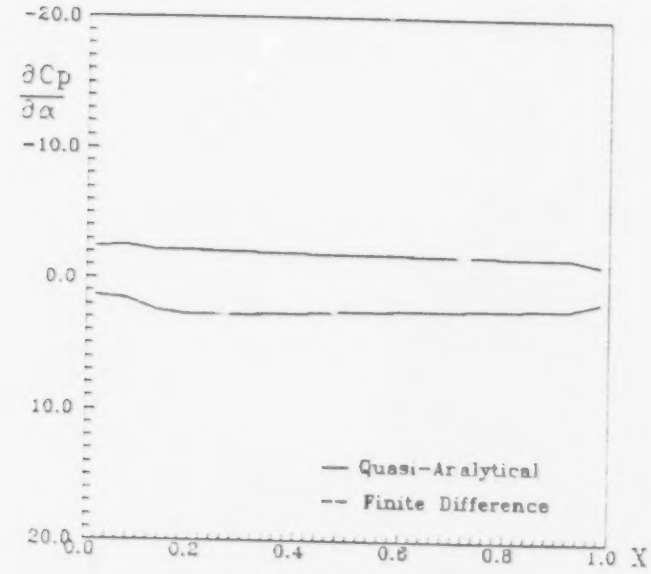

(a)

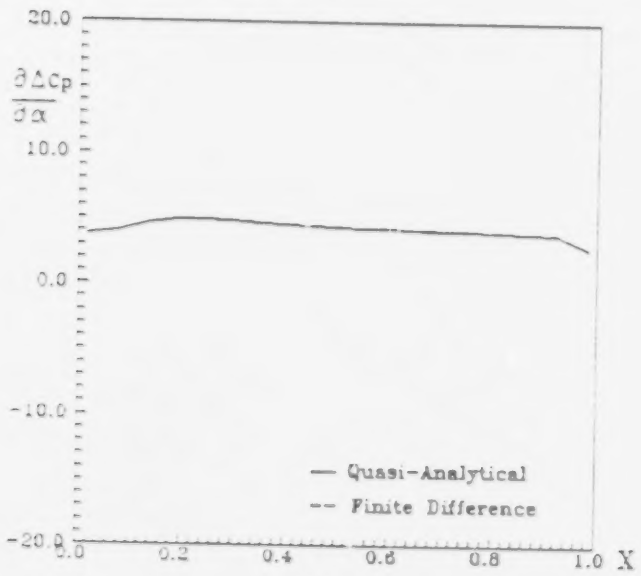

(b)

Fig.36 Sensitivity of Pressure to Angle of Attack, NACA 1406 Airfoil, M_∞ = 1.2, α = 1 °

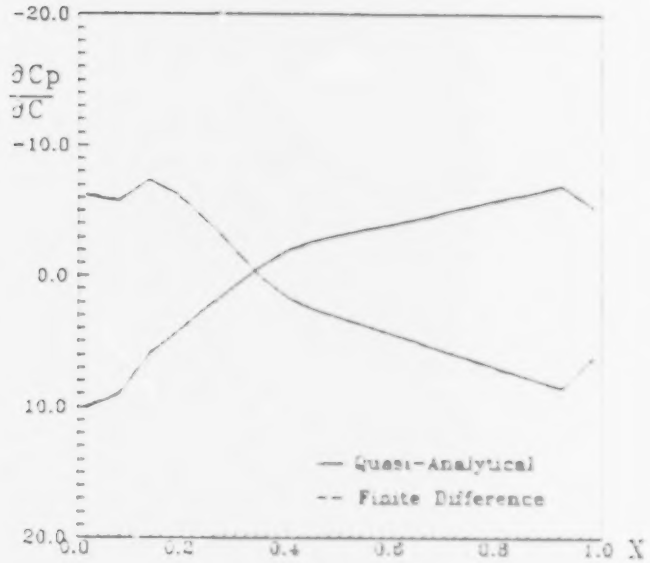

(a)

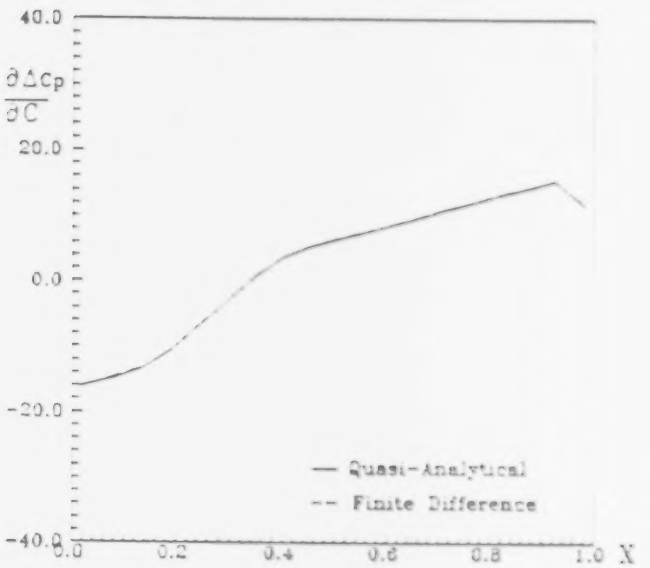

(b)

Fig.37 Sensitivity of Pressure to Maximum Camber, NACA 1406 Airfoil, $M_\infty = 1.2$, $\alpha = 1°$

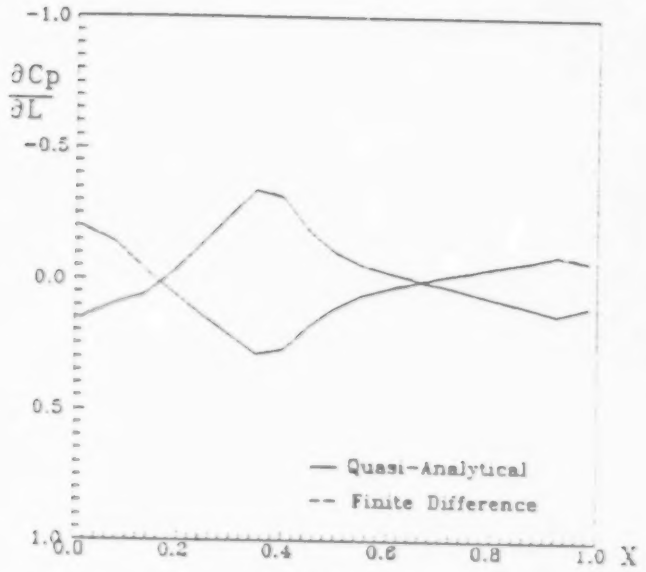

(a)

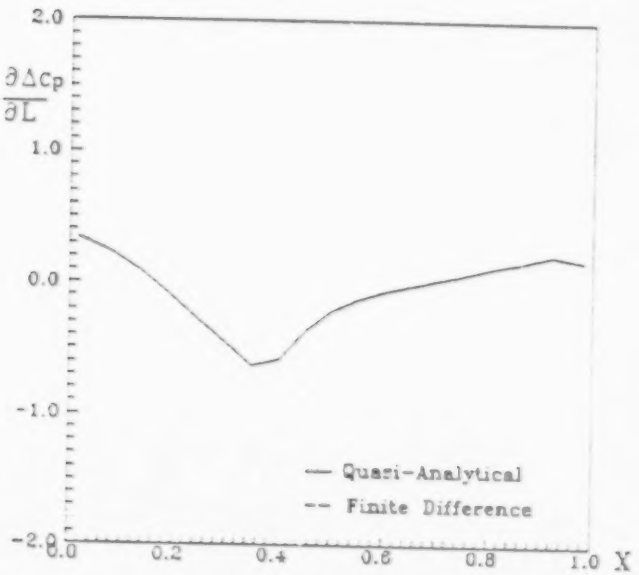

(b)

Fig.38 Sensitivity of Pressure to Location of Maximum Camber, NACA 1406 Airfoil, $M_\infty = 1.2$, $\alpha = 1°$

supercritical conditions, Figs.16-20 and 22-26, and that they are approaching the form expected from supersonic linear theory. These changes are particularly evident in the lift derivatives presented in Table 2. Notice that the derivatives with respect to the design variables maximum thickness, Mach number, and location of maximum camber have switched sign. In addition, as expected from linear theory, the influence of camber on lift has decreased significantly; and at $M_\infty = 1.2$ is only about 25% of the angle of attack effect as compared to a factor of about two at $M_\infty = 0.8$.

Time Comparisons

Obviously, in the development of the quasi-analytical method it was hoped that not only would this approach yield accurate values for the aerodynamic sensitivity coefficients but also that it would be more efficient than the brute force finite difference approach. Tables 3 and 4 present some comparisons concerning the amount of computational effort required to obtain solutions by the two approaches.

In comparing the values, several items should be kept in mind. First, it has been assumed that the finite difference approach will require six independent

Table 3

Time Comparisons for Obtaining Sensitivity Coefficients for Five Design Variables, Grid 41*20

P1406 airfoil

Method	M_∞ = 0.2	M_∞ = 0.8	M_∞ = 1.2
Flowfield Solver	1.00	2.95	2.30
Finite Difference Approch (6 Flowfield Solutions)	6.00	17.70	13.80
Quasi-Analytical Approach (1 Flowfield Solution plus Sensitivity Coefficient Solution via Gauss-Seidel)	4.54	7.45	5.52
Ratio —— QA / FD	0.76	0.42	0.40

NACA1406 airfoil

Method	M_∞ = 0.2	M_∞ = 0.8	M_∞ = 1.2
Flowfield Solver	1.00	2.66	2.81
Finite Difference Approch (6 Flowfield Solutions)	6.00	15.96	16.86
Quasi-Analytical Approach (1 Flowfield Solution plus Sensitivity Coefficient Solution via Gauss-Seidel)	4.63	10.75	5.60
Ratio —— QA / FD	0.77	0.61	0.33

Note: All times are normalized by the flowfield solver at Mach 0.2.

Table 4

Time Comparisons for Obtaining Sensitivity Coefficients for Five Design Variables, Grid 81*20

P1406 airfoil

Method	M_∞ = 0.2	M_∞ = 0.8
Flowfield Solver	1.00	1.93
Finite Difference Approch (6 Flowfield Solutions)	6.00	11.58
Quasi-Analytical Approach (1 Flowfield Solution plus Sensitivity Coefficient Solution via Gauss-Seidel)	5.56	14.65
Ratio —— QA / FD	0.93	1.27

NACA1406 airfoil

Method	M_∞ = 0.2	M_∞ = 0.8
Flowfield Solver	1.00	2.46
Finite Difference Approch (6 Flowfield Solutions)	6.00	14.76
Quasi-Analytical Approach (1 Flowfield Solution plus Sensitivity Coefficient Solution via Gauss-Seidel)	7.39	26.29
Ratio —— QA / FD	1.23	1.78

Note: All times are normalized by the flowfield solver at Mach 0.2.

solutions. In practice it might be possible to start each finite difference solution from a previous solution and, thus, decrease the time to convergence. However, to be accurate, the finite difference approach will probably require double precision and will have to be extremely well converged (i.e.1.E-08). Nevertheless, the values for the finite difference approach probably should be viewed as maximum values.

Second, the Gauss-Seidel method for obtaining the sensitivity coefficients has not been optimized and may not even be an efficient method; and the flowfield solution required for the quasi-analytical approach may not need double precision and may not have to be as tightly converged. Thus the values shown for the quasi-analytical approach should also be viewed as maximum values.

In spite of these limitations, the results do indicate, for the 41*20 grid, that the quasi-analytical method is at transonic conditions potentially more computationally efficient than the brute force finite difference approach.

As for the fine grid (81*20), it is seen that the finite differece method is generally more efficient than the quasi-analytical method. This result implies the need

to improve the efficiency of the sensitivity coefficient solver, which could be achieved thru the use of an optimum acceleration procedure. Another alternative explanation could be that the Gauss-Seidel solver might not be an efficient algorithm in the case of fine grids. This possibility will be discussed in the following section.

CONCLUSIONS AND RECOMMENDATIONS

Based upon the investigations and results described in the previous sections, it is concluded that

(1) The Quasi-Analytical Method is feasible as applied to the transonic small perturbation residual expression.

(2) The results obtained from the quasi-analytical method are almost identical to those obtained by the brute force technique (finite difference).

(3) The Gauss-Seidel iterative procedure used in solving the sensitivity equation is potentially more computationally efficient than the brute force direct approach for the 41*20 medium grid.

(4) For fine grids (81*20), the Gauss-Seidel solver is not as competitive.

It is recommended to

(1) Conduct more studies using refined grids at a variety of free stream Mach numbers.

(2) Consider new solution schemes for the quasi-analytical equation, Eq.(1).

(3) Examine the concept of only including part of the flowfield in attempt to reduce the size of system (1).

(4) Extend the calculation of the lift coefficient sensitivity derivates to that of the moment coefficient sensitivity derivates.

It is also recommended that further studies be carried out to examine the structure and properties of the coefficient matrix for special cases, as for example, that of the non-lifting problem ($\alpha = 0$, $C = 0$), and accordingly determine the feasibilty and efficiency of new fast solvers that exploit this structure. In addition, other iterative tridiagonal solvers need to be investigated.

REFERENCES

1. Sobieski, J.,"The Case for Aerodynamic Sensitivity Analysis", Paper presented to NASA/VPI&SU Symposium on Sensitivity Analysis in Engineering, September 25-26, 1986.

2. Adelman, M.; and Haftka, T., "Sensitivity Analysis and Discrete Structural Systems", AIAA Journal, Vol.24, No.5, May 1986, pp.823-832.

3. Sobieszczanski-Sobieski, J.; Barthelemy, J.-F.M.; and Riley, M.F.: Sensitivity of Optimum Solutions of Problem Parameters. AIAA Paper No.81-0548 R. AIAA Journal, Vol.20, No.9, September 1982, pp.1291-1299.

4. Bristow, D.R.; and Hawk, J.D.: Subsonic Panel Method for Designing Wing Surfaces from Pressure Distributions. NASA CR-3713, 1983.

5. Barthelemy, J.-F.M.; and Sobieszczanski-Sobieski, J.: Optimum Sensitivity Derivatives of Objective Functions in Nonlinear Programming. AIAA Journal, Vol.21, No.6, June 1983, pp.913-915.

6. Ballhaus, W.F.; Jameson, A.; and Albert, J.: Implicit Approximate Factorization Schemes for Steady Transonic Flow Problems. AIAA Journal, Vol.16, No.6, June 1978, pp.573-579.

7. Abbott, I.H. and Von Doenhoff, A.E., Theory of Wing Sections, Dover, New York., 1959.

8. Vanderplaats, N.; Hicks, M.; and Murman, M., "Application of Numerical Optimization Techniques To Airfoil Design", NASA SP-047, Part II, March, 1975, pp.749-768.

9. Sergio Pissanetzky, Sparse Matrix Technology, Academic Press, Inc., New York, 1984.

APPENDIX A

GENERAL EQUATION FOR SENSITIVITY

This Appendix[1] is a self-contained tutorial on sensitivity analysis arising in a generic problem whose governing equations are given. Let

$$F(y,x) = 0 \qquad \text{(A1)}$$

represent governing equations of a problem in which y is unknown to be obtained by solving Eq.(A1), and x are given constants. The quantities y and x may be vectors, and F may be a vector of functions. If y is a vector, Eq.(A1) implies a set of equations whose number is equal to the length of vector y; however, the x vector may be shorter than y. Existence of the solution of Eq.(A1) makes, implicitly, $y = f(x)$. The functions F may be anything computable : linear algebraical equations, partial differential equations, integral equations, or integral-differential equations, transcendental functions, etc. It may be nonlinear, and may require an iterative method for solution of Eq.(A1).

If Eq.(A1) governs a physical system being designed, then the designer wants to know not only the y for a given x, but also the sensitivity of y to those x-quantities that he controls as design variables For instance, F(y,x) might be the Euler equations from which to compute y - the

pressure distribution on a body in airflow, and x might be the body geometry variables. The designer of the body shape needs to know $\partial y/\partial x$.

One way to obtain $\partial y/\partial x$ is by finite differences. This requires solving Eq.(A1) for a given x to obtain y. Then assume, for one element of x, a perturbation, $x = x + \Delta x$, and repeat solution of Eq.(A1) to get $y + \Delta y$. Then, an approximation to $\partial y/\partial x$ is

$$\partial y/\partial x = \Delta y/\Delta x. \qquad (A2)$$

This operation must be repeated for all x-quantities of interest and may be prohibitively computer-intensive, if Eq.(A1) is expensive to solve. In addition, the accuracy of $\partial y/\partial x$ will depend on the proper choice of Δx.

An alternative is the quasi-analytical approach. It is called "quasi-" because the y(x) is known only numerically. However, for Δx, it must be true that

$$F(y+\Delta y,\ x+\Delta x) = 0 \qquad (A3)$$

In other words, increase of x must be compensated for by a change in y to preserve the zero value of F. Hence, recognizing that the total derivative of f with respect to x is according to the textbook rules of differentiation for implicit functions

$$dF/dx = \partial F/\partial x + (\partial F/\partial y)\ (\partial y/\partial x) \qquad (A4)$$

Eq.(A2) will be satisfied if

$$(dF/dx)\,\Delta x = 0 \qquad \text{(A5)}$$

Substituting Eq.(A4) into (A5), and rearranging, yields

$$(\partial F/\partial y)\,(\partial y/\partial x) = -(\partial F/\partial x) \qquad \text{(A6)}$$

Eq.(A6) is a general sensitivity equation in which the desired sensitivity appears directly as the unknown $(\partial y/\partial x)$. For a vector y of length n, the term $(\partial F/\partial y)$ is a matrix n*n whose each column is a vector of gradients with respect to y (a Jacobian matrix), the term $(\partial y/\partial x)$ is a vector of unknown derivatives of y with respect to one particular x variable, and the term $(\partial F/\partial x)$ is a vector of derivatives with respect to the same particular variable x. Computation of the derivatives of y with respect to several variables x requires solutions of Eq.(A6) with many right hand sides, one per each variable x. Since the Jacobian matrix remains the same for all variables x, a solution algorithm arranged so as to factor the matrix only once will be preferred for computational economy.

It is important that Eq.(A6) is simply a set of linear, algebraical equations even though Eq.(A1) may be far more complicated than that. The terms $(\partial F/\partial y)$ and $(\partial F/\partial x)$ may still not be obtainable analytically. If so, they can be computed by finite difference, i.e., assuming perturbation $x = x + \Delta x$ and $y = y + \Delta y$ for each element of

x and each element of y separately, and substituting into Eq.(A1), one obtains the respective ΔF values (upon substitution of $x + \Delta x$, or $y + \Delta y$, F in Eq.(A1) is no longer equal to zero, it becomes ΔF) from which the terms $(\partial F/\partial y)$ and $(\partial F/\partial x)$ can be computed as in Eq.(A2).

Computation of the terms $(\partial F/\partial y)$ and $(\partial F/\partial x)$ by finite difference is accomplished by repetitive evaluations of F(y,x) for known y and x, as opposed to repetitive solutions of Eq.(A1) for unknown y required by Eq.(A2). Hence, the quasi-analytical approach is inherently less computer intensitive than the finite difference procedure based on Eq.(A2).

APPENDIX B

RESIDUAL EXPRESSIONS AND DERIVATIVES

The residual expression at a general point (i,j) is given by,

$$R_{i,j} = c_1\varphi_{i,j} + c_2\varphi_{i+1,j}\varphi_{i-1,j} + c_3\varphi_{i+1,j}\varphi_{i,j} + c_4\varphi_{i-1,j}\varphi_{i,j} + c_5\varphi_{i+1,j}\varphi_{i-2,j} + c_6\varphi_{i-1,j}\varphi_{i-2,j} + c_7\varphi_{i-1,j}^2 + c_8\varphi_{i+1,j}^2 + c_9\varphi_{i+1,j} + c_{10}\varphi_{i-1,j} + c_{11}\varphi_{i,j+1} + c_{12}\varphi_{i,j-1} + c_{13}\varphi_{i-2,j}$$

For points designated [1]-[4], we have,

[1] $$R_{i,j} = (c_1+c_{11})\varphi_{i,j} + c_2\varphi_{i+1,j}\varphi_{i-1,j} + c_3\varphi_{i+1,j}\varphi_{i,j} + c_4\varphi_{i-1,j}\varphi_{i,j} + c_5\varphi_{i+1,j}\varphi_{i-2,j} + c_6\varphi_{i-1,j}\varphi_{i-2,j} + c_7\varphi_{i-1,j}^2 + c_8\varphi_{i+1,j}^2 + c_9\varphi_{i+1,j} + c_{10}\varphi_{i-1,j} + c_{12}\varphi_{i,j-1} + c_{13}\varphi_{i-2,j} + c_{11}\Delta\eta F_1/g_{j+\frac{1}{2}}$$

[2] $$R_{i,j} = (c_1+c_{12})\varphi_{i,j} + c_2\varphi_{i+1,j}\varphi_{i-1,j} + c_3\varphi_{i+1,j}\varphi_{i,j} + c_4\varphi_{i-1,j}\varphi_{i,j} + c_5\varphi_{i+1,j}\varphi_{i-2,j} + c_6\varphi_{i-1,j}\varphi_{i-2,j} + c_7\varphi_{i-1,j}^2 + c_8\varphi_{i+1,j}^2 + c_9\varphi_{i+1,j} + c_{10}\varphi_{i-1,j} + c_{11}\varphi_{i,j+1} + c_{13}\varphi_{i-2,j} - c_{12}\Delta\eta F_u/g_{j-\frac{1}{2}}$$

[3] $$R_{i,j} = c_1\varphi_{i,j} + c_2\varphi_{i+1,j}\varphi_{i-1,j} + c_3\varphi_{i+1,j}\varphi_{i,j} + c_4\varphi_{i-1,j}\varphi_{i,j} + c_5\varphi_{i+1,j}\varphi_{i-2,j} + c_6\varphi_{i-1,j}\varphi_{i-2,j} + c_7\varphi_{i-1,j}^2 + c_8\varphi_{i+1,j}^2 + c_9\varphi_{i+1,j} + c_{10}\varphi_{i-1,j} + c_{11}\varphi_{i,j+1} + c_{12}\varphi_{i,j-1} + c_{13}\varphi_{i-2,j} - c_{11}\Gamma$$

[4] $$R_{i,j} = c_1\varphi_{i,j} + c_2\varphi_{i+1,j}\varphi_{i-1,j} + c_3\varphi_{i+1,j}\varphi_{i,j} + c_4\varphi_{i-1,j}\varphi_{i,j} + c_5\varphi_{i+1,j}\varphi_{i-2,j} + c_6\varphi_{i-1,j}\varphi_{i-2,j} + c_7\varphi_{i-1,j}^2 + c_8\varphi_{i+1,j}^2 + c_9\varphi_{i+1,j} + c_{10}\varphi_{i-1,j} + c_{11}\varphi_{i,j+1} + c_{12}\varphi_{i,j-1} + c_{13}\varphi_{i-2,j} + c_{12}\Gamma$$

For a subsonic free stream,

$$[5]\quad R_{i,j} = c_1\varphi_{i,j} + c_4\varphi_{i-1,j}\varphi_{i,j} + c_6\varphi_{i-1,j}\varphi_{i-2,j} + c_7\varphi_{i-1,j}^2 + c_{10}\varphi_{i-1,j} + c_{11}\varphi_{i,j+1} + c_{12}\varphi_{i,j-1} + c_{13}\varphi_{i-2,j}$$

$$[6]\quad R_{i,j} = c_1\varphi_{i,j} + c_2\varphi_{i+1,j}\varphi_{i-1,j} + c_3\varphi_{i+1,j}\varphi_{i,j} + c_4\varphi_{i-1,j}\varphi_{i,j} + c_5\varphi_{i+1,j}\varphi_{i-2,j} + c_6\varphi_{i-1,j}\varphi_{i-2,j} + c_7\varphi_{i-1,j}^2 + c_8\varphi_{i+1,j}^2 + c_9\varphi_{i+1,j} + c_{10}\varphi_{i-1,j} + c_{11}(-\Gamma/4) + c_{12}\varphi_{i,j-1} + c_{13}\varphi_{i-2,j}$$

$$[7]\quad R_{i,j} = c_1\varphi_{i,j} + c_2\varphi_{i+1,j}(-\Gamma/2) + c_3\varphi_{i+1,j}\varphi_{i,j} + c_4(-\Gamma/2)\varphi_{i,j} + c_5\varphi_{i+1,j}\varphi_{i-2,j} + c_6(-\Gamma/2)\varphi_{i-2,j} + c_7(-\Gamma/2)^2 + c_8\varphi_{i+1,j}^2 + c_9\varphi_{i+1,j} + c_{10}(-\Gamma/2) + c_{11}\varphi_{i,j+1} + c_{12}\varphi_{i,j-1} + c_{13}\varphi_{i-2,j}$$

$$[8]\quad R_{i,j} = c_1\varphi_{i,j} + c_2\varphi_{i+1,j}\varphi_{i-1,j} + c_3\varphi_{i+1,j}\varphi_{i,j} + c_4\varphi_{i-1,j}\varphi_{i,j} + c_5\varphi_{i+1,j}\varphi_{i-2,j} + c_6\varphi_{i-1,j}\varphi_{i-2,j} + c_7\varphi_{i-1,j}^2 + c_8\varphi_{i+1,j}^2 + c_9\varphi_{i+1,j} + c_{10}\varphi_{i-1,j} + c_{11}\varphi_{i,j+1} + c_{12}(-3\Gamma/4) + c_{13}\varphi_{i-2,j}$$

$$[9]\quad R_{i,j} = c_1\varphi_{i,j} + c_2(-\Gamma)\varphi_{i-1,j} + c_3(-\Gamma)\varphi_{i,j} + c_4\varphi_{i-1,j}\varphi_{i,j} + c_5(-\Gamma)\varphi_{i-2,j} + c_6\varphi_{i-1,j}\varphi_{i-2,j} + c_7\varphi_{i-1,j}^2 + c_8(-\Gamma)^2 + c_9(-\Gamma) + c_{10}\varphi_{i-1,j} + c_{11}\varphi_{i,j+1} + c_{12}\varphi_{i,j-1} + c_{13}\varphi_{i-2,j}$$

$$[10]\quad R_{i,j} = c_1\varphi_{i,j} + c_4\varphi_{i-1,j}\varphi_{i,j} + c_6\varphi_{i-1,j}\varphi_{i-2,j} + c_7\varphi_{i-1,j}^2 + c_{10}\varphi_{i-1,j} + c_{11}(-\Gamma/4) + c_{12}\varphi_{i,j-1} + c_{13}\varphi_{i-2,j}$$

$$[11]\quad R_{i,j} = c_1\varphi_{i,j} + c_2\varphi_{i+1,j}(-\Gamma/2) + c_3\varphi_{i+1,j}\varphi_{i,j} + c_4(-\Gamma/2)\varphi_{i,j} + c_5\varphi_{i+1,j}\varphi_{i-2,j} + c_6(-\Gamma/2)\varphi_{i-2,j} + c_7(-\Gamma/2)^2 + c_8\varphi_{i+1,j}^2 + c_9\varphi_{i+1,j} + c_{10}(-\Gamma/2) + c_{11}(-\Gamma/4) + c_{12}\varphi_{i,j-1} + c_{13}\varphi_{i-2,j}$$

$$[12]\quad R_{i,j} = c_1\varphi_{i,j} + c_2\varphi_{i+1,j}(-\Gamma/2) + c_3\varphi_{i+1,j}\varphi_{i,j} + c_4(-\Gamma/2)\varphi_{i,j} + c_5\varphi_{i+1,j}\varphi_{i-2,j} + c_6(-\Gamma/2)\varphi_{i-2,j} + c_7(-\Gamma/2)^2 + c_8\varphi_{i+1,j}^2 + c_9\varphi_{i+1,j} + c_{10}(-\Gamma/2) + c_{11}\varphi_{i,j+1} + c_{12}(-3\Gamma/4) + c_{13}\varphi_{i-2,j}$$

$$[13]\quad R_{i,j} = c_1\varphi_{i,j} + c_2(-\Gamma)\varphi_{i-1,j} + c_3(-\Gamma)\varphi_{i,j} + c_4\varphi_{i-1,j}\varphi_{i,j} + c_5(-\Gamma)\varphi_{i-2,j} + c_6\varphi_{i-1,j}\varphi_{i-2,j} + c_7\varphi_{i-1,j}^2 + c_8(-\Gamma)^2 + c_9(-\Gamma) + c_{10}\varphi_{i-1,j} + c_{11}\varphi_{i,j+1} + c_{12}(-3\Gamma/4) + c_{13}\varphi_{i-2,j}$$

$$[14]\quad R_{i,j} = c_1\varphi_{i,j} + c_4\varphi_{i-1,j}\varphi_{i,j} + c_6\varphi_{i-1,j}\varphi_{i-2,j} + c_7\varphi_{i-1,j}^2 + c_{10}\varphi_{i-1,j} + c_{11}\varphi_{i,j+1} + c_{12}\varphi_{i,j-1} + c_{13}\varphi_{i-2,j} + c_{12}\Gamma$$

$$[15]\quad R_{i,j} = c_1\varphi_{i,j} + c_2(-\Gamma)\varphi_{i-1,j} + c_3(-\Gamma)\varphi_{i,j} + c_4\varphi_{i-1,j}\varphi_{i,j} + c_5(-\Gamma)\varphi_{i-2,j} + c_6\varphi_{i-1,j}\varphi_{i-2,j} + c_7\varphi_{i-1,j}^2 + c_8(-\Gamma)^2 + c_9(-\Gamma) + c_{10}\varphi_{i-1,j} + c_{11}\varphi_{i,j+1} + c_{12}\varphi_{i,j-1} + c_{13}\varphi_{i-2,j} - c_{11}\Gamma$$

For a supersonic free stream,

$$[5]\quad R_{i,j} = c_1\varphi_{i,j} + c_2\varphi_{i,j}\varphi_{i-1,j} + c_3\varphi_{i,j}^2 + c_4\varphi_{i-1,j}\varphi_{i,j} + c_5\varphi_{i,j}\varphi_{i-2,j} + c_6\varphi_{i-1,j}\varphi_{i-2,j} + c_7\varphi_{i-1,j}^2 + c_8\varphi_{i,j}^2 + c_9\varphi_{i,j} + c_{10}\varphi_{i-1,j} + c_{11}\varphi_{i,j+1} + c_{12}\varphi_{i,j-1} + c_{13}\varphi_{i-2,j}$$

$$[6]\quad R_{i,j} = c_1\varphi_{i,j} + c_2\varphi_{i+1,j}\varphi_{i-1,j} + c_3\varphi_{i+1,j}\varphi_{i,j} + c_4\varphi_{i-1,j}\varphi_{i,j} + c_5\varphi_{i+1,j}\varphi_{i-2,j} + c_6\varphi_{i-1,j}\varphi_{i-2,j} + c_7\varphi_{i-1,j}^2 + c_8\varphi_{i+1,j}^2 + c_9\varphi_{i+1,j} + c_{10}\varphi_{i-1,j} + c_{12}\varphi_{i,j-1} + c_{13}\varphi_{i-2,j}$$

$$[7]\quad R_{i,j} = c_1\varphi_{i,j} + c_3\varphi_{i+1,j}\varphi_{i,j} + c_5\varphi_{i+1,j}\varphi_{i-2,j} + c_8\varphi_{i+1,j}^2 + c_9\varphi_{i+1,j} + c_{11}\varphi_{i,j+1} + c_{12}\varphi_{i,j-1} + c_{13}\varphi_{i-2,j}$$

$$[8]\quad R_{i,j} = c_1\varphi_{i,j} + c_2\varphi_{i+1,j}\varphi_{i-1,j} + c_3\varphi_{i+1,j}\varphi_{i,j} + c_4\varphi_{i-1,j}\varphi_{i,j} + c_5\varphi_{i+1,j}\varphi_{i-2,j} + c_6\varphi_{i-1,j}\varphi_{i-2,j} + c_7\varphi_{i-1,j}^2 + c_8\varphi_{i+1,j}^2 + c_9\varphi_{i+1,j} + c_{10}\varphi_{i-1,j} + c_{11}\varphi_{i,j+1} + c_{13}\varphi_{i-2,j}$$

$$[9]\quad R_{i,j} = c_1\varphi_{i,j} + c_2\varphi_{i,j}\varphi_{i-1,j} + c_3\varphi_{i,j}^2 + c_4\varphi_{i-1,j}\varphi_{i,j} + c_5\varphi_{i,j}\varphi_{i-2,j} + c_6\varphi_{i-1,j}\varphi_{i-2,j} + c_7\varphi_{i-1,j}^2 + c_8\varphi_{i,j}^2 + c_9\varphi_{i,j} + c_{10}\varphi_{i-1,j} + c_{11}\varphi_{i,j+1} + c_{12}\varphi_{i,j-1} + c_{13}\varphi_{i-2,j}$$

$$[10]\quad R_{i,j} = c_1\varphi_{i,j} + c_2\varphi_{i,j}\varphi_{i-1,j} + c_3\varphi_{i,j}^2 + c_4\varphi_{i-1,j}\varphi_{i,j} + c_5\varphi_{i,j}\varphi_{i-2,j} + c_6\varphi_{i-1,j}\varphi_{i-2,j} + c_7\varphi_{i-1,j}^2 + c_8\varphi_{i,j}^2 + c_9\varphi_{i,j} + c_{10}\varphi_{i-1,j} + c_{12}\varphi_{i,j-1} + c_{13}\varphi_{i-2,j}$$

[11] $R_{i,j} = c_1\varphi_{i,j} + c_3\varphi_{i+1,j}\varphi_{i,j} + c_5\varphi_{i+1,j}\varphi_{i-2,j}$
$+ c_8\varphi_{i+1,j}^2 + c_9\varphi_{i+1,j} + c_{12}\varphi_{i,j-1} + c_{13}\varphi_{i-2,j}$

[12] $R_{i,j} = c_1\varphi_{i,j} + c_3\varphi_{i+1,j}\varphi_{i,j} + c_5\varphi_{i+1,j}\varphi_{i-2,j}$
$+ c_8\varphi_{i+1,j}^2 + c_9\varphi_{i+1,j} + c_{11}\varphi_{i,j+1} + c_{13}\varphi_{i-2,j}$

[13] $R_{i,j} = c_1\varphi_{i,j} + c_2\varphi_{i,j}\varphi_{i-1,j} + c_3\varphi_{i,j}^2$
$+ c_4\varphi_{i-1,j}\varphi_{i,j} + c_5\varphi_{i,j}\varphi_{i-2,j} + c_6\varphi_{i-1,j}\varphi_{i-2,j}$
$+ c_7\varphi_{i-1,j}^2 + c_8\varphi_{i,j}^2 + c_9\varphi_{i,j} + c_{10}\varphi_{i-1,j}$
$+ c_{11}\varphi_{i,j+1} + c_{13}\varphi_{i-2,j}$

[14] $R_{i,j} = c_1\varphi_{i,j} + c_2\varphi_{i,j}\varphi_{i-1,j} + c_3\varphi_{i,j}^2$
$+ c_4\varphi_{i-1,j}\varphi_{i,j} + c_5\varphi_{i,j}\varphi_{i-2,j} + c_6\varphi_{i-1,j}\varphi_{i-2,j}$
$+ c_7\varphi_{i-1,j}^2 + c_8\varphi_{i,j}^2 + c_9\varphi_{i,j} + c_{10}\varphi_{i-1,j}$
$+ c_{11}\varphi_{i,j+1} + c_{12}\varphi_{i,j-1} + c_{13}\varphi_{i-2,j} + c_{12}\Gamma$

[15] $R_{i,j} = c_1\varphi_{i,j} + c_2\varphi_{i,j}\varphi_{i-1,j} + c_3\varphi_{i,j}^2$
$+ c_4\varphi_{i-1,j}\varphi_{i,j} + c_5\varphi_{i,j}\varphi_{i-2,j} + c_6\varphi_{i-1,j}\varphi_{i-2,j}$
$+ c_7\varphi_{i-1,j}^2 + c_8\varphi_{i,j}^2 + c_9\varphi_{i,j} + c_{10}\varphi_{i-1,j}$
$+ c_{11}\varphi_{i,j+1} + c_{12}\varphi_{i,j-1} + c_{13}\varphi_{i-2,j} - c_{11}\Gamma$

Now, the previous expressions are differentiated with respect to $\varphi_{ii,jj}$ to give the elements of the jacobian matrix $(\partial R_{i,j}/\partial \varphi_{ii,jj})$. This is achieved as follows :

For a general point (i,j),

ii	jj	Derivative of $R_{i,j}$
i	j-1	c_{12}
i	j	$c_1 + c_3\varphi_{i+1,j} + c_4\varphi_{i-1,j}$
i	j+1	c_{11}
i-2	j	$c_5\varphi_{i+1,j} + c_6\varphi_{i-1,j} + c_{13}$
i-1	j	$c_2\varphi_{i+1,j} + c_4\varphi_{i,j} + c_6\varphi_{i-2,j} + 2c_7\varphi_{i-1,j} + c_{10}$
i+1	j	$c_2\varphi_{i-1,j} + c_3\varphi_{i,j} + c_5\varphi_{i-2,j} + 2c_8\varphi_{i+1,j} + c_9$
ITE-1	JB-2	0
ITE-1	JB-1	0
ITE-1	JB	0
ITE-1	JB+1	0
ITE	JB-2	0
ITE	JB-1	0
ITE	JB	0
ITE	JB+1	0

For points [1],

ii	jj	Derivative of $R_{i,j}$
i	j-1	c_{12}
i	j	$c_1 + c_3\varphi_{i+1,j} + c_4\varphi_{i-1,j} + c_{11}$
i	j+1	0
i-2	j	$c_5\varphi_{i+1,j} + c_6\varphi_{i-1,j} + c_{13}$
i-1	j	$c_2\varphi_{i+1,j} + c_4\varphi_{i,j} + c_6\varphi_{i-2,j} + 2c_7\varphi_{i-1,j} + c_{10}$
i+1	j	$c_2\varphi_{i-1,j} + c_3\varphi_{i,j} + c_5\varphi_{i-2,j} + 2c_8\varphi_{i+1,j} + c_9$
ITE-1	JB-2	0
ITE-1	JB-1	0
ITE-1	JB	0
ITE-1	JB+1	0
ITE	JB-2	0
ITE	Jb-1	0
ITE	JB	0
ITE	JB+1	0

For points [2],

ii	jj	Derivative of $R_{i,j}$
i	j-1	0
i	j	$c_1 + c_3\varphi_{i+1,j} + c_4\varphi_{i-1,j} + c_{12}$
i	j+1	c_{11}
i-2	j	$c_5\varphi_{i+1,j} + c_6\varphi_{i-1,j} + c_{13}$
i-1	j	$c_2\varphi_{i+1,j} + c_4\varphi_{i,j} + c_6\varphi_{i-2,j} + 2c_7\varphi_{i-1,j} + c_{10}$
i+1	j	$c_2\varphi_{i-1,j} + c_3\varphi_{i,j} + c_5\varphi_{i-2,j} + 2c_8\varphi_{i+1,j} + c_9$
ITE-1	JB-2	0
ITE-1	JB-1	0
ITE-1	JB	0
ITE-1	JB+1	0
ITE	JB-2	0
ITE	JB-1	0
ITE	JB	0
ITE	JB+1	0

For points [3],

ii	jj	Derivative of $R_{i,j}$
i	j-1	c_{12}
i	j	$c_1 + c_3\varphi_{i+1,j} + c_4\varphi_{i-1,j}$
i	j+1	c_{11}
i-2	j	$c_5\varphi_{i+1,j} + c_6\varphi_{i-1,j} + c_{13}$
i-1	j	$c_2\varphi_{i+1,j} + c_4\varphi_{i,j} + c_6\varphi_{i-2,j} + 2c_7\varphi_{i-1,j} + c_{10}$
i+1	j	$c_2\varphi_{i-1,j} + c_3\varphi_{i,j} + c_5\varphi_{i-2,j} + 2c_8\varphi_{i+1,j} + c_9$
ITE-1	JB-2	$- c_{11}(+0.5T_1)$
ITE-1	JB-1	$- c_{11}(-1.5T_1)$
ITE-1	JB	$- c_{11}(+1.5T_1)$
ITE-1	JB+1	$- c_{11}(-0.5T_1)$
ITE	JB-2	$- c_{11}(+0.5T_2)$
ITE	JB-1	$- c_{11}(-1.5T_2)$
ITE	JB	$- c_{11}(+1.5T_2)$
ITE	JB+1	$- c_{11}(-0.5T_2)$

For points [4],

ii	jj	Derivative of $R_{i,j}$
i	j-1	c_{12}
i	j	$c_1 + c_3\varphi_{i+1,j} + c_4\varphi_{i-1,j}$
i	j+1	c_{11}
i-2	j	$c_5\varphi_{i+1,j} + c_6\varphi_{i-1,j} + c_{13}$
i-1	j	$c_2\varphi_{i+1,j} + c_4\varphi_{i,j} + c_6\varphi_{i-2,j}$ $+ 2c_7\varphi_{i-1,j} + c_{10}$
i+1	j	$c_2\varphi_{i-1,j} + c_3\varphi_{i,j} + c_5\varphi_{i-2,j}$ $+ 2c_8\varphi_{i+1,j} + c_9$
ITE-1	JB-2	$+ c_{12}(+0.5T_1)$
ITE-1	JB-1	$+ c_{12}(-1.5T_1)$
ITE-1	JB	$+ c_{12}(+1.5T_1)$
ITE-1	JB+1	$+ c_{12}(-0.5T_1)$
ITE	JB-2	$+ c_{12}(+0.5T_2)$
ITE	JB-1	$+ c_{12}(-1.5T_2)$
ITE	JB	$+ c_{12}(+1.5T_2)$
ITE	JB+1	$+ c_{12}(-0.5T_2)$

For a subsonic free stream :

For points [5],

ii	jj	Derivative of $R_{i,j}$
i	j-1	c_{12}
i	j	$c_1 + c_4\varphi_{i-1,j}$
i	j+1	c_{11}
i-2	j	$c_6\varphi_{i-1,j} + c_{13}$
i-1	j	$c_4\varphi_{i,j} + c_6\varphi_{i-2,j} + 2c_7\varphi_{i-1,j} + c_{10}$
i+1	j	0
ITE-1	JB-2	0
ITE-1	JB-1	0
ITE-1	JB	0
ITE-1	JB+1	0
ITE	JB-2	0
ITE	JB-1	0
ITE	JB	0
ITE	JB+1	0

For points [6],

ii	jj	Derivative of $R_{i,j}$
i	j-1	c_{12}
i	j	$c_1 + c_3\varphi_{i+1,j} + c_4\varphi_{i-1,j}$
i	j+1	0
i-2	j	$c_5\varphi_{i+1,j} + c_6\varphi_{i-1,j} + c_{13}$
i-1	j	$c_2\varphi_{i+1,j} + c_4\varphi_{i,j} + c_6\varphi_{i-2,j} + 2c_7\varphi_{i-1,j} + c_{10}$
i+1	j	$c_2\varphi_{i-1,j} + c_3\varphi_{i,j} + c_5\varphi_{i-2,j} + 2c_8\varphi_{i+1,j} + c_9$
ITE-1	JB-2	$- c_{11}(+0.5T_1)/4$
ITE-1	JB-1	$- c_{11}(-1.5T_1)/4$
ITE-1	JB	$- c_{11}(+1.5T_1)/4$
ITE-1	JB+1	$- c_{11}(-0.5T_1)/4$
ITE	JB-2	$- c_{11}(+0.5T_2)/4$
ITE	JB-1	$- c_{11}(-1.5T_2)/4$
ITE	JB	$- c_{11}(+1.5T_2)/4$
ITE	JB+1	$- c_{11}(-0.5T_2)/4$

For points [7],

ii	jj	Derivative of $R_{i,j}$
i	j-1	c_{12}
i	j	$c_1 + c_3\varphi_{i+1,j} - c_4\Gamma/2$
i	j+1	c_{11}
i-2	j	$c_5\varphi_{i+1,j} - c_6\Gamma/2 + c_{13}$
i-1	j	0
i+1	j	$-c_2\Gamma/2 + c_3\varphi_{i,j} + c_5\varphi_{i-2,j} + 2c_8\varphi_{i+1,j} + c_9$
ITE-1	JB-2	$(-c_2\varphi_{i+1,j}/2-c_4\varphi_{i,j}/2-c_6\varphi_{i-2,j}/2 +c_7\Gamma/2-c_{10}/2)\ (+0.5T_1)$
ITE-1	JB-1	$(-c_2\varphi_{i+1,j}/2-c_4\varphi_{i,j}/2-c_6\varphi_{i-2,j}/2 +c_7\Gamma/2-c_{10}/2)\ (-1.5T_1)$
ITE-1	JB	$(-c_2\varphi_{i+1,j}/2-c_4\varphi_{i,j}/2-c_6\varphi_{i-2,j}/2 +c_7\Gamma/2-c_{10}/2)\ (+1.5T_1)$
ITE-1	JB+1	$(-c_2\varphi_{i+1,j}/2-c_4\varphi_{i,j}/2-c_6\varphi_{i-2,j}/2 +c_7\Gamma/2-c_{10}/2)\ (-0.5T_1)$
ITE	JB-2	$(-c_2\varphi_{i+1,j}/2-c_4\varphi_{i,j}/2-c_6\varphi_{i-2,j}/2 +c_7\Gamma/2-c_{10}/2)\ (+0.5T_2)$
ITE	JB-1	$(-c_2\varphi_{i+1,j}/2-c_4\varphi_{i,j}/2-c_6\varphi_{i-2,j}/2 +c_7\Gamma/2-c_{10}/2)\ (-1.5T_2)$
ITE	JB	$(-c_2\varphi_{i+1,j}/2-c_4\varphi_{i,j}/2-c_6\varphi_{i-2,j}/2 +c_7\Gamma/2-c_{10}/2)\ (+1.5T_2)$
ITE	JB+1	$(-c_2\varphi_{i+1,j}/2-c_4\varphi_{i,j}/2-c_6\varphi_{i-2,j}/2 +c_7\Gamma/2-c_{10}/2)\ (-0.5T_2)$

For points [8],

ii	jj	Derivative of $R_{i,j}$
i	j-1	0
i	j	$c_1 + c_3\varphi_{i+1,j} + c_4\varphi_{i-1,j}$
i	j+1	c_{11}
i-2	j	$c_5\varphi_{i+1,j} + c_6\varphi_{i-1,j} + c_{13}$
i-1	j	$c_2\varphi_{i+1,j} + c_4\varphi_{i,j} + c_6\varphi_{i-2,j} + 2c_7\varphi_{i-1,j} + c_{10}$
i+1	j	$c_2\varphi_{i-1,j} + c_3\varphi_{i,j} + c_5\varphi_{i-2,j} + 2c_8\varphi_{i+1,j} + c_9$
ITE-1	JB-2	$-3\,c_{12}\,(+0.5T_1)\,/\,4$
ITE-1	JB-1	$-3\,c_{12}\,(-1.5T_1)\,/\,4$
ITE-1	JB	$-3\,c_{12}\,(+1.5T_1)\,/\,4$
ITE-1	JB+1	$-3\,c_{12}\,(-0.5T_1)\,/\,4$
ITE	JB-2	$-3\,c_{12}\,(+0.5T_2)\,/\,4$
ITE	JB-1	$-3\,c_{12}\,(-1.5T_2)\,/\,4$
ITE	JB	$-3\,c_{12}\,(+1.5T_2)\,/\,4$
ITE	JB+1	$-3\,c_{12}\,(-0.5T_2)\,/\,4$

For points [9],

ii	jj	Derivative of $R_{i,j}$
i	j-1	c_{12}
i	j	$c_1 - c_3\Gamma + c_4\varphi_{i-1,j}$
i	j+1	c_{11}
i-2	j	$- c_5\Gamma + 6\varphi_{i-1,j} + c_{13}$
i-1	j	$- c_2\Gamma + 4\varphi_{i,j} + c_6\varphi_{i-2,j}$ $+ 2c_7\varphi_{i-1,j} + c_{10}$
i+1	j	0
ITE-1	JB-2	$(-c_2\varphi_{i-1,j} - c_3\varphi_{i,j} - c_5\varphi_{i-2,j}$ $+2c_8\Gamma - c_9)\ (+0.5T_1)$
ITE-1	JB-1	$(-c_2\varphi_{i-1,j} - c_3\varphi_{i,j} - c_5\varphi_{i-2,j}$ $+2c_8\Gamma - c_9)\ (-1.5T_1)$
ITE-1	JB	$(-c_2\varphi_{i-1,j} - c_3\varphi_{i,j} - c_5\varphi_{i-2,j}$ $+2c_8\Gamma - c_9)\ (+1.5T_1)$
ITE-1	JB+1	$(-c_2\varphi_{i-1,j} - c_3\varphi_{i,j} - c_5\varphi_{i-2,j}$ $+2c_8\Gamma - c_9)\ (-0.5T_1)$
ITE	JB-2	$(-c_2\varphi_{i-1,j} - c_3\varphi_{i,j} - c_5\varphi_{i-2,j}$ $+2c_8\Gamma - c_9)\ (+0.5T_2)$
ITE	JB-1	$(-c_2\varphi_{i-1,j} - c_3\varphi_{i,j} - c_5\varphi_{i-2,j}$ $+2c_8\Gamma - c_9)\ (-1.5T_2)$
ITE	JB	$(-c_2\varphi_{i-1,j} - c_3\varphi_{i,j} - c_5\varphi_{i-2,j}$ $+2c_8\Gamma - c_9)\ (+1.5T_2)$
ITE	JB+1	$(-c_2\varphi_{i-1,j} - c_3\varphi_{i,j} - c_5\varphi_{i-2,j}$ $+2c_8\Gamma - c_9)\ (-0.5T_2)$

For points [10],

ii	jj	Derivative of $R_{i,j}$
i	j-1	c_{12}
i	j	$c_1 + c_4\varphi_{i-1,j}$
i	j+1	0
i-2	j	$c_6\varphi_{i-1,j} + c_{13}$
i-1	j	$c_4\varphi_{i,j} + c_6\varphi_{i-2,j} + 2c_7\varphi_{i-1,j} + c_{10}$
i+1	j	0
ITE-1	JB-2	$- c_{11} (+0.5T_1) / 4$
ITE-1	JB-1	$- c_{11} (-1.5T_1) / 4$
ITE-1	JB	$- c_{11} (+1.5T_1) / 4$
ITE-1	JB+1	$- c_{11} (-0.5T_1) / 4$
ITE	JB-2	$- c_{11} (+0.5T_2) / 4$
ITE	JB-1	$- c_{11} (-1.5T_2) / 4$
ITE	JB	$- c_{11} (+1.5T_2) / 4$
ITE	JB+1	$- c_{11} (-0.5T_2) / 4$

For points [11],

ii	jj	Derivative of $R_{i,j}$
i	j-1	c_{12}
i	j	$c_1 + c_3\varphi_{i+1,j} - c_4\Gamma/2$
i	j+1	0
i-2	j	$c_5\varphi_{i+1,j} - c_6\Gamma/2 + c_{13}$
i-1	j	0
i+1	j	$-c_2\Gamma + c_3\varphi_{i,j} + c_5\varphi_{i-2,j} + 2c_8\varphi_{i+1,j} + c_9$
ITE-1	JB-2	$(-c_2\varphi_{i+1,j}/2-c_4\varphi_{i,j}/2-c_6\varphi_{i-2,j}/2 +c_7/2-c_{10}/2-c_{11}/4)\ (+0.5T_1)$
ITE-1	JB-1	$(-c_2\varphi_{i+1,j}/2-c_4\varphi_{i,j}/2-c_6\varphi_{i-2,j}/2 +c_7/2-c_{10}/2-c_{11}/4)\ (-1.5T_1)$
ITE-1	JB	$(-c_2\varphi_{i+1,j}/2-c_4\varphi_{i,j}/2-c_6\varphi_{i-2,j}/2 +c_7/2-c_{10}/2-c_{11}/4)\ (+1.5T_1)$
ITE-1	JB+1	$(-c_2\varphi_{i+1,j}/2-c_4\varphi_{i,j}/2-c_6\varphi_{i-2,j}/2 +c_7/2-c_{10}/2-c_{11}/4)\ (-0.5T_1)$
ITE	JB-2	$(-c_2\varphi_{i+1,j}/2-c_4\varphi_{i,j}/2-c_6\varphi_{i-2,j}/2 +c_7/2-c_{10}/2-c_{11}/4)\ (+0.5T_2)$
ITE	JB-1	$(-c_2\varphi_{i+1,j}/2-c_4\varphi_{i,j}/2-c_6\varphi_{i-2,j}/2 +c_7/2-c_{10}/2-c_{11}/4)\ (-1.5T_2)$
ITE	JB	$(-c_2\varphi_{i+1,j}/2-c_4\varphi_{i,j}/2-c_6\varphi_{i-2,j}/2 +c_7/2-c_{10}/2-c_{11}/4)\ (+1.5T_2)$
ITE	JB+1	$(-c_2\varphi_{i+1,j}/2-c_4\varphi_{i,j}/2-c_6\varphi_{i-2,j}/2 +c_7/2-c_{10}/2-c_{11}/4)\ (-0.5T_2)$

For points [12],

ii	jj	Derivative of $R_{i,j}$
i	j-1	0
i	j	$c_1 + c_3\varphi_{i+1,j} - c_4\Gamma/2$
i	j+1	c_{11}
i-2	j	$c_5\varphi_{i+1,j} - c_6\Gamma/2 + c_{13}$
i-1	j	0
i+1	j	$- c_2\Gamma/2 + c_3\varphi_{i,j} + c_5\varphi_{i-2,j} + 2c_8\varphi_{i+1,j} + c_9$
ITE-1	JB-2	$(-c_2\varphi_{i+1,j}/2-c_4\varphi_{i,j}/2-c_6\varphi_{i-2,j}/2 +c_7\Gamma/2-c_{10}/2-3c_{12}/4)\ (+0.5T_1)$
ITE-1	JB-1	$(-c_2\varphi_{i+1,j}/2-c_4\varphi_{i,j}/2-c_6\varphi_{i-2,j}/2 +c_7\Gamma/2-c_{10}/2-3c_{12}/4)\ (-1.5T_1)$
ITE-1	JB	$(-c_2\varphi_{i+1,j}/2-c_4\varphi_{i,j}/2-c_6\varphi_{i-2,j}/2 +c_7\Gamma/2-c_{10}/2-3c_{12}/4)\ (+1.5T_1)$
ITE-1	JB+1	$(-c_2\varphi_{i+1,j}/2-c_4\varphi_{i,j}/2-c_6\varphi_{i-2,j}/2 +c_7\Gamma/2-c_{10}/2-3c_{12}/4)\ (-0.5T_1)$
ITE	JB-2	$(-c_2\varphi_{i+1,j}/2-c_4\varphi_{i,j}/2-c_6\varphi_{i-2,j}/2 +c_7\Gamma/2-c_{10}/2-3c_{12}/4)\ (+0.5T_2)$
ITE	JB-1	$(-c_2\varphi_{i+1,j}/2-c_4\varphi_{i,j}/2-c_6\varphi_{i-2,j}/2 +c_7\Gamma/2-c_{10}/2-3c_{12}/4)\ (-1.5T_2)$
ITE	JB	$(-c_2\varphi_{i+1,j}/2-c_4\varphi_{i,j}/2-c_6\varphi_{i-2,j}/2 +c_7\Gamma/2-c_{10}/2-3c_{12}/4)\ (+1.5T_2)$
ITE	JB+1	$(-c_2\varphi_{i+1,j}/2-c_4\varphi_{i,j}/2-c_6\varphi_{i-2,j}/2 +c_7\Gamma/2-c_{10}/2-3c_{12}/4)\ (-0.5T_2)$

For points [13],

ii	jj	Derivative of $R_{i,j}$
i	j-1	0
i	j	$c_1 - c_3\Gamma + c_4\varphi_{i-1,j}$
i	j+1	c_{11}
i-2	j	$- c_5\Gamma + c_6\varphi_{i-1,j} + c_{13}$
i-1	j	$- c_2\Gamma + c_4\varphi_{i,j} + c_6\varphi_{i-2,j} + 2c_7\varphi_{i-1,j} + c_{10}$
i+1	j	0
ITE-1	JB-2	$(-c_2\varphi_{i-1,j}-c_3\varphi_{i,j}-c_5\varphi_{i-2,j} +2c_8\Gamma-c_9-3c_{12}/4)\ (+0.5T_1)$
ITE-1	JB-1	$(-c_2\varphi_{i-1,j}-c_3\varphi_{i,j}-c_5\varphi_{i-2,j} +2c_8\Gamma-c_9-3c_{12}/4)\ (-1.5T_1)$
ITE-1	JB	$(-c_2\varphi_{i-1,j}-c_3\varphi_{i,j}-c_5\varphi_{i-2,j} +2c_8\Gamma-c_9-3c_{12}/4)\ (+1.5T_1)$
ITE-1	JB+1	$(-c_2\varphi_{i-1,j}-c_3\varphi_{i,j}-c_5\varphi_{i-2,j} +2c_8\Gamma-c_9-3c_{12}/4)\ (-1.5T_1)$
ITE	JB-2	$(-c_2\varphi_{i-1,j}-c_3\varphi_{i,j}-c_5\varphi_{i-2,j} +2c_8\Gamma-c_9-3c_{12}/4)\ (+0.5T_2)$
ITE	JB-1	$(-c_2\varphi_{i-1,j}-c_3\varphi_{i,j}-c_5\varphi_{i-2,j} +2c_8\Gamma-c_9-3c_{12}/4)\ (-1.5T_2)$
ITE	JB	$(-c_2\varphi_{i-1,j}-c_3\varphi_{i,j}-c_5\varphi_{i-2,j} +2c_8\Gamma-c_9-3c_{12}/4)\ (+1.5T_2)$
ITE	JB+1	$(-c_2\varphi_{i-1,j}-c_3\varphi_{i,j}-c_5\varphi_{i-2,j} +2c_8\Gamma-c_9-3c_{12}/4)\ (-0.5T_2)$

For points [14],

ii	jj	Derivative of $R_{i,j}$
i	j-1	c_{12}
i	j	$c_1 + c_4\varphi_{i-1,j}$
i	j+1	c_{11}
i-2	j	$c_6\varphi_{i-1,j} + c_{13}$
i-1	j	$c_4\varphi_{i,j} + c_6\varphi_{i-2,j} + 2c_7\varphi_{i-1,j} + c_{10}$
i+1	j	0
ITE-1	JB-2	c_{12} $(+0.5T_1)$
ITE-1	JB-1	c_{12} $(-1.5T_1)$
ITE-1	JB	c_{12} $(+1.5T_1)$
ITE-1	JB+1	c_{12} $(-0.5T_1)$
ITE	JB-2	c_{12} $(+0.5T_2)$
ITE	JB-1	c_{12} $(-1.5T_2)$
ITE	JB	c_{12} $(+1.5T_2)$
ITE	JB+1	c_{12} $(-0.5T_2)$

For points [15],

ii	jj	Derivative of $R_{i,j}$
i	j-1	c_{12}
i	j	$c_1 - c_3\Gamma + c_4\varphi_{i-1,j}$
i	j+1	c_{11}
i-2	j	$- c_5\Gamma + c_6\varphi_{i-1,j} + c_{13}$
i-1	j	$- c_2\Gamma + c_4\varphi_{i,j} + c_6\varphi_{i-2,j} + 2c_7\varphi_{i-1,j} + c_{10}$
i+1	j	0
ITE-1	JB-2	$(-c_2\varphi_{i-1,j}-c_3\varphi_{i,j}-c_5\varphi_{i-2,j} +2c_8\Gamma-c_9-c_{11})\ (+0.5T_1)$
ITE-1	JB-1	$(-c_2\varphi_{i-1,j}-c_3\varphi_{i,j}-c_5\varphi_{i-2,j} +2c_8\Gamma-c_9-c_{11})\ (-1.5T_1)$
ITE-1	JB	$(-c_2\varphi_{i-1,j}-c_3\varphi_{i,j}-c_5\varphi_{i-2,j} +2c_8\Gamma-c_9-c_{11})\ (+1.5T_1)$
ITE-1	JB+1	$(-c_2\varphi_{i-1,j}-c_3\varphi_{i,j}-c_5\varphi_{i-2,j} +2c_8\Gamma-c_9-c_{11})\ (-0.5T_1)$
ITE	JB-2	$(-c_2\varphi_{i-1,j}-c_3\varphi_{i,j}-c_5\varphi_{i-2,j} +2c_8\Gamma-c_9-c_{11})\ (+0.5T_2)$
ITE	JB-1	$(-c_2\varphi_{i-1,j}-c_3\varphi_{i,j}-c_5\varphi_{i-2,j} +2c_8\Gamma-c_9-c_{11})\ (-1.5T_2)$
ITE	JB	$(-c_2\varphi_{i-1,j}-c_3\varphi_{i,j}-c_5\varphi_{i-2,j} +2c_8\Gamma-c_9-c_{11})\ (+1.5T_2)$
ITE	JB+1	$(-c_2\varphi_{i-1,j}-c_3\varphi_{i,j}-c_5\varphi_{i-2,j} +2c_8\Gamma-c_9-c_{11})\ (-0.5T_2)$

For a supersonic free stream :

For points [5],

ii	jj	Derivative of $R_{i,j}$
i	j-1	c_{12}
i	j	$c_1 + c_2\varphi_{i-1,j} + 2c_3\varphi_{i,j} + c_4\varphi_{i-1,j} + c_5\varphi_{i-2,j} + 2c_8\varphi_{i,j} + c_9$
i	j+1	c_{11}
i-2	j	$c_5\varphi_{i,j} + c_6\varphi_{i-1,j} + c_{13}$
i-1	j	$(c_2+c_4)\varphi_{i,j} + c_6\varphi_{i-2,j} + 2c_7\varphi_{i-1,j} + c_{10}$
i+1	j	0
ITE-1	JB-2	0
ITE-1	JB-1	0
ITE-1	JB	0
ITE-1	JB+1	0
ITE	JB-2	0
ITE	JB-1	0
ITE	JB	0
ITE	JB+1	0

For points [6],

ii	jj	Derivative of $R_{i,j}$
i	j-1	c_{12}
i	j	$c_1 + c_3\varphi_{i+1,j} + c_4\varphi_{i-1,j}$
i	j+1	0
i-2	j	$c_5\varphi_{i+1,j} + c_6\varphi_{i-1,j} + c_{13}$
i-1	j	$c_2\varphi_{i+1,j} + c_4\varphi_{i,j} + c_6\varphi_{i-2,j} + 2c_7\varphi_{i-1,j} + c_{10}$
i+1	j	$c_2\varphi_{i-1,j} + c_3\varphi_{i,j} + c_5\varphi_{i-2,j} + 2c_8\varphi_{i+1,j} + c_9$
ITE-1	JB-2	0
ITE-1	JB-1	0
ITE-1	JB	0
ITE-1	JB+1	0
ITE	JB-2	0
ITE	JB-1	0
ITE	JB	0
ITE	JB+1	0

For points [7],

ii	jj	Derivative of $R_{i,j}$
i	j-1	c_{12}
i	j	$c_1 + c_3\varphi_{i+1,j}$
i	j+1	c_{11}
i-2	j	$c_5\varphi_{i+1,j} + c_{13}$
i-1	j	0
i+1	j	$c_3\varphi_{i,j} + c_5\varphi_{i-2,j} + 2c_8\varphi_{i+1,j} + c_9$
ITE-1	JB-2	0
ITE-1	JB-1	0
ITE-1	JB	0
ITE-1	JB+1	0
ITE	JB-2	0
ITE	JB-1	0
ITE	JB	0
ITE	JB+1	0

For points [8],

ii	jj	Derivative of $R_{i,j}$
i	j-1	0
i	j	$c_1 + c_3\varphi_{i+1,j} + c_4\varphi_{i-1,j}$
i	j+1	c_{11}
i-2	j	$c_5\varphi_{i+1,j} + c_6\varphi_{i-1,j} + c_{13}$
i-1	j	$c_2\varphi_{i+1,j} + c_4\varphi_{i,j} + c_6\varphi_{i-2,j} + 2c_7\varphi_{i-1,j} + c_{10}$
i+1	j	$c_2\varphi_{i-1,j} + c_3\varphi_{i,j} + c_5\varphi_{i-2,j} + 2c_8\varphi_{i+1,j} + c_9$
ITE-1	JB-2	0
ITE-1	JB-1	0
ITE-1	JB	0
ITE-1	JB+1	0
ITE	JB-2	0
ITE	JB-1	0
ITE	JB	0
ITE	JB+1	0

For points [9],

ii	jj	Derivative of $R_{i,j}$
i	j-1	c_{12}
i	j	$c_1 + c_2\varphi_{i-1,j} + 2c_3\varphi_{i,j} + c_4\varphi_{i-1,j} + c_5\varphi_{i-2,j} + 2c_8\varphi_{i,j} + c_9$
i	j+1	c_{11}
i-2	j	$c_5\varphi_{i,j} + c_6\varphi_{i-1,j} + c_{13}$
i-1	j	$(c_2+c_4)\varphi_{i,j} + c_6\varphi_{i-2,j} + 2c_7\varphi_{i-1,j} + c_{10}$
i+1	j	0
ITE-1	JB-2	0
ITE-1	JB-1	0
ITE-1	JB	0
ITE-1	JB+1	0
ITE	JB-2	0
ITE	JB-1	0
ITE	JB	0
ITE	JB+1	0

For points [10],

ii	jj	Derivative of $R_{i,j}$
i	j-1	c_{12}
i	j	$c_1 + c_2\varphi_{i-1,j} + 2c_3\varphi_{i,j} + c_4\varphi_{i-1,j} + c_5\varphi_{i-2,j} + 2c_8\varphi_{i,j} + c_9$
i	j+1	0
i-2	j	$c_5\varphi_{i+1,j} + c_6\varphi_{i-1,j} + c_{13}$
i-1	j	$c_2\varphi_{i+1,j} + c_4\varphi_{i,j} + c_6\varphi_{i-2,j} + 2c_7\varphi_{i-1,j} + c_{10}$
i+1	j	0
ITE-1	JB-2	0
ITE-1	JB-1	0
ITE-1	JB	0
ITE-1	JB+1	0
ITE	JB-2	0
ITE	JB-1	0
ITE	JB	0
ITE	JB+1	0

For points [11],

ii	jj	Derivative of $R_{i,j}$
i	j-1	c_{12}
i	j	$c_1 + c_3\varphi_{i+1,j}$
i	j+1	0
i-2	j	$c_5\varphi_{i+1,j} + c_{13}$
i-1	j	0
i+1	j	$c_3\varphi_{i,j} + c_5\varphi_{i-2,j} + 2c_8\varphi_{i+1,j} + c_9$
ITE-1	JB-2	0
ITE-1	JB-1	0
ITE-1	JB	0
ITE-1	JB+1	0
ITE	JB-2	0
ITE	JB-1	0
ITE	JB	0
ITE	JB+1	0

For points [12],

ii	jj	Derivative of $R_{i,j}$
i	j-1	0
i	j	$c_1 + c_3\varphi_{i+1,j}$
i	j+1	c_{11}
i-2	j	$c_5\varphi_{i+1,j} + c_{13}$
i-1	j	0
i+1	j	$c_3\varphi_{i,j} + c_5\varphi_{i-2,j} + 2c_8\varphi_{i+1,j} + c_9$
ITE-1	JB-2	0
ITE-1	JB-1	0
ITE-1	JB	0
ITE-1	JB+1	0
ITE	JB-2	0
ITE	JB-1	0
ITE	JB	0
ITE	JB+1	0

For points [13],

ii	jj	Derivative of $R_{i,j}$
i	j-1	0
i	j	$c_1 + c_2\varphi_{i-1,j} + 2c_3\varphi_{i,j} + c_4\varphi_{i-1,j} + c_5\varphi_{i-2,j} + 2c_8\varphi_{i,j} + c_9$
i	j+1	c_{11}
i-2	j	$c_5\varphi_{i+1,j} + c_6\varphi_{i-1,j} + c_{13}$
i-1	j	$c_2\varphi_{i+1,j} + c_4\varphi_{i,j} + c_6\varphi_{i-2,j} + 2c_7\varphi_{i-1,j} + c_{10}$
i+1	j	0
ITE-1	JB-2	0
ITE-1	JB-1	0
ITE-1	JB	0
ITE-1	JB+1	0
ITE	JB-2	0
ITE	JB-1	0
ITE	JB	0
ITE	JB+1	0

For points [14],

ii	jj	Derivative of $R_{i,j}$
i	j-1	c_{12}
i	j	$c_1 + c_2\varphi_{i-1,j} + 2c_3\varphi_{i,j}$ $+ c_4\varphi_{i-1,j} + c_5\varphi_{i-2,j} + 2c_8\varphi_{i,j}$ $+ c_9$
i	j+1	c_{11}
i-2	j	$c_5\varphi_{i+1,j} + c_6\varphi_{i-1,j} + c_{13}$
i-1	j	$c_2\varphi_{i+1,j} + c_4\varphi_{i,j} + c_6\varphi_{i-2,j}$ $+ 2c_7\varphi_{i-1,j} + c_{10}$
i+1	j	0
ITE-1	JB-2	c_{12} $(+0.5T_1)$
ITE-1	JB-1	c_{12} $(-1.5T_1)$
ITE-1	JB	c_{12} $(+1.5T_1)$
ITE-1	JB+1	c_{12} $(-0.5T_1)$
ITE	JB-2	c_{12} $(+0.5T_2)$
ITE	JB-1	c_{12} $(-1.5T_2)$
ITE	JB	c_{12} $(+1.5T_2)$
ITE	JB+1	c_{12} $(-0.5T_2)$

For points [15],

ii	jj	Derivative of $R_{i,j}$
i	j-1	c_{12}
i	j	$c_1 + c_2\varphi_{i-1,j} + 2c_3\varphi_{i,j} + c_4\varphi_{i-1,j} + c_5\varphi_{i-2,j} + 2c_8\varphi_{i,j} + c_9$
i	j+1	c_{11}
i-2	j	$c_5\varphi_{i+1,j} + c_6\varphi_{i-1,j} + c_{13}$
i-1	j	$c_2\varphi_{i+1,j} + c_4\varphi_{i,j} + c_6\varphi_{i-2,j} + 2c_7\varphi_{i-1,j} + c_{10}$
i+1	j	0
ITE-1	JB-2	$- c_{11} (+0.5T_1)$
ITE-1	JB-1	$- c_{11} (-1.5T_1)$
ITE-1	JB	$- c_{11} (+1.5T_1)$
ITE-1	JB+1	$- c_{11} (-0.5T_1)$
ITE	JB-2	$- c_{11} (+0.5T_2)$
ITE	JB-1	$- c_{11} (-1.5T_2)$
ITE	JB	$- c_{11} (+1.5T_2)$
ITE	JB+1	$- c_{11} (-0.5T_2)$

The derivates of the residual with respect to the design variables (i.e. right hand sides of Eq.(1)) are given by,

XD_i	Points	Derivates
T	[1]	$(+c_{11}\Delta\eta/g_{j+\frac{1}{2}})\ F'_l$
	[2]	$(-c_{12}\Delta\eta/g_{j-\frac{1}{2}})\ F'_u$
M_∞	General	$c_1'\varphi_{i,j} + c_2'\varphi_{i+1,j}\varphi_{i-1,j}$
		$+ c_3'\varphi_{i+1,j}\varphi_{i,j} + c_4'\varphi_{i-1,j}\varphi_{i,j}$
		$+ c_5'\varphi_{i+1,j}\varphi_{i-2,j} + c_6'\varphi_{i-1,j}\varphi_{i-2,j}$
		$+ c_7'\varphi_{i-1,j}^2 + c_8'\varphi_{i+1,j}^2 + c_9'\varphi_{i+1,j}$
		$+ c_{10}'\varphi_{i-1,j} + c_{13}'\varphi_{i-2,j}$
α	[1]	$(-c_{11}\Delta\eta/g_{j+\frac{1}{2}})$
	[2]	$(+c_{12}\Delta\eta/g_{j-\frac{1}{2}})$
C	[1]	$(+c_{11}\Delta\eta/g_{j+\frac{1}{2}})\ F'_l$
	[2]	$(-c_{12}\Delta\eta/g_{j-\frac{1}{2}})\ F'_u$
L	[1]	$(+c_{11}\Delta\eta/g_{j+\frac{1}{2}})\ F'_l$
	[2]	$(-c_{12}\Delta\eta/g_{j-\frac{1}{2}})\ F'_u$

Note that the primes (') denote the partial derivative with respect to the design variable (XD_i).

VITA

Hesham Mahmoud Elbanna was born in Cairo, EGYPT, on July 12, 1962, and is the son of Mahmoud E. and Zeinab Fahmy. He graduated from Port Said School, Zamalek, Cairo, EGYPT, in 1980, and entered Cairo University in the fall of that year. In May, 1985, he received a Bachelor of Science in Mechanical Engineering from Cairo University and began graduate studies in the summer of 1986.

His interests include computational aerodynamics and mathematics. Leisure time interests include squash, chess, and swimming. His permanent address is, 16 Saleh Ayoub St., Apt.63, Zamalek, Cairo, Egypt.